

UNCLASSIFIED

AD NUMBER
AD474616
NEW LIMITATION CHANGE
TO Approved for public release, distribution unlimited
FROM Distribution authorized to U.S. Gov't. agencies and their contractors; Administrative/Operational Use; Sep 1965. Other requests shall be referred to Air Force Flight Dynamics Laboratory, Research and Technology Division, Wright-Patterson AFB, OH 45433.
AUTHORITY
AFFDL ltr, 24 Jan 1973

THIS PAGE IS UNCLASSIFIED

SECURITY

MARKING

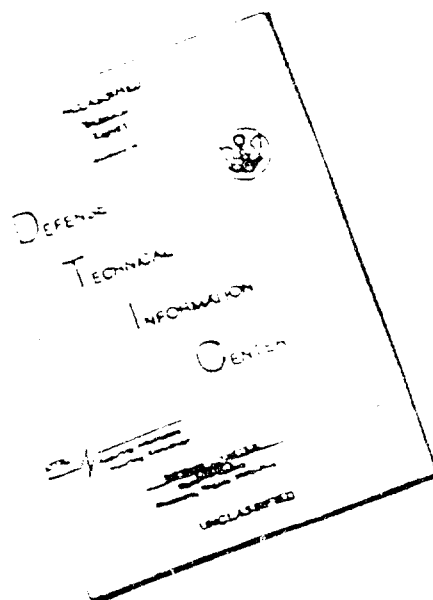
The classified or limited status of this report applies to each page, unless otherwise marked.

Separate page printouts MUST be marked accordingly.

THIS DOCUMENT CONTAINS INFORMATION AFFECTING THE NATIONAL DEFENSE OF THE UNITED STATES WITHIN THE MEANING OF THE ESPIONAGE LAWS, TITLE 18, U.S.C., SECTIONS 793 AND 794. THE TRANSMISSION OR THE REVELATION OF ITS CONTENTS IN ANY MANNER TO AN UNAUTHORIZED PERSON IS PROHIBITED BY LAW.

NOTICE: When government or other drawings, specifications or other data are used for any purpose other than in connection with a definitely related government procurement operation, the U. S. Government thereby incurs no responsibility, nor any obligation whatsoever; and the fact that the Government may have formulated, furnished, or in any way supplied the said drawings, specifications, or other data is not to be regarded by implication or otherwise as in any manner licensing the holder or any other person or corporation, or conveying any rights or permission to manufacture, use or sell any patented invention that may in any way be related thereto.

DISCLAIMER NOTICE



THIS DOCUMENT IS BEST
QUALITY AVAILABLE. THE COPY
FURNISHED TO DTIC CONTAINED
A SIGNIFICANT NUMBER OF
PAGES WHICH DO NOT
REPRODUCE LEGIBLY.

REPRODUCED FROM
BEST AVAILABLE COPY

AFFDL-TR-65-144

464316

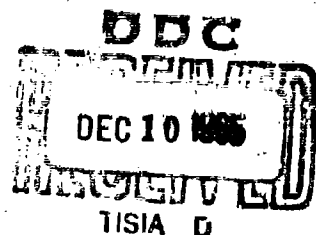
HIGH ALTITUDE CLEAR AIR TURBULENCE

WALTER CROOKS

LOCKHEED-CALIFORNIA COMPANY

TECHNICAL REPORT No. AFFDL-TR-65-144

SEPTEMBER 1965



AF FLIGHT DYNAMICS LABORATORY
RESEARCH AND TECHNOLOGY DIVISION
AIR FORCE SYSTEMS COMMAND
WRIGHT-PATTERSON AIR FORCE BASE, OHIO

NOTICES

When Government drawings, specifications, or other data are used for any purpose other than in connection with a definitely related Government procurement operation, the United States Government thereby incurs no responsibility nor any obligation whatsoever; and the fact that the Government may have formulated, furnished, or in any way supplied the said drawings, specifications, or other data, is not to be regarded by implication or otherwise as in any manner licensing the holder or any other person or corporation, or conveying any rights or permission to manufacture, use, or sell any patented invention that may in any way be related thereto.

Copies of this report should not be returned to the Research and Technology Division unless return is required by security considerations, contractual obligations, or notice on a specific document.

HIGH ALTITUDE CLEAR AIR TURBULENCE

WALTER CROOKS

FOREWORD

This report discusses the research accomplished on the High Altitude Clear Air Turbulence project prior to its redirection on 15 February 1965 and was prepared by the Lockheed-California Company, on Air Force Contract AF 33(657)-11143, under Task No. 146902 of Project 1469. The work was administered under the direction of Structures Division of the Air Force Flight Dynamics Laboratory. Mr. Neal Loving was Project Engineer for the Laboratory.

This work was conducted from 15 April 1963 to 15 February 1965. This manuscript was released for publication as an RTD Technical Report 19 June 1965.

This technical report has been reviewed and is approved.



RICHARD F. HOENER
Acting Chief
Structures Division

ABSTRACT

The purpose of this report is to describe the high altitude clear air turbulence (HICAT) program accomplishments and results as of 15 February 1965, when the program was redirected. The program effort consists of the measurement of HICAT velocity components at altitudes above 50,000 feet in several world areas. The program objective is the statistical definition of the characteristics of HICAT so as to improve structural design criteria.

In the work accomplished thus far, an analog FM instrumentation system utilizing a fixed vane gust probe and a 7-hour recording system was installed aboard an Air Force U-2. HICAT searches were conducted at Air Force bases in California, Florida and Puerto Rico. Over seven hours of HICAT associated with jet streams, convective activity due to low level heating, and mountain wave activity were recorded. The latter category provided the most severe turbulence experienced to date, i.e., c.g. normal acceleration incremental peaks up to about $\pm 1g$ and RMS gust velocities in excess of 5 ft/sec.

Actual vertical gust velocity time histories containing gust wavelengths from 70 to 2500 feet have been calculated from the measurements and used to obtain gust velocity peak counts and power spectra. Derived equivalent gust velocities, U_{de} , were also calculated and found to be comparable with similar NASA data.

The redirected and extended HICAT program will utilize a new digital (PCM) instrumentation system. This system will include a stable platform which will greatly improve the precision of HICAT measurements and permit turbulence wavelengths in excess of 12,000 feet to be measured.

CONTENTS

SECTION I	INTRODUCTION	1
SECTION II	HICAT INSTRUMENTATION SYSTEM	3
	GENERAL	3
	FUNCTIONAL DESCRIPTION	4
SECTION III	DATA ACQUISITION	11
	HICAT SEARCHES	11
	HICAT FLIGHT DESCRIPTION	11
SECTION IV	DATA PROCESSING AND ANALYSIS METHODS	12
	GENERAL	12
	PEAK COUNTING	12
	POWER SPECTRA ANALYSIS	13
SECTION V	INTERIM RESULTS	13
	TIME HISTORIES	13
	PEAK COUNTS	15
	POWER SPECTRA	16
SECTION VI	METEOROLOGICAL ASPECTS	18
	SAMPLING SITE SELECTION	18
	FORECASTING	19
	ANALYSIS AND INTERPRETATION	19
SECTION VII	CONCLUSIONS	21
APPENDIX I	HICAT GUST SENSOR SPECIFICATIONS AND CALIBRATIONS.	85
APPENDIX II	HICAT FLIGHT TEST LOG AND TRACK MAPS	87
APPENDIX III	GUST VELOCITY EQUATIONS	112
APPENDIX IV	DERIVED EQUIVALENT GUST VELOCITY FORMULA	113
REFERENCES		114

ILLUSTRATIONS

<u>Figure No.</u>	<u>Title</u>	
1	U-2 Aircraft Used for HICAT Searches	22
2	HICAT Gust Probe and Boom Installation on Nose of U-2.	23
3	HICAT Gust Probe Closeup Showing Vertical and Lateral Gust Sensing Vanes and Air Force MA-1 Pitot-Static Tube	23
4	HICAT Data Acquisition System Block Diagram for Aircraft	24
5	Double Beam Sensor with Strain Gage Installation for Shear Measurement	25
6	Angular Deflection of Simple Sensor	25
7	Aircraft Instrumentation Location Diagram	26
8	Pilot's Total Pressure Head and Nose Boom Attachment	27

<u>Figure No.</u>	<u>Title</u>	<u>Page</u>
9	Total Temperature Sensor Installation on Nose of Aircraft	27
10	Magnetic Tape Recorder Installation in Equipment Bay	28
11	Time Code Generator Installation in Equipment Bay (Upper Hatch Removed)	28
12	Instrumentation Installation on Lower Hatch of Equipment Bay	29
13	Mobile Data Systems Van	29
14	Van Instrumentation Showing Magnetic Tape Reproducer, Patch Panel, Electronic Test Equipment, and Subcarrier Discriminator Array . . .	30
15	Van "Quick-Look" Oscillograph Recorder and Control Panel	30
16	HICAT Data Acquisition System Block Diagram for the Mobile Data Systems Van	31
17	HICAT Data Acquisition System Block Diagram for the Ground Station	31
18	Time History of Vertical Gust Velocity, Test 33, Run 3. 0 - 60 Sec.	32
19	Time History of Vertical Gust Velocity, Test 33, Run 3. 60 - 120 Sec.	33
20	Time History of C.G. Normal Acceleration and Left Wing Nodal Acceleration, Test 33, Run 3. 0 - 60 Sec.	34
21	Time History of C.G. Normal Acceleration and Left Wing Nodal Acceleration, Test 33, Run 3. 60 - 120 Sec.	35
22	Time History of Derived Equivalent Gust Velocity (U_{ge}) and Equivalent Velocity (V_e) Test 33, Run 3. 0 - 60 Sec.	36
23	Time History of Derived Equivalent Gust Velocity (U_{ge}) and Equivalent Velocity (V_e) Test 33, Run 3. 60 - 120 Sec.	37
24	Frequency of Exceedance Per Mile of Vertical Gust Velocity, Tests 28 and 33	38
25	Frequency of Exceedance Per Mile of Derived Equivalent Gust Velocity, Test 26	39
26	Frequency of Exceedance Per Mile of Derived Equivalent Gust Velocity, Test 28	40
27	Frequency of Exceedance Per Mile of Derived Equivalent Gust Velocity, Test 30	41
28	Frequency of Exceedance Per Mile of Derived Equivalent Gust Velocity, Test 33, Runs 3-7	42
29	Frequency of Exceedance Per Mile of Derived Equivalent Gust Velocity, Test 33, All Runs Combined	43
30	Frequency of Exceedance Per Mile of Incremental C.G. Normal Acceleration, Test 26	44
31	Frequency of Exceedance Per Mile of Incremental C.G. Normal Acceleration, Test 28	45

<u>Figure No.</u>	<u>Title</u>	<u>Page</u>
32	Frequency of Exceedance Per Mile of Incremental C.G. Normal Acceleration, Test 30	46
33	Frequency of Exceedance Per Mile of Incremental C.G. Normal Acceleration, Test 33	47
34	Comparison of HICAT Frequency of Exceedance of Gust Velocity Per Mile of Flight With TN D-548	48
35	Comparison of HICAT Derived Equivalent Gust Velocities With U_{dc} Design Envelope	49
36	Power Spectrum of $V_T \Delta \alpha$, Test 26, Run 1	50
37	Power Spectrum of $V_T \Delta \beta$, Test 26, Run 1	51
38	Power Spectrum of $V_T \Delta \alpha$, Test 26, Run 2	52
39	Power Spectrum of $V_T \Delta \beta$, Test 26, Run 2	53
40	Power Spectrum of $V_T \Delta \alpha$, Test 26, Run 3	54
41	Power Spectrum of $V_T \Delta \beta$, Test 26, Run 3	55
42	Power Spectrum of Vertical Gust Velocity, Test 28, Run 2	56
43	Power Spectrum of $V_T \Delta \alpha$, Test 28, Run 2	57
44	Power Spectrum of $V_T \Delta \beta$, Test 28, Run 2	58
45	Power Spectrum of Vertical Gust Velocity, Test 28, Run 3	59
46	Power Spectrum of $V_T \Delta \alpha$, Test 28, Run 3	60
47	Power Spectrum of $V_T \Delta \beta$, Test 28, Run 3	61
48	Power Spectrum of Vertical Gust Velocity, Test 30, Run 3	62
49	Power Spectrum of $V_T \Delta \alpha$, Test 30, Run 3	63
50	Power Spectrum of $V_T \Delta \beta$, Test 30, Run 3	64
51	Power Spectrum of Vertical Gust Velocity, Test 33, Run 1	65
52	Power Spectrum of $V_T \Delta \alpha$, Test 33, Run 1	66
53	Power Spectrum of $V_T \Delta \beta$, Test 33, Run 1	67
54	Power Spectrum of Vertical Gust Velocity, Test 33, Run 3	68
55	Power Spectrum of $V_T \Delta \alpha$, Test 33, Run 3	69
56	Power Spectrum of $V_T \Delta \beta$, Test 33, Run 3	70
57	Power Spectrum of Vertical Gust Velocity, Test 33, Run 4	71
58	Power Spectrum of $V_T \Delta \alpha$, Test 33, Run 4	72
59	Power Spectrum of $V_T \Delta \beta$, Test 33, Run 4	73
60	Power Spectrum of Vertical Gust Velocity, Test 33, Run 5	74
61	Power Spectrum of $V_T \Delta \alpha$, Test 33, Run 5	75
62	Power Spectrum of $V_T \Delta \beta$, Test 33, Run 5	76
63	Power Spectrum of Vertical Gust Velocity, Test 33, Run 6	77
64	Power Spectrum of $V_T \Delta \alpha$, Test 33, Run 6	78
65	Power Spectrum of $V_T \Delta \beta$, Test 33, Run 6	79

<u>Figure No.</u>	<u>Title</u>	<u>Page</u>
66	Power Spectrum of Vertical Gust Velocity, Test 33, Run 7	80
67	Power Spectrum of $V_T \Delta\alpha$, Test 33, Run 7	81
68	Power Spectrum of $V_T \Delta\beta$, Test 33, Run 7	82
69	Sensitivity Versus Vane Temperature for Semi- Conductor Gage System	83
70	HICAT Gust Sensor Load Calibration	84
71	HICAT Track Map, Test 7	93
72	HICAT Track Map, Test 8	94
73	HICAT Track Map, Test 10	95
74	HICAT Track Map, Test 11	96
75	HICAT Track Map, Test 12	97
76	HICAT Track Map, Test 17	98
77	HICAT Track Map, Test 18	99
78	HICAT Track Map, Test 19	100
79	HICAT Track Map, Test 20	101
80	HICAT Track Map, Test 22	102
81	HICAT Track Map, Test 23	103
82	HICAT Track Map, Test 24	104
83	HICAT Track Map, Test 25	105
84	HICAT Track Map, Test 26	106
85	HICAT Track Map, Test 27	107
86	HICAT Track Map, Test 28	108
87	HICAT Track Map, Test 29	109
88	HICAT Track Map, Test 30	110
89	HICAT Track Map, Test 33	111

TABLES

<u>Table No.</u>	<u>Title</u>	<u>Page</u>
I.	HICAT AIRCRAFT INSTRUMENTATION	6
II.	SUBCARRIER FREQUENCIES	7
III.	HICAT DATA SUMMARY	14
IV.	HICAT GUST SENSOR LOAD CALIBRATION RESPONSES	86
V.	HICAT FLIGHT TEST LOG	88

SYMBOLS

a_p	Gust probe longitudinal acceleration (ft/sec ²); positive acceleration is forward.
a_L	Gust probe lateral acceleration (ft/sec ²); positive to the right.
\bar{a}_L	Average value of a_L .
a_N	Gust probe normal acceleration (ft/sec ²); positive upward.
\bar{a}_N	Average value of a_N .
\bar{c}	Mean aerodynamic chord, wing area/wing span (ft).
$C_{L\alpha}$	Wing lift curve slope (1/rad).
$C_{N\alpha}$	Alpha-vane rate of change of normal force coefficient with angle-of-attack (1/rad).
$C_{N\beta}$	Beta-vane rate of change of normal force coefficient with sideslip angle (1/rad).
g	Acceleration of gravity (ft/sec ²).
K_g	Gust alleviation factor = $.83\mu_g/(5.3 + \mu_g)$.
L	Scale of turbulence (ft).
m_v	Mass of gust sensing vane (lb-sec ² /ft).
P_α	Alpha-vane normal force (lb); positive upward.
\bar{P}_α	Average value of P_α .
P_β	Beta-vane normal force (lb); positive force is from the right.
\bar{P}_β	Average value of P_β .
S	Wing area (ft ²).
S_v	Vane area (ft ²).
t_o, t_n	Turbulence start and end times (sec).
U_{de}	Derived equivalent gust velocity (ft/sec); positive upwards.
U_F	Longitudinal gust velocity (ft/sec); positive aft.

U_L	Lateral gust velocity (ft/sec); positive to the right.
U_V	Vertical gust velocity (ft/sec); positive upwards.
v_e	Equivalent airspeed = $V_T (\rho/\rho_0)^{1/2}$ (knots)
V_T	Aircraft true airspeed (ft/sec).
\bar{V}_T	Average value of V_T .
W	Aircraft weight (lb).
β	Gust probe sideslip angle (rad); positive relative wind is from the right.
$\bar{\beta}$	Average value of β .
θ	Aircraft pitch attitude angle (rad); positive for aircraft nose up.
$\bar{\theta}$	Average value of θ .
$\phi ()$	Spectrum of ().
ϕ	Aircraft roll attitude angle (rad); positive right wing down.
$\bar{\phi}$	Average value of ϕ .
ψ	Aircraft yaw angle (rad); positive for aircraft nose right.
$\bar{\psi}$	Average value of ψ .
ρ	Air density (lb-sec ² /ft ⁴).
ρ_0	Air density at sea level (lb-sec ² /ft ⁴).
μ_g	Aircraft mass ratio = $2W/\rho C_{L\alpha} \bar{c} S_g$.
Δa_{CG}	Incremental C.G. normal acceleration (g), positive up.
Δa_N	$a_N - \bar{a}_N$
Δa_L	$a_L - \bar{a}_L$
ΔP_α	$P_\alpha - \bar{P}_\alpha$
ΔP_β	$P_\beta - \bar{P}_\beta$

$$\Delta v_T \quad v_T - \bar{v}_T$$

$$\Delta \theta \quad \theta - \bar{\theta}$$

$$\Delta \phi \quad \phi - \bar{\phi}$$

$$\Delta \psi \quad \psi - \bar{\psi}$$

$$\bar{v}_T \quad \text{Root mean square gust velocity (ft/sec).}$$

$$\Omega \quad \text{Reduced frequency} = 2\pi / \lambda \text{ (rad/ft).}$$

$$\lambda \quad \text{Turbulence wavelength (ft).}$$

SECTION I

INTRODUCTION

BACKGROUND

A distinguishing characteristic of advanced flight vehicles is the increased size of their operating envelope in terms of speed and altitude. Optimum design of such a vehicle is essential and requires detailed knowledge of the intended operating environment.

Sometime before 1962 the Air Force recognized the need for better definition of the clear air turbulence environment, particularly for altitudes above 50,000 feet (Reference 1). Information available then was derived almost entirely from NASA VGH¹ recordings acquired during 192 U-2 flights in five world areas (Reference 2). These flights were made for purposes not directly related to atmospheric turbulence or the penetration of turbulence. Only about half of the data from these flights or approximately 5-1/2 hours were for turbulence above 50,000 feet.

The Air Force realized the danger of relying solely on the acceleration response of the U-2 aircraft as a measure of turbulence at high altitudes. A supersonic or hypersonic vehicle of possibly radical shape, flying four to ten or more times the speed of the U-2, will obviously have a somewhat different response to turbulence than the U-2. An aircraft flying at these high speeds would be affected much more by longer turbulence wavelengths and less by the shorter than the relatively slow flying U-2. For these reasons, the Air Force enlisted Lockheed's aid to measure high altitude clear air turbulence (HICAT) at altitudes above 50,000 feet in several world areas. The principal objective of the program was to statistically define the characteristics of high altitude CAT so as to improve structural design criteria. To accomplish this result, an Air Force U-2 was to be instrumented so that true gust velocity components encountered along the aircraft flight path could be determined.

Lockheed was directed to install and maintain the turbulence measuring instrumentation in the U-2 as well as to process and analyze the data. In this joint effort, the Air Force was to supply the instrumentation, maintain and fly the HICAT aircraft, and provide overall direction of the program. Under a separate contract (Reference 4) Lockheed was directed to utilize the data gathered in the flight program to develop a statistical model of high altitude CAT. The model would then provide meteorologists with a basis for the prediction of atmospheric rough spots.

HICAT PROGRAM HISTORY

Most of the aircraft instrumentation was provided off-the-shelf from Air Force inventory in order to keep within the modest HICAT budget. In many instances standard instruments were supplied which were not particularly intended for turbulence research.

¹ Aircraft velocity, center-of-gravity acceleration, and altitude

Installation of the instrumentation was begun at Edwards AFB on 18 March 1963 after inspection and preliminary calibration. Installation work was halted 14 June 1963 when the aircraft was required for a higher priority Air Force program. The aircraft was unavailable to the program almost continuously until 26 December 1963. In this period, it was established that the Giannini type gust probe originally supplied to the program was a Douglas prototype model, and hence not repairable by Giannini, the licensed manufacturer. This probe (a low altitude device used in the B-66B program, Reference 3) was intended for interim use only until a more sensitive probe could be purchased. However, a new Giannini probe could not be built to meet the requirements for high altitude gust measurements because appropriate 1 psi pressure transducers were unavailable.

Consequently, at the request of the Air Force, Lockheed designed and built a high altitude gust sensor. The sensor design was based upon the fixed vane principle (for description, see page 4) utilized successfully in a recent investigation of tail buffeting turbulence on the USN F3A patrol bomber. Fortunately, it was possible to adapt the Lockheed gust sensors to the nose boom previously fabricated for the Giannini probe.

On 27 December 1963, the Mobile Data Systems Van (a mobile ground station for instrument maintenance and calibration and for rapidly converting flight recorded magnetic tapes to analog oscillograms; see page 9) was moved to EAFB. The HICAT field team, consisting of an instrumentation engineer and three technicians, followed on 30 December and completed the van equipment checkout on site 10 January 1964.

After two more delays, totalling approximately a month because of aircraft and then engine unavailability, the first HICAT checkout flight was made on 20 February 1964 and the first HICAT search on 3 April 1964. In the period ending 15 July 1964, 18 HICAT search flights were completed, five from EAFB, California, four from Patrick AFB, Florida, and nine from Ramey AFB, Puerto Rico. Approximately six hours of high altitude CAT of predominantly light to moderate intensity² was encountered on these flights. (See HICAT log, page 88.) Turbulence in the wavelength range from 60 to 2500 feet was located and recorded approximately 14 percent of the time at altitudes above 50,000 feet.

In the work accomplished thus far, the HICAT aircraft had to be shared on a day-to-day basis with other higher priority Air Force programs. This mode of operation caused HICAT flights to be made during daytime hours on a more or less scheduled basis. For this reason, the flights only occasionally coincided with optimum turbulence forecasts.

On 15 February 1965, the HICAT program was redirected and extended. HICAT searches are expected to be resumed near the end of 1965 with improved instrumentation capable of accurately measuring the very long turbulence waves, i.e., those up to 12,000 feet or more in length. The new instrumentation system will be a digital (PCM) type. It will have sufficient capacity to

² Approximately $\pm 0.1g$ to $\pm 0.7g$ in terms of c.g. acceleration

to record up to 12 channels of data in addition to those required for the HICAT measurements. Thus, measurements related to HICAT research such as electric field strength, ozone concentration, particle counts and the like, can also be recorded.

SECTION II

HICAT INSTRUMENTATION SYSTEM

GENERAL

The HICAT instrumentation system is composed of three main elements. The first, of course, is the aircraft and the airborne instrumentation (Figure 1). Basically this consists of sensitive vertical and lateral gust sensing vanes mounted on the end of a long stiff boom on the nose of the aircraft (Figures 2 and 3). These vanes detect the fluctuating turbulence velocities by small changes in angle-of-attack relative to the airplane. Analog signals proportional to the angle changes are generated by the gust sensors during the flight and recorded in frequency modulated (FM) form on one inch magnetic tape. Also recorded and used in the gust velocity equations to correct for the effects of aircraft motion are measurements of aircraft attitude angles, angular rates, and three axis accelerations. All the gust measurements are recorded using the lowest speed mode of the tape recorder. In this way a continuous recording of the entire flight from takeoff to landing is obtained.

The second element in the instrumentation scheme is the Mobile Data Systems Van which accompanies the aircraft to all bases of operation. The Van provides facilities for instrumentation maintenance, calibration and pre- and post-flight checkout. Perhaps more important, the Van contains equipment for the rapid production of an analog oscillograph record (i.e., a time history) from the high speed playback of the flight recorded magnetic tape. This record is called the "Quick-Look" and is made immediately after a HICAT search flight. The "Quick-Look" record is examined to determine the extent and intensity of turbulence encountered and to check the performance of the instrumentation system.

After evaluation, the flight recorded tape and the "Quick-Look" records are transmitted to the third element in the HICAT instrumentation scheme, the ground station. The ground station converts the flight recorded magnetic data tape to a computer compatible data tape based upon editing information derived from the "Quick-Look" record. Three significant functions are performed in this process. The ground station electronically filters the data to eliminate electrical noise as well as those signals at frequencies above those of interest, i.e., greater than 10 cps. At the same time, the ground station reads the selected portions of the analog recorded signals and converts them into calibrated signals in binary digits. This information is reformatted and recorded on half inch computer compatible tape for use in the various HICAT computing programs.

FUNCTIONAL DESCRIPTION

Airborne Instrumentation

The airborne instrumentation consists basically of the gust probe with associated transducers for making the gust measurements, strain controlled oscillators, and magnetic tape recorder as shown in the system block diagram in Figure 4. A transducer simulator is used to calibrate the performance of the strain controlled oscillators and the time code generator supplies time base reference signals. These components are described in detail below.

HICAT Gust Sensor. The determination of the gust velocity components of atmospheric turbulence from an aircraft flying through it generally requires the measurement of two quantities:

1. Motion of the air disturbances or gusts relative to the aircraft.
2. Motion of the aircraft with respect to the ground.

The first measurement is normally accomplished by detecting component changes in flow direction, flow velocity, or flow pressure. The second is obtained by observing the vehicle's motion from the ground by optical or electrical means or by recording the motion with respect to an inertial or gravity reference carried aboard the vehicle. Accelerometers and gyros were used for this latter purpose on the HICAT program.

The measurement of item 1. above at altitudes of 50,000 feet or more from a vehicle operating at high subsonic speeds requires a sensor designed to satisfy some fairly restrictive requirements. It must operate at temperatures ranging from 130°F on the ground to -100°F and atmospheric pressures varying from 14.7 psi to about 0.5 psi at altitude without significant change in its zero reference or sensitivity. The instrument must be able to accurately detect atmospheric gusts with velocities as small as 1/2 ft/sec over a frequency range from near zero to 10 cps. In practice this requires an ability to resolve angular changes in flow direction of the order of 1/20 of a degree.

The fixed vane sensor developed by Lockheed meets these requirements. The sensor consists of a light weight wedgeshaped vane (4-inch span and 2-inch chord) attached to a specially constructed strain gaged beam. The slotted construction of the beam allows the wedge to deflect parallel to itself under load. Figure 5 shows how this deflection takes place without change of angle-of-incidence. Note that this would not be the case if the wedge were mounted on a simple beam as shown in Figure 6. Here the aerodynamic lift load bends the beam and causes the vane to rotate changing the angle-of-incidence by a small and undesired amount ($\Delta \alpha$).

By measuring the lift load in terms of shear instead of bending moment, considerations of moment arm changes due to center-of-pressure shifts on the vane can be entirely eliminated. Figure 5 shows the strain gage installation used to accomplish the measurements of the vane vertical shear or lift. The shear is a function of the difference in the bending strains between the fore and aft gage stations. The Wheatstone bridge circuit arrangement of the

strain gages produces an electrical signal directly proportional to this difference. At the same time, the strain gage circuit cancels out all unwanted responses. That is, there is no electrical response due to twisting of the vane about its longitudinal axis, no response to sideways loading of the vane, and lastly no response due to fore and aft forces on the vane.

The gust sensor design is comparatively rugged. It will withstand airloads as large as ± 12 lb without damage. The sensor is also very stiff. The fundamental or natural bending frequency is 155 cps when the sensor is mounted on the gust probe. This frequency is so much greater than the turbulence frequencies of interest (approximately 0-10 cps) that maximum amplitude distortion in the measurement is less than 1% for frequencies below 10 cps.

Despite its comparatively stiff and rugged construction, the gust sensor is extremely sensitive with an output of about 12 mv/v per pound of lift or about 0.15 mv/v for a 1 ft/sec vertical or lateral gust at 60,000 feet. This relatively large output results from the use of semiconductor strain gages which have an output over 25 times larger than the usual wire or foil strain gage. Detailed specification and calibration data for the gust sensor are included in Appendix I.

The HICAT Gust Probe consists of vertical and lateral gust sensors grouped about a central pitot-static tube (AF type MA-1), as shown in Figure 3. Vertical and lateral accelerometers and a very sensitive airspeed (pressure) transducer installed internally just behind the gust sensor attach points complete the gust probe instrumentation.

HICAT Nose Boom. The nose boom is used to support the gust probe sufficiently far ahead of the aircraft nose as to be relatively unaffected by the aircraft flow field. Normally it would be attached on the centerline to the most forward part of the nose of the aircraft. However, radio gear in the nose of the U-2 precluded this type of installation. The boom was therefore installed just under the nose as shown in Figures 2 and 8. This also caused the pilot's pitot to be relocated as shown in Figure 8.

The boom was originally designed to mount the Giannini gust probe. For this purpose, it was made of 6061 aluminum alloy tubing, 3-1/2 inches in diameter and .188 inches thick. Overall length from the nose of the aircraft to the gust sensing head was to have been 80 inches. As explained on page 2, this gust probe could not be made to satisfy the requirements for high altitude gust measurement so a Lockheed-designed sensor was installed.

With the Lockheed probe installed, overall length to the tip of the pitot-static head was 77.3 inches. The gust sensing vanes were located 10.0 inches back of this point as shown in Figure 3. Despite the somewhat greater mass of the Lockheed sensor, boom stiffness was considered adequate without additional modification. Vertical and lateral boom bending frequencies were 14.1 and 12.7 cps, respectively, or about twice the highest frequency of interest.

Transducers. A total of twenty flight data and turbulence parameters comprise the HICAT measurement list shown in Table I, page 6. A summary of transducer specifications is also included for each measurement. In order to be com-

TABLE I

HICAT AIRCRAFT INSTRUMENTATION

No.	Measurement	Location	Maker	Model No.	Serial No.	Inst. Freq. (cps)	Inst. Range	Meas. Range	Sys. Avg. Res.	Hysteresis
1	α-Vane Normal Force	Gust Probe	Lockheed	PT 3809	4	155	±12 lb	±2 lb	.0031g	±.1%
2	β-Vane Lateral Force	Gust Probe	Lockheed	PT 3809	5	155	±12 lb	±2 lb	.0030g	±.1%
3	Probe Normal Accel.	Gust Probe	Statham	AJ43-3-350	10440	60	± 3g	± 3g	.0046g	±.1%
4	Probe Lateral Accel.	Gust Probe	Statham	AJ43-3-350	10441	60	± 3g	± 3g	.0046g	±.1%
5	C.G. Normal Accel.	FS408	BMF	LF-5-15-120	577	15	± 5g	0, +2g	.0023g	±.1%
6	C.G. Longitudinal Ac.	FS408	Statham	A26-1-350	184	70	± 1g	± 1g	.0015g	±.1%
7	L. Wing Nodal Accel.	WS175	Statham	A43-2-350	215	70	± 2g	± 2g	.0036g	±.1%
8	R. Wing Nodal Accel.	WS175	Statham	A43-4-350	350	70	± 1g	± 2g	.0036g	±.1%
9	Indicated Airspeed	Gust Probe	Statham	PL283TC-1-350	722	3500	0-1.0 psi	0-200K	.164K	±.1%
10	Pressure Altitude	A/C Nose	Rosemount	80085A4	101	2.5*	0-4.0 lb	32-30Kft	26.5 ft	±.02475
11	Total Temperature	A/C Nose	Lockheed	PT210F-17	-	1.3*	±250°F	±100°F	.20°F	--
12	Pitch Angle	A/C Nose	Minn-Honey	JG7044A0	M-169	10	±85°	-5, +10°	.011°	--
13	Roll Angle	A/C Nose	Minn-Honey	JG7044A0	M-169	10	360°	±20°	.035°	--
14	Yaw Angle	A/C Nose	Minn-Honey	JG7044	-	10	360°	±10°	.017°	--
15	Pitch Rate	A/C Nose	Humphrey	RC02-C501-1	AF50-H24	10	60°/sec	±20°/sec	.031°/sec	--
16	Roll Rate	A/C Nose	Humphrey	RC02-C501-1	AF50-H24	10	50°/sec	±30°/sec	.051°/sec	--
17	Yaw Rate	A/C Nose	Humphrey	RC02-C501-1	AF50-H24	10	60°/sec	±10°/sec	.017°/sec	--
18	L. Aileron Position	Left Wing	Spectrol	100STD	-	-	±15°	±15°	.025°	--
19	Elevator Position	Tail	Spectrol	100STD	-	-	-25, +30°	-25, +30°	.037°	--
20	Rudder Position	Thill	Spectrol	100STD	-	-	±30°	±30°	.083°	--

* 1 ÷ 5 x time constant

patible with the strain controlled oscillators, all of the transducers except the altimeter³ utilize resistance type strain gages or variable resistance type pickups. The location of the transducers and related measuring equipment is shown on the aircraft planview in Figure 7. Installation photographs of the significant items of aircraft instrumentation appear in Figures 8 through 12.

Strain Controlled Oscillators. These oscillators use a resistance bridge (of which the transducer is the main element) as source of signal voltage which linearly shifts the frequency of the oscillator. The magnitude and direction of the frequency shift is proportional to the magnitude and direction of the resistive unbalance produced by the transducer. Thus the measured quantity modulates the oscillator frequency signal which is then recorded on tape.

The oscillators are G.F.E. Bendix-Pacific Models TOR-7 of 1956 manufacture⁴. Four of the five subcarrier frequencies used are changed slightly from the standard IRIG values as indicated in Table II below.

TABLE II. SUBCARRIER FREQUENCIES

(1)	(2)	(3)	(4)	(5)	(6)
Band	IRIG (cps)	HICAT Recording (cps)	XL7.5 HICAT Playback (cps)	IRIG (cps)	Band
4	960	829	14,500	14,500	13
5	1300	1257	22,000	22,000	14
6	1700	1714	30,000	30,000	15
7	2300	2286	40,000	40,000	16
8	3000	3000	52,000	52,000	17

The frequencies in column 3 are selected in place of the IRIG standard in column 2 in order to permit playback of the flight data on the ground at 17.5 times the record speed or 30 in/sec. At this speed the data appear at standard IRIG frequencies corresponding to bands 13 through 17 as shown in the last three columns of the table.

The strain controlled oscillators are installed on the lower hatch. They are just discernible in the center of Figure 12.

3 The altimeter transducer is a variable capacitance type device and comes equipped with its own oscillator.

4 Although replaced in most modern FM systems by the low level voltage controlled oscillator, the SCO's performed adequately during the HICAT tests. Standard deviation of center frequency and change in sensitivity during a given test was generally less than 2% of the bandwidth.

Airborne Recorder. The airborne recording is done with an Ampex AR 200 magnetic tape recorder equipped with a 1-inch 1 $\frac{1}{4}$ -track analog head. By placing several channels of data on each tape track, only 8 tracks are required to record all the HICAT data including the various timing and control signals and the pilot's voice. Figure 10 shows the recorder installed in the upper part of the aircraft equipment bay.

To accommodate the speed scaling described above (tape record speed/tape playback speed = 1/17.5), the recorder is modified to operate at 1-5/7 in/sec instead of the standard 1-7/8 in/sec. By this means a 7-hour flight recording capability is obtained with 1 mil tape. At the same time, the capability for rapid playback of the data at the standard tape speed of 30 in/sec is provided.

Time Code Generator. The primary function of the time code generator is to provide time base reference signals for the recorded data. For this purpose two time codes are recorded simultaneously with the test data. The codes used are IRIG B and C.

IRIG B provides the basic time reference used when converting the FM analog tape to a digital computer compatible tape. IRIG B time is resolved to the millisecond and carries year, day, hour, minute, and second information.

When playing back the data to make the "Quick-Look" oscillograph record, the tape speed is normally increased by a factor of 17.5 over the record speed. At this speed the IRIG B code is too compressed to be legible on the oscillograph record. Consequently, the slower IRIG C code furnishes the oscillograph time reference.

The time code generator also provides two reference signals to enable errors in playback speed to be corrected. These are the capstan control signal and the wow and flutter or tape speed compensation signal. Finally, the time code generator supplies the tape recorder motor drive frequency.

The necessity for providing these last three signals (normally supplied by the tape recorder electronics) is the non-standard 1-5/7 in/sec record speed which is in turn governed by the 17.5 to 1 speed scaling requirement to conform to the IRIG standards of the van and the ground digitizing station.

All the time code generator signals are derived by means of flip-flop count down circuits from one source, a 750,000 cps crystal controlled oscillator. Figure 11 shows the time code generator installed in the upper forward part of the aircraft equipment bay.

Calibrator. The calibrator or transducer simulator, when actuated by the pilot, replaces each transducer with a Wheatstone bridge circuit of fixed resistance and then sequentially shunts a calibrate resistor across adjacent legs of the bridge. In this way a stable center band reference level signal and upper and lower band edge reference signals are obtained. These calibrate signals then provide a direct measure of the center frequency drift and sensitivity change of the strain controlled oscillators.

Mobile Data Systems Van

The HICAT Mobile Data Systems Van is a specially equipped Fruehauf trailer, Figure 13. The equipment in the MDS Van used during the normal playback function consists of a tape reproducer, amplifiers, subcarrier discriminators and analog oscillograph recorder (see Figures 14 and 15). Tape speed corrections are provided by a wow and flutter compensation system. A block diagram of the Mobile Data Systems Van is shown in Figure 16. A detailed description of the system components appears below.

Magnetic Tape Reproducer. The magnetic tape reproducer is a Consolidated Electrodynamics Corporation Model 5-752. The transport can be operated at 1-7/8, 3-3/4, 7-1/2, 15, 30 and 60 inches per second and has 1-inch heads installed. Normal HICAT playback operations are performed at 30 inches per second or 17.5 times record speed. Electronics to play back 8 tracks simultaneously are available and are used to reproduce the 6 tracks of data, 1 track of time and 1 track of voice. The voice track is not normally readable due to the increased playback speed but the presence of voice activity is observable.

Amplifiers. The tape reproducer output is passed through MacIntosh MC-30 or MC-40 high fidelity amplifiers to insure a proper impedance match and drive level to the following circuits. The amplifiers are low distortion, high power gain devices providing 30 and 40 watts drive capability.

Subcarrier Discriminators. Twenty-four Electromagnetic Research Model 67 subcarrier discriminators are installed in the Van to process the data. These devices select the subcarrier band of the tape track and convert the frequency modulated data to voltage data. In addition to channel selection, the discriminator controls provide for adjustment of the gain (volts per cycle per second), zero balance and zero signal level. The output filter characteristic is selectable. For HICAT the output filters have a corner frequency of about 17/4 cps equivalent to 174/17.5 or about 10 cps in real time.

Tape Speed Compensation System. Two Electromagnetic Research Model 96F tape speed compensation systems each having 12 channels capability provide a correction signal for tape speed wow and flutter. This system eliminates more than 97% of the wow and flutter errors over the system bandwidth and thus makes practical the slow record speed and subsequent speed scaling.

Recording Oscillograph. The output signal is fed to a Consolidated Electrodynamics Corporation Model 5-119-P3 oscillograph using 32 C.E.C. 7-319 galvanometers for data signals and 4 C.E.C. 7-316 galvanometers for the timing signals (see Figure 15). The data galvanometers have an undamped natural frequency of 585 cps and when damped are flat to 350 cps. This latter frequency corresponds to about 20 cps in real time for the data and represents the upper limit of the data system bandwidth (i.e., for all practical purposes, signal frequencies higher than 20 cps are completely eliminated by the low pass output filters of the discriminators).

The oscillograph is equipped with a C.E.C. Datarite Magazine Type 5-036 which develops the flight record almost instantaneously and provides the dry "Quick-Look" oscillogram ready for evaluation.

Accessory Test Equipment. In addition to the above main line elements of the Van data system, several items of test equipment and minor components are required to complete the operating system. Patching, switching and controlling circuits are provided to route data and test signals to the discriminators, establish specific programmed run connections, and provide for rapid connection of test equipment for trouble shooting.

A rack of test equipment including a counter, an oscilloscope, a voltmeter and two oscillators fulfill most of the Van and some of the aircraft trouble shooting requirements.

Portable test equipment consisting of a voltmeter, two harmonic analyzers, two frequency counters, and an oscilloscope complete the trouble shooting equipment needs for the aircraft and provide the electronics to perform pre- and post-flight calibration and time setting.

Ground Station

The FM analog tapes were processed at the Edwards Air Force Base Aerospace Data Systems Branch ground station. The conversion process is illustrated in the block diagram in Figure 17.

Upon playback, the multiplexed signals from the six data tracks were routed to discriminators where the subcarrier signals were separated and d.c. voltage signals proportional to the output of the transducers in the HICAT aircraft were recovered. The d.c. voltage signals were then fed into the analog-to-digital (A/D) converter where the data were sampled and converted to an eleven bit binary word through a convergent process of successive comparisons of the sample amplitude with precise reference voltages. The range of the eleven bit binary words in decimal mode is ± 1024 counts providing maximum resolution of 1 part in 2040. Signals from the time code track are also read during playback and serve as control input for the sampling rate of the A/D converter. The sampling rate used throughout the program was 40 samples per second. The function of the output control is to serve as a buffer (temporary storage) for the incoming binary data words and the decoded time words, provide computer compatible output formatting for the information in storage, and have capability for writing this information on half inch digital tape.

Calibration of the sampled data on the digital tape was performed on the IBM 7094 computer under the control of RAFF FM Calibration Program. The calibrated data in engineering units was output in a binary time frame format on a standard half inch digital tape. Each data frame consists of the time of day with the sampled data for each of the twenty parameters recorded at that time.

SECTION III
DATA ACQUISITION

HICAT SEARCHES

A general requirement of the HICAT data acquisition phase is that turbulence data be accumulated during different seasons of the year and over varying geographical terrain. In the HICAT program to date, flights have been conducted from Edwards Air Force Base, California; Patrick Air Force Base, Florida; and Ramey Air Force Base, Puerto Rico. The flights from Edwards covered large portions of California, Nevada and Arizona. Those from Patrick passed over Florida, Georgia, South Carolina and the Bahama Islands. The Ramey based flights were over the West Indies area and the Caribbean Sea.

The U-2 HICAT flights were carried out by pilots of the Edwards Air Force Base Special Projects Branch of Flight Test Operations under the command of Lt. Col. Harry Andonian. As indicated by the Flight Log in Appendix II, Col. Andonian, Capt. R. B. Lowell, and Capt. W. H. Shawler together made 33 HICAT test flights totaling 94.7 flight hours. Eighteen of these flights were planned searches for high CAT and 14 of the 18 resulted in CAT encounters of light to moderate roughness. In addition, high CAT was penetrated in three of the 15 incidental flight tests. These were aircraft check flights, instrumentation check flights, and ferry flights. Overall, 7.4 hours of high CAT was recorded, 6.1 of them coming from planned searches based on CAT forecasts.

Track maps of the HICAT flights are included in Appendix II with the flight log.

In ideal circumstances, a preparation for a HICAT search flight begins a day or two before the aircraft actually flies. At this time the developing weather trends are studied to determine if conditions are likely to be favorable for CAT and a decision is made as to whether support aircraft will be needed.

HICAT FLIGHT DESCRIPTION

HICAT support aircraft were of two types. A B-47 was frequently used as a low altitude turbulence scout and to furnish navigational support to the U-2. For overwater flights, a C-54 Air Rescue transport patrolled near the HICAT search area to provide immediate aid in event of a mishap.

On the day of the HICAT flight (assuming conditions are still favorable) a flight plan is prepared and the pilot briefed on high CAT conditions and any special flight tests to be performed. Meanwhile, the aircraft is preflighted in the hangar. The instrumentation is checked and then the time code generator is turned on and the time set in. The aircraft is then towed to the takeoff point on the runway.

The pilot arrives, garbed in his high altitude pressure suit, and climbs aboard. He has prepared for the HICAT flight by breathing pure oxygen for an hour or more prior to takeoff to eliminate nitrogen from his blood.

The engine is started and all test instrumentation comes on, including the tape recorder. The aircraft takes off and climbs to above 50,000 feet and flies to predicted or suspected areas of turbulence. By monitoring his c.g.

accelerometer, the pilot can readily evaluate the intensity of any rough air. If significant ($+ .1g$ or better) turbulence is encountered, the aircraft maneuvers so as to define the turbulent area. Fairly level straight runs are then made through the turbulence. When not in turbulence, control pulses as well as occasional smooth symmetric pitch maneuvers or rollercoasters are performed to check the instrumentation. The average HICAT flight lasts about three hours.

Upon returning from a CAT search, the aircraft is towed to the hangar for postflight instrumentation procedures and checks. The pilot is debriefed and the "Quick-Look" oscillograph record examined to evaluate the turbulence penetrated as well as for evidence of instrument malfunctions. Maximum and minimum turbulence accelerations and equivalent derived gust velocities are determined at this time for comparison with the pilot's report.

SECTION IV

DATA PROCESSING AND ANALYSIS METHODS

GENERAL

The main purpose of the HICAT data processing and analysis is to statistically define the essential characteristics of high altitude clear air turbulence in a manner useful to the aircraft structural designer. Secondly, the analysis will attempt to correlate the turbulence measurements with significant geophysical and meteorological factors.

The first step in processing of the digitized data after it is reformatted is numerical filtering. This filtering process further improves that already performed electronically and completely eliminates frequencies greater than 10 cps. Corrected gust velocities are then computed utilizing the equations shown in Appendix II and plotted in graphical form along with the other flight parameters (i.e., airspeed, altitude, temperature, Mach number, c.g. acceleration, etc.).

Because of the apparently random character of atmospheric turbulence, statistical methods of analysis are employed. These consist primarily of peak counts of the gust velocity time histories and computations of gust velocity power spectra.

PEAK COUNTING

This program counts and classifies into pre-established positive and negative intervals the maxima or minima (peaks) in a set of discrete time data points such as could be obtained from a gust velocity time history. A peak is defined as the maximum or minimum value between two intersections of a certain narrow band. For most of the peak counts contained herein, this band was the mean value of all the data plus and minus .1 of the smallest peak count interval.

Individual peak count plots are obtained by an accumulation process wherein

all the positive and negative peaks within a velocity or acceleration interval are first added together and then summed over all intervals beginning with the largest velocities or accelerations. In this way a cumulative peak count distribution is obtained. By dividing by the total number of miles in the turbulence sample, the distribution becomes an estimate of the frequency of equaling or exceeding a given velocity or acceleration level per mile of flight, e.g., see Figures 24 through 34.

POWER SPECTRA ANALYSIS

This method of analysis involves the mean-square value of a function and has by electrical analogy come to be considered in terms of average power. The power spectrum or power spectral density of a function (e.g., a gust velocity time history) describes the manner in which the total average power of the function (velocity amplitude squared/cycles per second) is distributed over the frequency range of interest. In essence it provides a statistical measure of the mean square amplitude of a measurement for each of a number of narrow but discrete frequency bands. The square root of the sum of all these values over the frequency range of the spectrum gives the RMS value of the spectrum data.

Normally, power spectra from uniform time series data are computed and plotted as a function of cycles per second or radians per second. However, in turbulence work it is desirable to interpret the cycles per second in terms of wavelengths in feet or inverse wavelength in cycles/foot. Thus, to obtain the ordinates of the spectra in cycles/foot requires dividing by the aircraft speed in ft/sec. The average true airspeed of the aircraft was the value used for the spectra appearing in Figures 36 through 68.

Further description of the HICAT data processing and analysis methods is contained in Reference 5.

SECTION V

INTERIM RESULTS

The results acquired in the HICAT program thus far include time histories, peak counts, and power spectra of gust velocities and related flight parameters. A summary of HICAT data processed and analyzed to date is presented in Table III.

TIME HISTORIES

Time histories were plotted of all the data for which gust velocities and gust velocity spectra could be determined.⁵ For this purpose, turbulence

⁵ Longitudinal gust velocities were not computed because of the frequency response limitations of the pitot-tube.

TABLE III
HICAT DATA SUMMARY

TEST NO.	DATE	AIR FORCE BASE	RUN NO.	START TIME* (Hr:Min:Sec)	RUN LENGTH (Sec.)	ALTITUDE (1000 Ft)	MAX. Δ ACCEL. (g)	MAX Δ U _v ** (Ft/Sec)	RMS U _v ** (Ft/Sec)
7	4-3-64	Edwards	1	21:53:25	300	61.8	-0.33	-5.9	--
8	4-10-64	Edwards	1	19:55:00	240	60.8	+0.22	+3.9	--
		Edwards	2	20:15:25	110	50.4	+0.28	+4.8	--
10	4-21-64	Edwards	2	19:44:21	239	69.6	+0.16	+2.6	--
26	7-1-64	Ramey	1	16:48:20	120	53.2	-0.55	-8.6	--
		Ramey	2	16:52:30	240	53.6	+0.70	+10.0	--
		Ramey	3	17:04:35	120	53.0	+0.31	+4.1	--
27	7-2-64	Ramey	1	16:37:40	170	60.0	+0.31	+4.4	--
		Ramey	2	17:14:38	220	59.0	+0.21	+3.0	--
28	7-6-64	Ramey	2	17:19:50	240	55.6	+0.36	+4.9	1.62
		Ramey	3	17:23:50	239	55.3	+0.22	+3.1	1.53
30	7-15-64	Ramey	3	16:09:35	240	52.0	+0.87	+11.3	3.70
		Ramey	4	16:38:30	240	52.4	+0.80	+10.4	1.90
33	10-29-64	Edwards	1	21:17:20	180	57.4	-0.35	-5.2	1.77
		Edwards	3	22:20:50	180	56.8	+1.10	+16.7	3.70
		Edwards	4	22:25:40	240	56.5	-0.65	-11.3	4.14
		Edwards	5	22:30:00	240	56.4	+0.60	+10.0	3.45
		Edwards	6	22:34:00	120	56.5	-0.56	-9.6	3.51
		Edwards	7	22:36:00	240	56.7	+0.61	+11.1	3.44

* Greenwich Time

** Truncated RMS Vertical Gust Velocities for Wavelengths 70 - 2500 Feet.

test data were divided into runs or samples of two to four minutes duration. The run time histories were used primarily to evaluate the quality of the data after digitizing and filtering and to check the gust velocity and peak count calculations. In general, the turbulence data samples selected appeared to be random and fairly continuous with no obvious periodicity or discrete gust peaks. The data also appeared to be sensibly stationary.

A two-minute sample time history selected from a run 3 of test 33 is shown in Figures 18 through 23. The data plotted include vertical gust velocity, c.g. normal acceleration, left wing nodal acceleration, derived equivalent gust velocity (U_{de}), and aircraft equivalent velocity (V_e). In the gust velocity time history shown, frequencies less than .2 cps and greater than 10 cps were removed by numerical filtering. Removal of the very low frequencies was required because of inherent limitations of the instrumentation.⁶

PEAK COUNTS

Figure 24 presents actual gust velocity peak count data in terms of frequency of exceedance per mile of a given value of vertical gust velocity. Since these data are the first of their kind at high altitude, no data are available for comparison except the runs shown. Comparison of the true gust velocities with derived equivalent gust velocities (U_{de}) is meaningless. A true gust velocity describes an atmospheric condition directly. A U_{de} on the other hand is a very indirect atmospheric description derived from an aircraft's c.g. acceleration experience utilizing simple but frequently inapplicable assumptions (see Appendix IV). The U_{de} concept has been utilized in years past for lack of actual gust velocity data and the analytical methods to use them.

Figures 25 through 33 present frequency of exceedance plots of U_{de} and c.g. normal accelerations. The accelerations data have been included to give a direct measure of aircraft response as well as to indicate approximately what the pilot feels.

The HICAT U_{de} data may be properly interpreted provided the following distinction is made. The HICAT data were obtained in flights made for the express purpose of encountering and continuously sampling turbulence above 50,000 feet. Consequently, all miles in the HICAT U_{de} plots are turbulent miles. However, the only U_{de} data available for comparison come from NASA TN D-548, reference 2. In reference 2, the turbulence described was encountered in non-random flights made for other purposes than to collect turbulence data. Consequently, the cumulative frequency curves of U_{de} contained therein are based upon total flight miles of which only a small percentage were turbulent.

Figure 34 presents the cumulative frequency data from reference 2 compared with the HICAT data from test 33. HICAT test 33 was selected for comparison for two reasons: (1) measured c.g. accelerations, and hence U_{de} values, were among the highest recorded to date, and (2) terrain and associated "mountain

⁶ This is not expected to be necessary in the redirected HICAT program because appropriate precision instrumentation will be available.

wave" turbulence are believed to be very similar to some of the Japanese data of reference 2.

The HICAT data shown at the top of Figure 34 are based only upon the length in miles of the total turbulence sample. By including all the miles above 50,000 feet on test 33, nonturbulent as well as turbulent, the curve may be shifted down as shown.

Note that these two HICAT curves differ by an order of magnitude indicating that for test 33 the aircraft was in turbulence about 10% of the time. The data at the bottom of the figure is for routine reference 2 flights in which turbulence was encountered about 2% of the time. The difference between the 10% and the 2% turbulence reflects directly the type of missions being flown.

Note that the adjusted HICAT U_{de} data most closely approach the data from the relatively severe turbulence encountered over Japan. Reference 2 indicates that two flights, CW-58-2 and CW-58-4, are responsible for most of the U_{de} peaks. These two flights include about 9% of the total miles flown in the Japanese area, yet they contribute more than 20% of the turbulence miles. Most significant of all, they contribute 90% of the data above 4 ft/sec and all the data above 10 ft/sec. By assuming as is very nearly the case that these two flights comprise all the significant turbulence experience over Japan, the cumulative frequency curve for the Japanese data will shift upwards by an order of magnitude. On this basis, the data are comparable to the HICAT data and in fact are seen to be nearly coincident with them.

Figure 35 presents the variation of U_{de} with altitude presently used in design of military aircraft (see reference 6). Superimposed on this figure are U_{de} data points obtained in various HICAT flights. Note that in approximately 24,000 miles of flight in HICAT searches, the design values between 50,000 and 60,000 feet have not been exceeded. Thus far, a significant margin exists between the highest recorded U_{de} and the design value in this altitude band. More data samples will be required to permit further generalization.

POWER SPECTRA

Power spectra of vertical gust velocities are presented along with power spectra of $V_T \Delta \alpha$ and $V_T \Delta \beta$ in Figures 36 through 68. The grouping of the spectra is by ascending test number.

The $V_T \Delta \alpha$ and $V_T \Delta \beta$ referred to above represent, respectively, the product of true airspeed and incremental angle-of-attack and true airspeed and sideslip angle. They are the uncorrected vertical and lateral gust velocity components. For frequencies above those to which the aircraft responds (i.e., about 2 cps corresponding to wavelengths of about 1/.003 or 330 feet) spectra of these quantities are accurate representations of gust velocity power. Below the frequency limit mentioned, correction is required for aircraft translation and rotation.

This correction could not be applied to the lateral gust measurements and to some of the vertical gust measurements due to malfunctioning rate and attitude gyros. Consequently, only uncorrected lateral gust velocity ($V_T \Delta \beta$) spectra are shown with (in most cases) both corrected and uncorrected vertical gust velocity spectra included for comparison.

The power spectra tables are somewhat abbreviated and require explanation. The first three digits after "Test" are the test number. The fourth digit is the run number. The letter stands for the field test site, 'E' for Edwards AFB, 'P' for Patrick AFB, and 'R' for Ramey AFB. The "Start Time" is the moment the run began in hours, minutes, and seconds of Greenwich time. "Duration" or run length is in minutes and seconds. The "No. Lags" is the number of estimates comprising the spectrum. The "Time Incr." is the time between data samples in seconds. "No. Points" is the number of data samples. "Deg. Freedom" is the number of degrees of freedom in the data sample and is used to evaluate the statistical reliability of the spectrum.

For statistical reliability the "Deg. Freedom" should be large, preferably 100 or more. For 100 degrees of freedom one may say that four out of five times the measured spectrum is within $\pm 10\%$ of the "true" long term average spectrum.

Mathematically, the gust power spectrum is defined in terms of a scale of turbulence, L , a mean square gust velocity intensity, σ_w^2 , and an exponent describing the reduction in gust velocity power with increasing frequency (decreasing wavelength). The scale of turbulence is normally determined by the location of the bend in the low-frequency end of the spectrum. Unfortunately, the spectrum could not be defined accurately below .25 cps because of inherent limitations in the instrumentation system. Consequently, a scale of turbulence cannot be specified from the present data. However, it would appear the " L " is not less than the 2500-foot end point of the present spectra since little if any bend is visible.

Too few data samples are available to enable meaningful discussion of root mean square gust intensity, σ_w , except to indicate that the RMS values shown in the spectra and in the data summary are values obtained by integration of the truncated spectra without extrapolation to zero frequency.

Data available at much lower altitudes than the 50,000 plus feet HICAT flights indicate that the gust spectrum may have a constant negative slope at higher frequencies. Two commonly used analytical approximations for the spectral shapes at these altitudes are defined as follows:

1. Liepmann equation:

$$\phi(\Omega) = \frac{\sigma_w^2 L}{\pi} \frac{(1 + 3 \Omega^2 L^2)}{(1 + \Omega^2 L^2)^2}$$

2. Isotropic turbulence equation:

$$\phi(\Omega) = \frac{\sigma_w^2 L}{\pi} \frac{1 + 8/3 (1.339 \Omega L)^2}{[1 + (1.339 \Omega L)^2]^{11/16}}$$

These expressions predict high-frequency slopes (on a log-log plot) of -2 and -5/3 respectively. The HICAT data plotted in Figures 54 and 66, for example, tend to follow similar slopes, lying closer to -5/3 than to -2. The gust data

contain a typical amount of scatter such that an average, overall slope is not well defined. More data are required before reliable average slopes can be determined.

SECTION VI

METEOROLOGICAL ASPECTS

The meteorological aspects of the HICAT program are basically threefold:

1. Selection of HICAT sampling sites.
2. Forecasting rough air in the site area and establishing flight plans.
3. Analysis and interpretation of data.

SAMPLING SITE SELECTION

Wind shear is the most important source of energy for the production and growth of atmospheric perturbations that cause rough air. Consequently, those regions having particularly high wind shears such as the jet streams would have the highest probability of also having rough air. The jet streams and the seasons considered optimum for encountering rough air are indicated below:

1. The mid-latitude (30° - 50°) jet that flows in the upper troposphere and lower stratosphere from west to east. This jet is strongest in the winter and accessible from Edwards AFB, California and Patrick AFB, Florida, for example.
2. The tropical jet that flows from east to west in upper stratosphere. This jet is accessible in the summer from Ramey AFB, Puerto Rico.
3. The polar night jet that flows from west to east over Alaska and Northern Canada in the upper stratosphere. The bottom of this jet would be accessible from Eielson AFB, Alaska.

Air flow and heating due to the varying characteristics of the underlying surface (i.e., ocean, mountains, plains, etc.) may cause perturbations in the troposphere and stratosphere under certain conditions of wind field and temperature structure. These perturbations may cause rough air or otherwise

⁷ The terms rough air and turbulence are often used interchangeably. However, in this section rough air refers to both the comparatively random turbulence oscillations as well as to the more regular oscillations identified as undulance.

modify the wind shear field. They can be investigated along with the jet stream phenomena from the sites indicated or from other sites in the areas described.

The above considerations were and continue to be the basis for HICAT site selection. As described in Section III, HICAT flights have thus far been conducted from Edwards AFB, Patrick AFB, and Ramey AFB. It is expected that the redirected and extended HICAT program will conduct additional flights from these bases as well as from Alaska and other untested areas.

FORECASTING

Forecasting is obviously important in order to improve the efficiency of locating and sampling the rough air. The basic forecast was provided by the Strategic Air Command. These forecasts were based on a numerical model that uses wind shear as the primary assessment for rough-air occurrence and intensity. Although this numerical model was developed for altitudes below 45,000 feet, it was the only method available at the start of the program.

This rough-air forecast was received from SAC Headquarters each afternoon at the field test site, i.e., Edwards AFB, Patrick AFB or Ramey AFB. Ideally, if the forecast was favorable for the occurrence of rough-air within range of the aircraft, the Officer in Charge was notified that the following day was favorable. If weather conditions still appeared favorable on checking the weather maps the following morning, a recommended flight pattern was established and the pilot briefed.

Several rough-air data gathering patterns were utilized. In this initial phase the basic objective was to sample as much rough air as possible and at the same time to cover as much area as practical in order to verify forecasts. In some cases where significant turbulence was encountered, a box or triangle pattern was flown at constant altitude in order to delineate the horizontal dimensions. In other cases where the rough air appeared to be associated with local features such as towering cumulus or mountains, several altitudes were sampled in order to determine not only the variation of rough air with altitude but also the variation of temperature with altitude.

ANALYSIS AND INTERPRETATION

The analysis and interpretation of the rough air data is concerned with developing physical and analytical models to relate the rough air characteristics to the meteorological and geophysical conditions. To assist in the evaluation of these relationships, each flight is plotted on a large scale aeronautical chart with contours to indicate major topographic features. The areas of rough air and smooth air are charted based upon the pilot's observation. These track maps appear in Appendix II. The meteorological data were provided by the Air Weather Service. These data consisted of the surface weather charts, 500 mb, 300 mb and where available, the 100 mb upper air constant pressure charts. In addition, the regular upper air wind and temperature data were provided for those stations near the flight track. Where available the upper air data used came from the USAF "listings" and from the rawinsonde records of Weather Bureau stations.

The "listings" are wind and temperature data that are automatically calculated

and printed from balloon runs. The Weather Bureau records consisted of form WRAN20 for winds and the original radiosonde recorder records for the temperatures. These records were used to determine the wind and temperature profiles in order to investigate the small scale details of the vertical atmospheric structure.

For reasons discussed in Section I, the "rough-air" data flights frequently could not be flown under meteorological conditions considered conducive to rough air, i.e., in vicinity of strong jet streams, and/or mountain wave activity. Nevertheless, a significant amount of light to moderate turbulence was encountered (6 hours in the searches and 7-1/2 hours overall). Examination of these data indicates that in the horizontal distribution of turbulence at least three categories of atmospheric activity are important:

1. Strong wind shear associated with jet streams (test 11).
2. Mountain wave activity (tests 7, 8 and 33).
3. Low level heating including convection.

In this latter category, tests 10, 12, 17-20, 23, 28-30 occurred above or near towering cumulus or cumulonimbus clouds in straight or anticyclonic flow. Tests 26 and 27 from Ramey AFB occurred over convective areas associated with easterly waves (cyclonic flow). On the other hand, tests 22, 24 and 25 occurred well away from visible low level convection yet in the same weather pattern.

In order to see if the occurrence of rough air over the Caribbean occurred under preferred conditions of wind shear and temperature change with height a 3 x 3 contingency or data classification table was prepared relating the two. The table indicated that most of the rough air occurrences were associated with near isothermal conditions or temperature definitely increasing with height. Less than 5% of the rough air occurred with temperature decreasing more than 1°C per thousand feet (3°C per 1000 feet is the adiabatic lapse rate). No clear-cut relation of rough air occurrence with wind shear was indicated. Approximately a fourth of the rough air occurred with wind shears less than one knot per thousand feet.

The lack of relationship between the wind shear, temperature change with height, and rough air occurrence cannot be explained at this time. It may simply be the result of attempting too detailed an analysis with wind and temperature observations not sufficiently close in time and distance to the rough air location. It is likely that some of the future HICAT searches will be conducted directly over weather observation stations to clarify this point.

Additional and more detailed analysis of the HICAT data from the meteorological standpoint is presented in reference 7 in conjunction with the "High Altitude Rough Air Model Study".

SECTION VII

CONCLUSIONS

It is not possible nor appropriate to present final conclusions at this juncture in the HICAT program. The major portion of the program is still ahead and many unknowns remain to be explored. However, certain observations can be made to summarize the results and accomplishments to date as follows:

1. A sensitive high altitude gust probe has been designed, developed, and combined with a 7-hour FM recording system to successfully measure turbulence velocities.
2. High CAT is relatively easy to locate. It was encountered in 14 of 18 HICAT searches at altitudes of 50,000 feet or more as well as in 3 of the 15 incidental flights.
3. High CAT encountered in the majority of flights appeared to be associated with low level (tropospheric) convective activity as indicated by swelling cumulus and cumulonimbus clouds.
4. The most severe turbulence encountered was associated with mountainous terrain and appeared to be of the "mountain wave" type. The NASA data of reference 2 appear to show a similar characteristic.
5. The vertical gust velocity power spectra thus far obtained indicate a scale of turbulence at altitudes above 50,000 feet in excess of 2500 feet.
6. Derived equivalent gust velocity (U_{d_g}) values obtained to date are well within the U_{d_g} design envelope specified by reference 6.

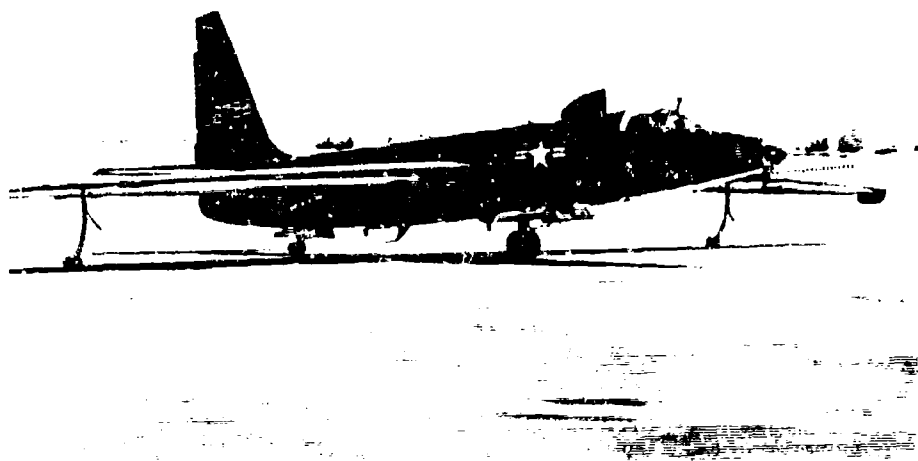


Figure 1. U-2 Aircraft Used For HICAT Searches

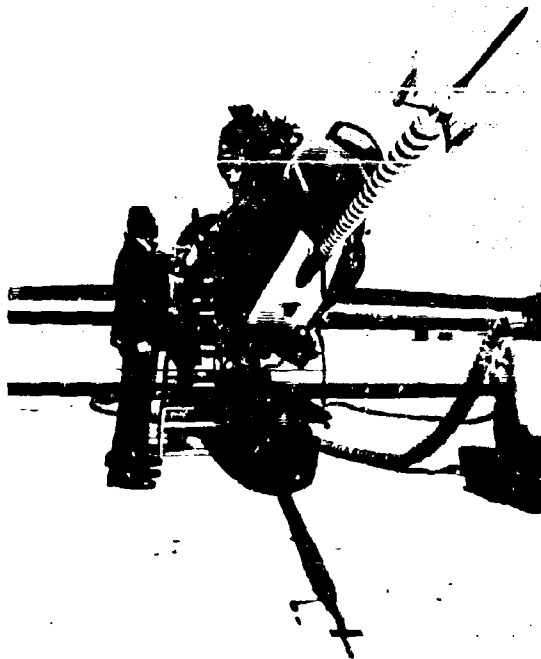


Figure 2. HICAT Gust Probe and Boom Installation on Nose of U-2

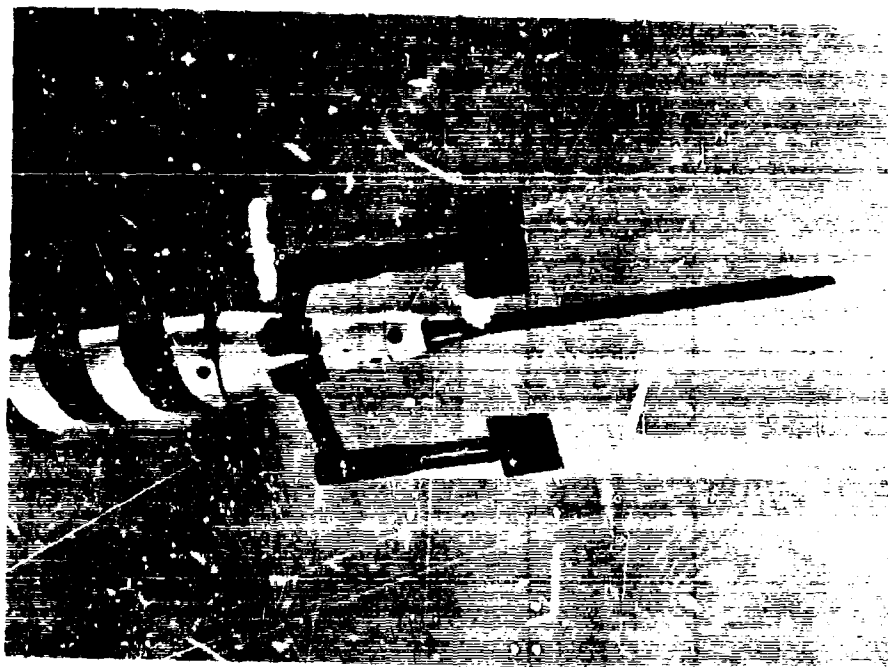


Figure 3. HICAT Gust Probe Closeup Showing Vertical and Lateral Gust Sensing Vanes and Air Force MA-1 Pitot-Static Tube

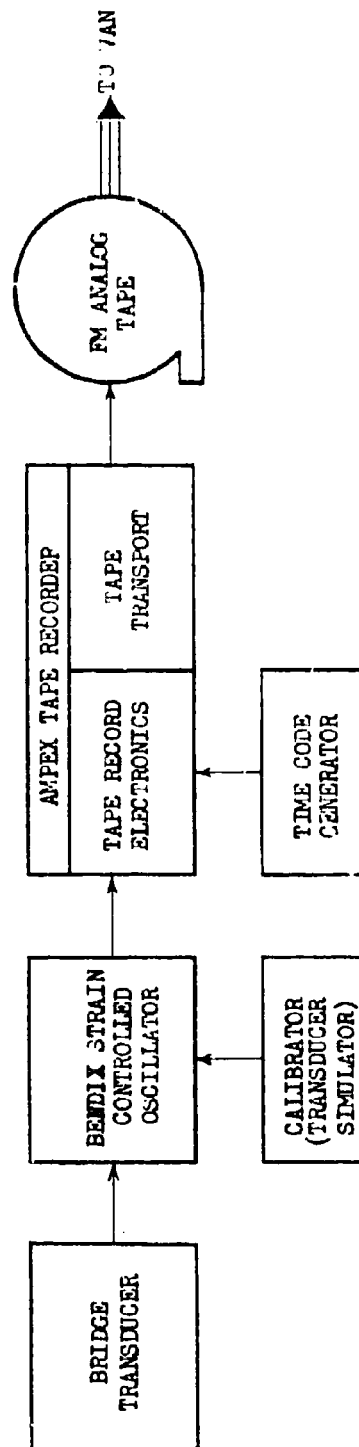


Figure 4. FICAT Data Acquisition System Block Diagram for Reference

Strain gage
circuit for
shear measurement

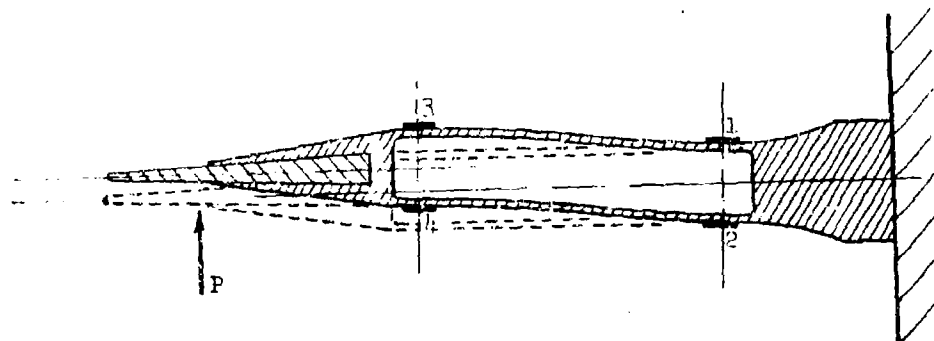
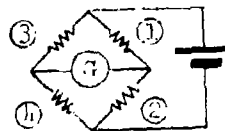


Figure 5. Double Beam Sensor With Strain Gage
Installation for Shear Measurement
(Sensor Shown Deflected Due to Airload)

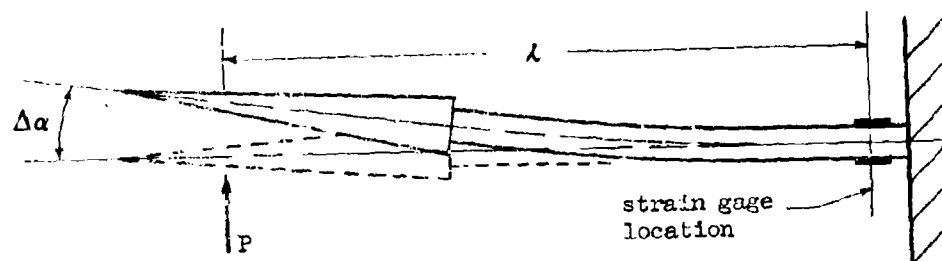


Figure 6. Angular Deflection of Simple Sensor

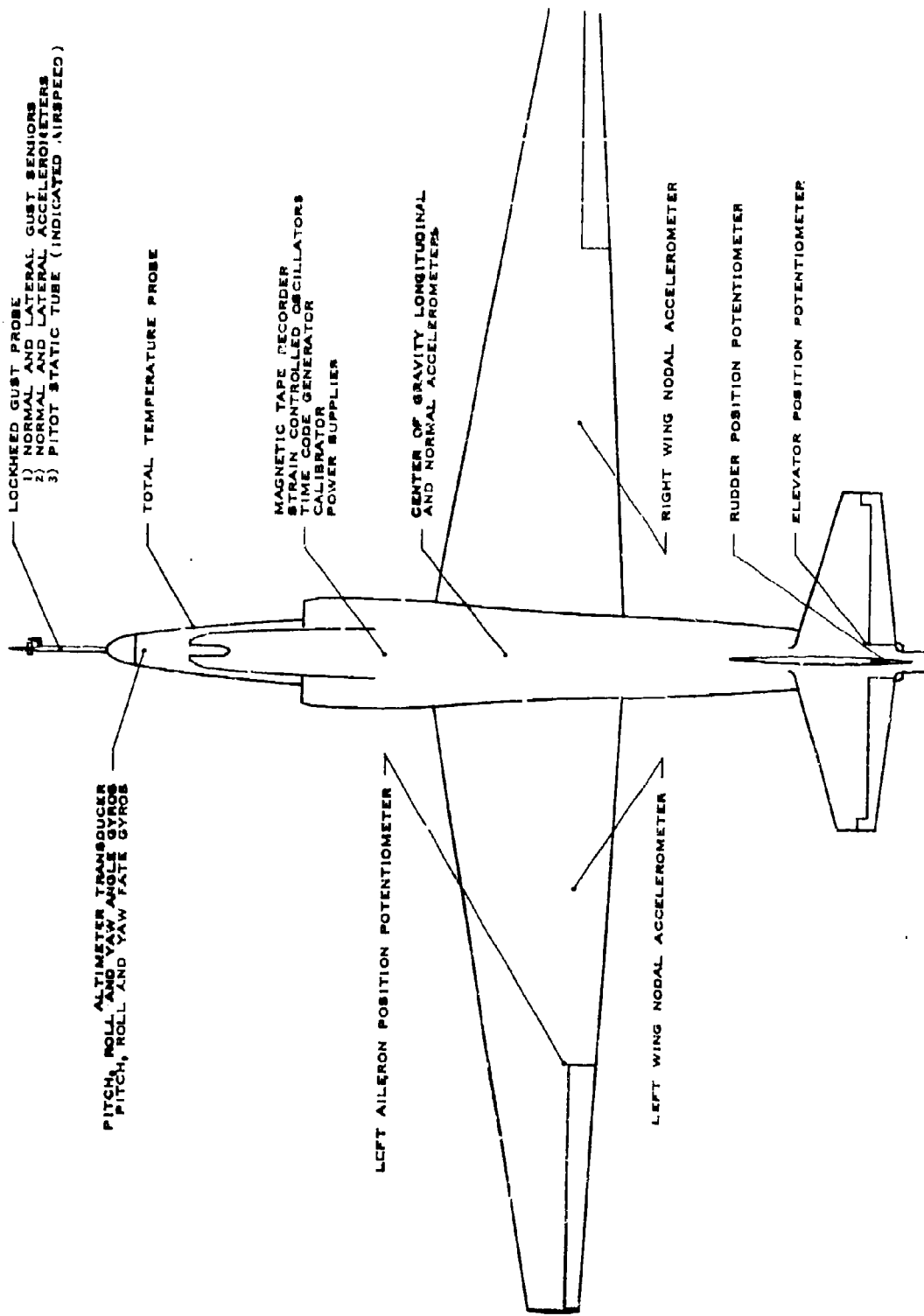


Figure 7. Aircraft Instrumentation Location Diagram



Figure 8. Pilot's Total Pressure Head and Nose Boom Attachment

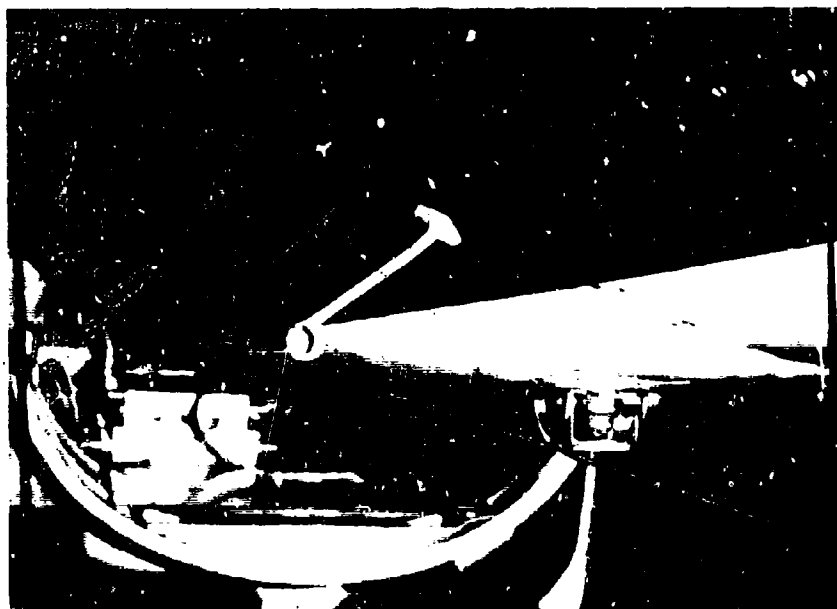


Figure 9. Total Temperature Sensor Installation on Nose of Aircraft

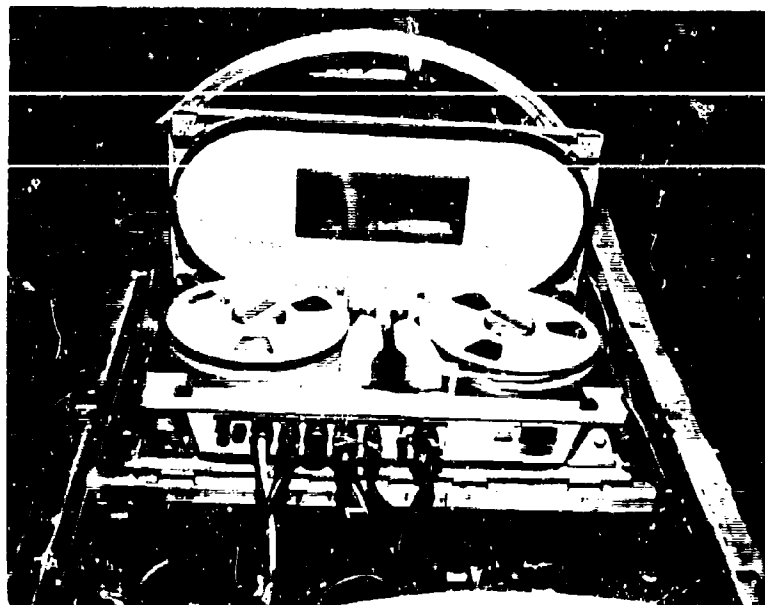


Figure 10. Magnetic Tape Recorder Installation in Equipment

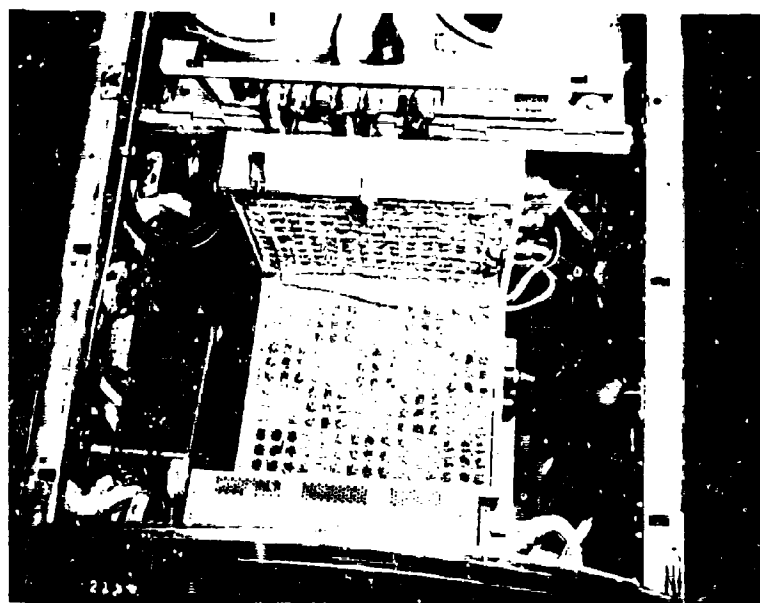


Figure 11. Time Code Generator Installation in Equipment Bay
(Upper Hatch Removed)



Figure 12. Instrumentation Installation on Lower Hatch of Equipment Bay

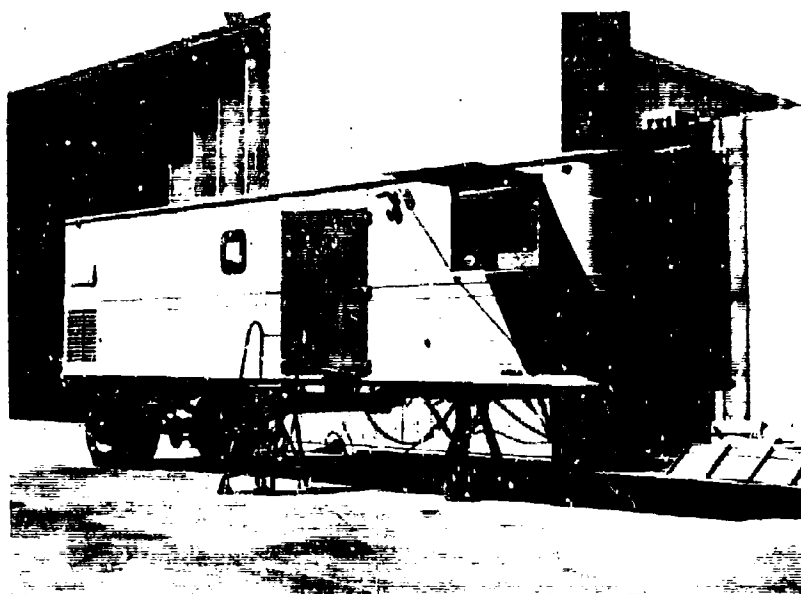


Figure 13. Mobile Data Systems Van



Figure 14. Van Instrumentation Showing Magnetic Tape Reproducer, Patch Panel, Electronic Test Equipment, and Subcarrier Discriminator Array



Figure 15. Van "Quick-Look" Oscillograph Recorder and Control Panel

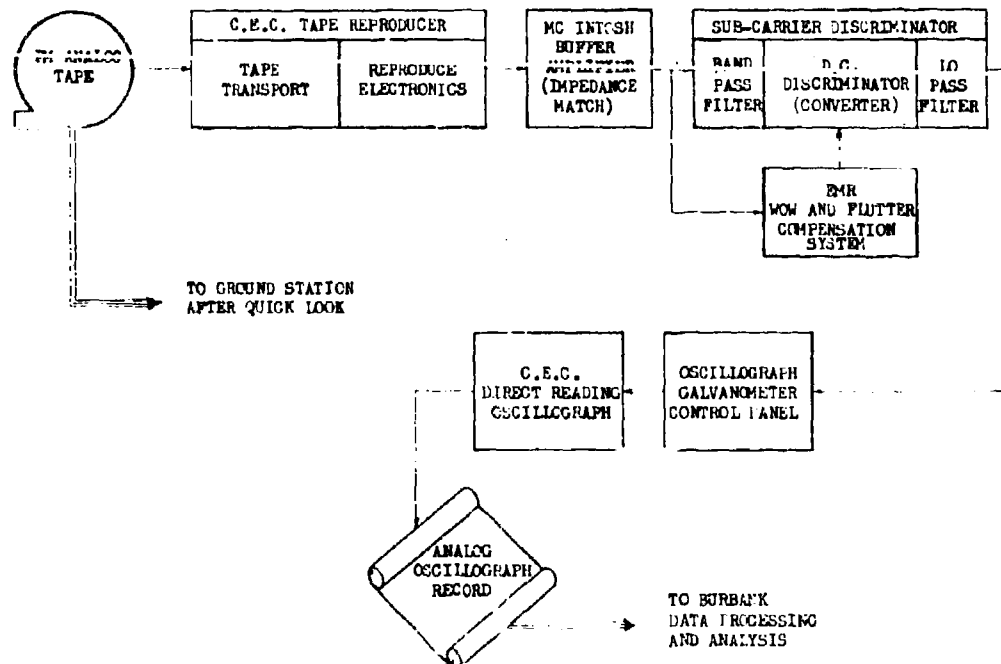


Figure 16. HICAT Data Acquisition System Block Diagram for the Mobile Data Systems Van

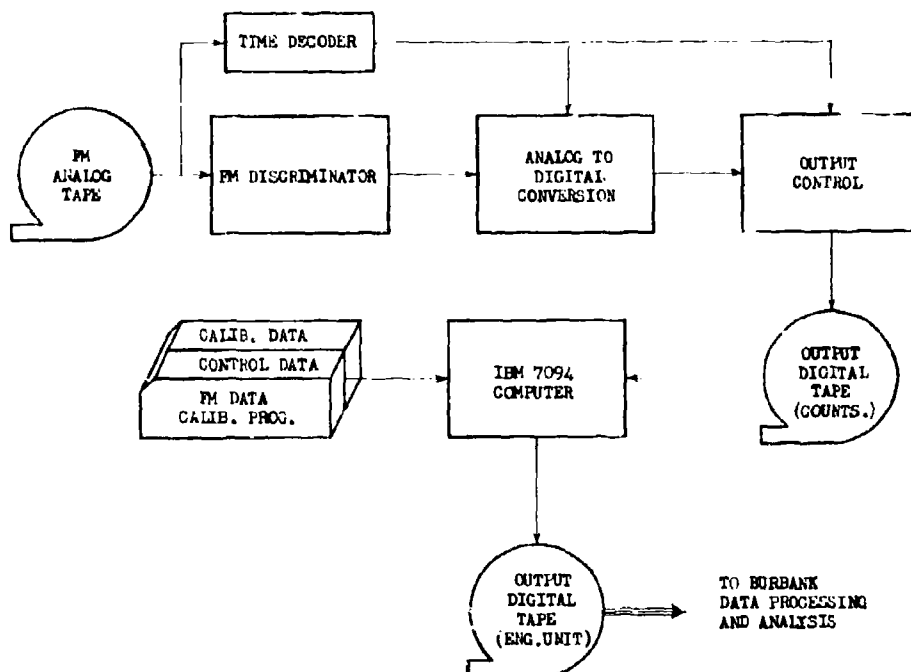


Figure 17. HICAT Data Acquisition System Block Diagram for the Ground Station

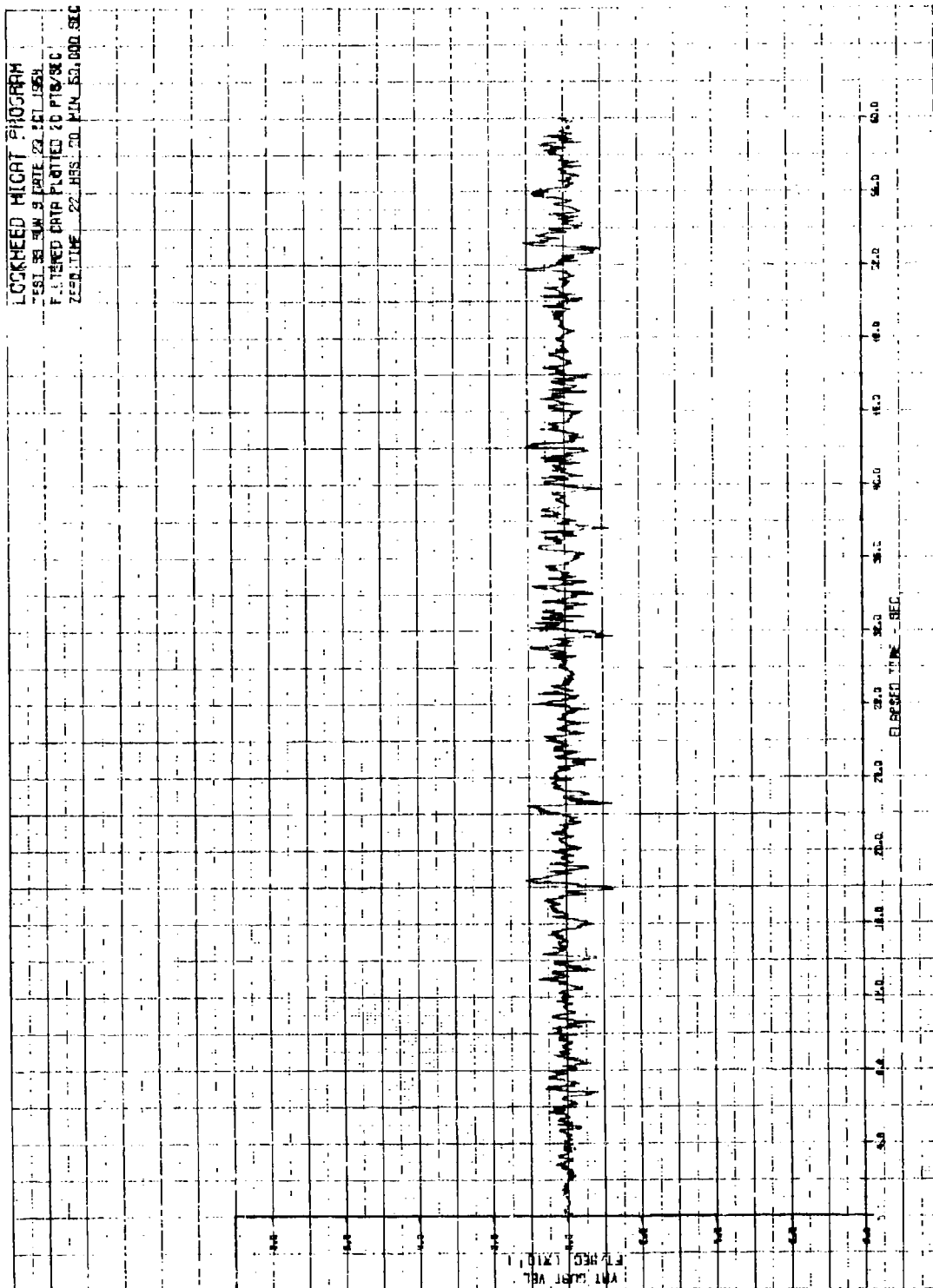


Figure 16. Time History of Vertical Gust Velocity.
 Test 33, Run 3, 0 - 60 Sec.

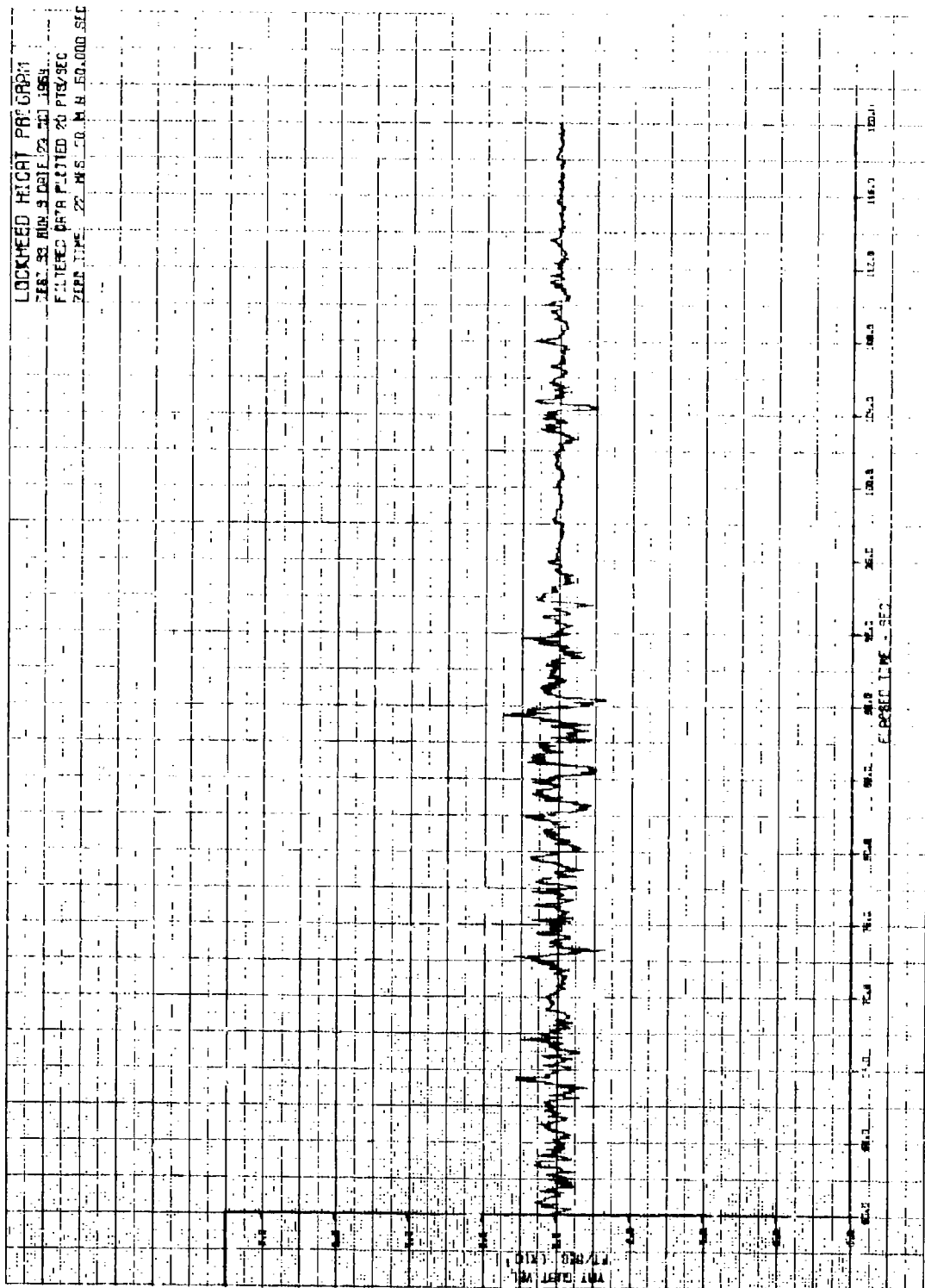


Figure 19. Time History of Vertical Gust Velocity. Test 33, Run 1, 6. - 12. Sec.

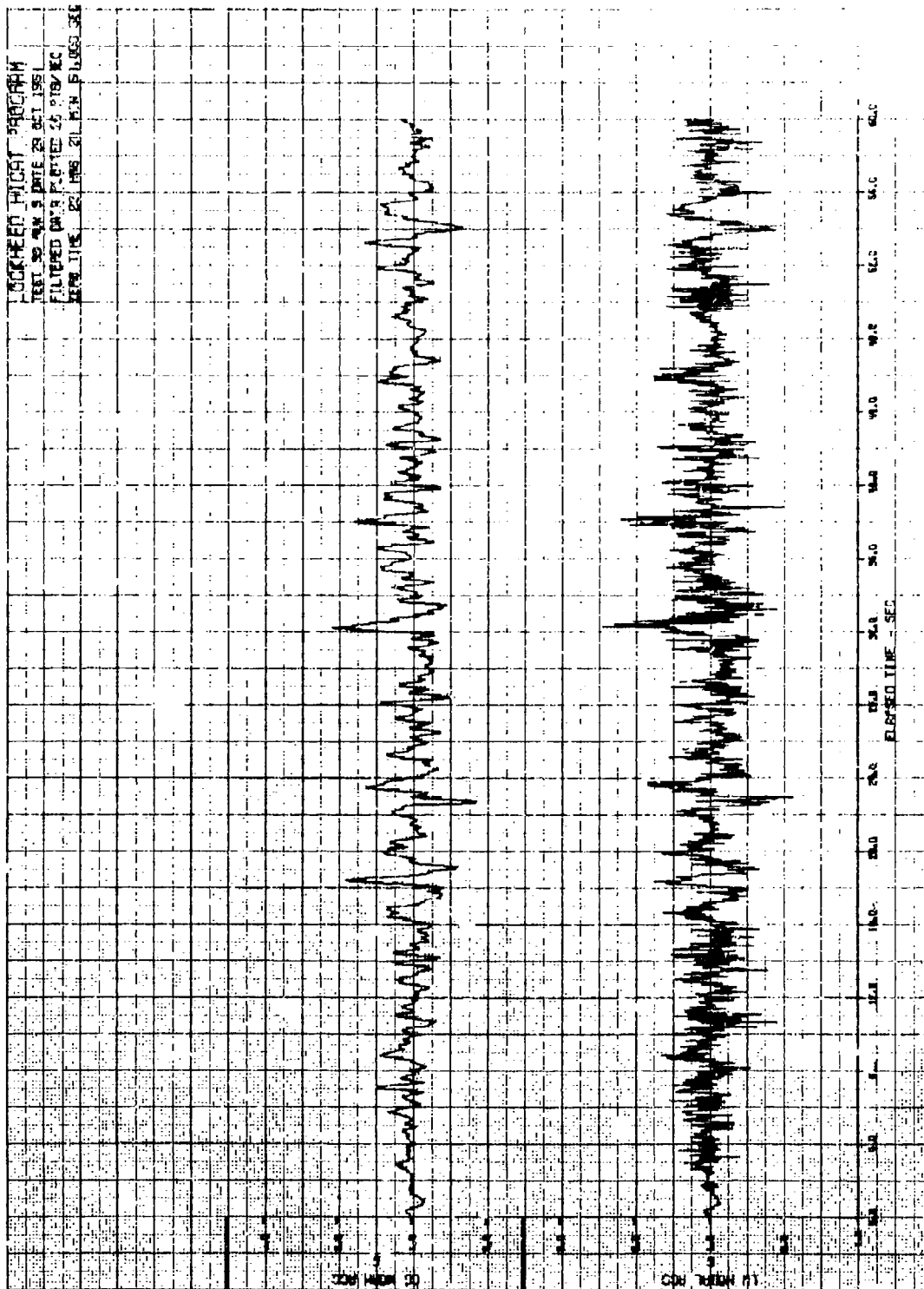


Figure 20. Time History of C.G. Normal Acceleration and Left Wing Root Bending Moment
 Test 33, Run 3. 0 - 60 Sec.

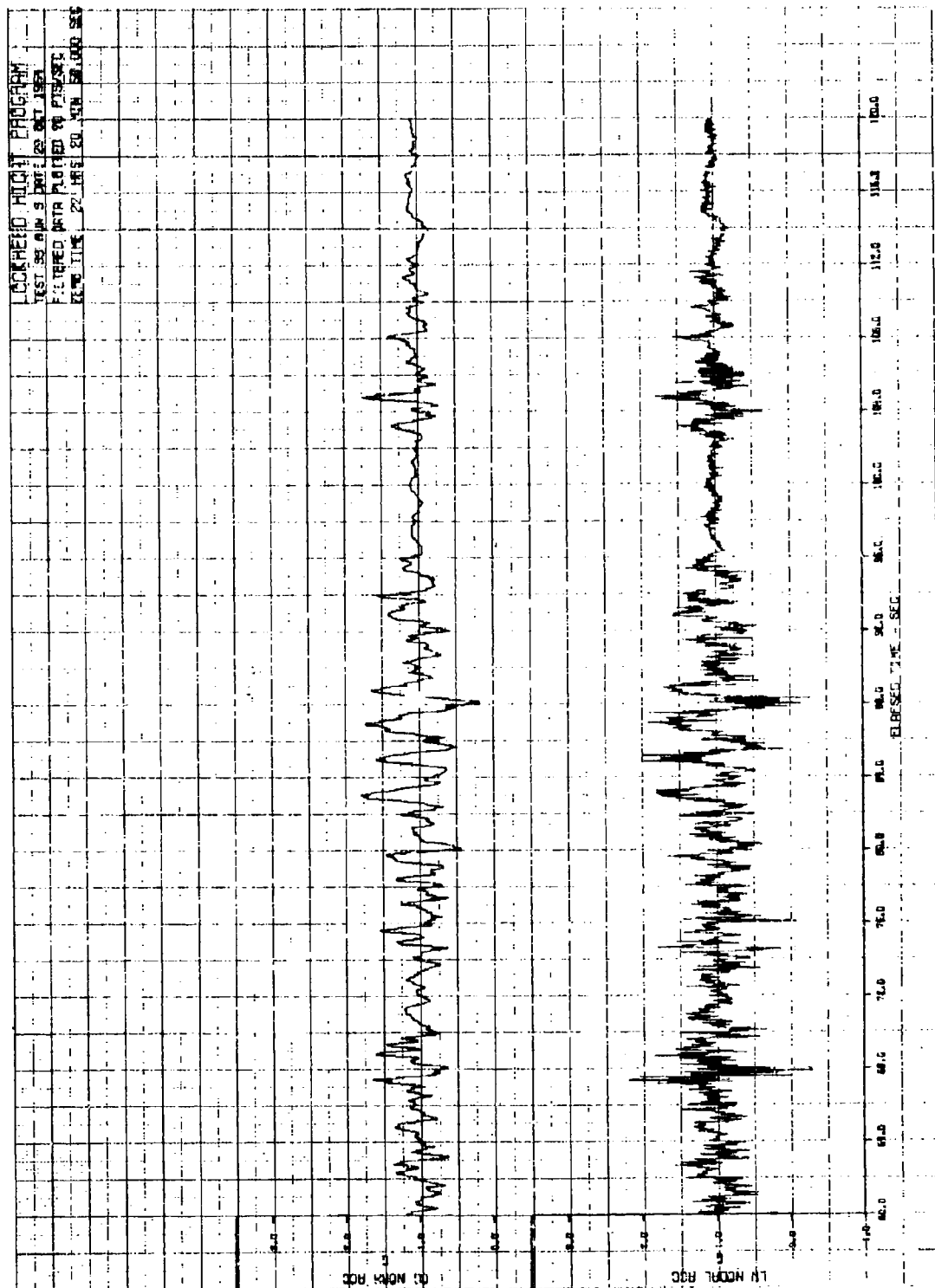


Figure 21. Time History of G.G. Normal Acceleration and Left Wing Root Acceleration.
 Test 50, Run 3. 50 - 120 sec.

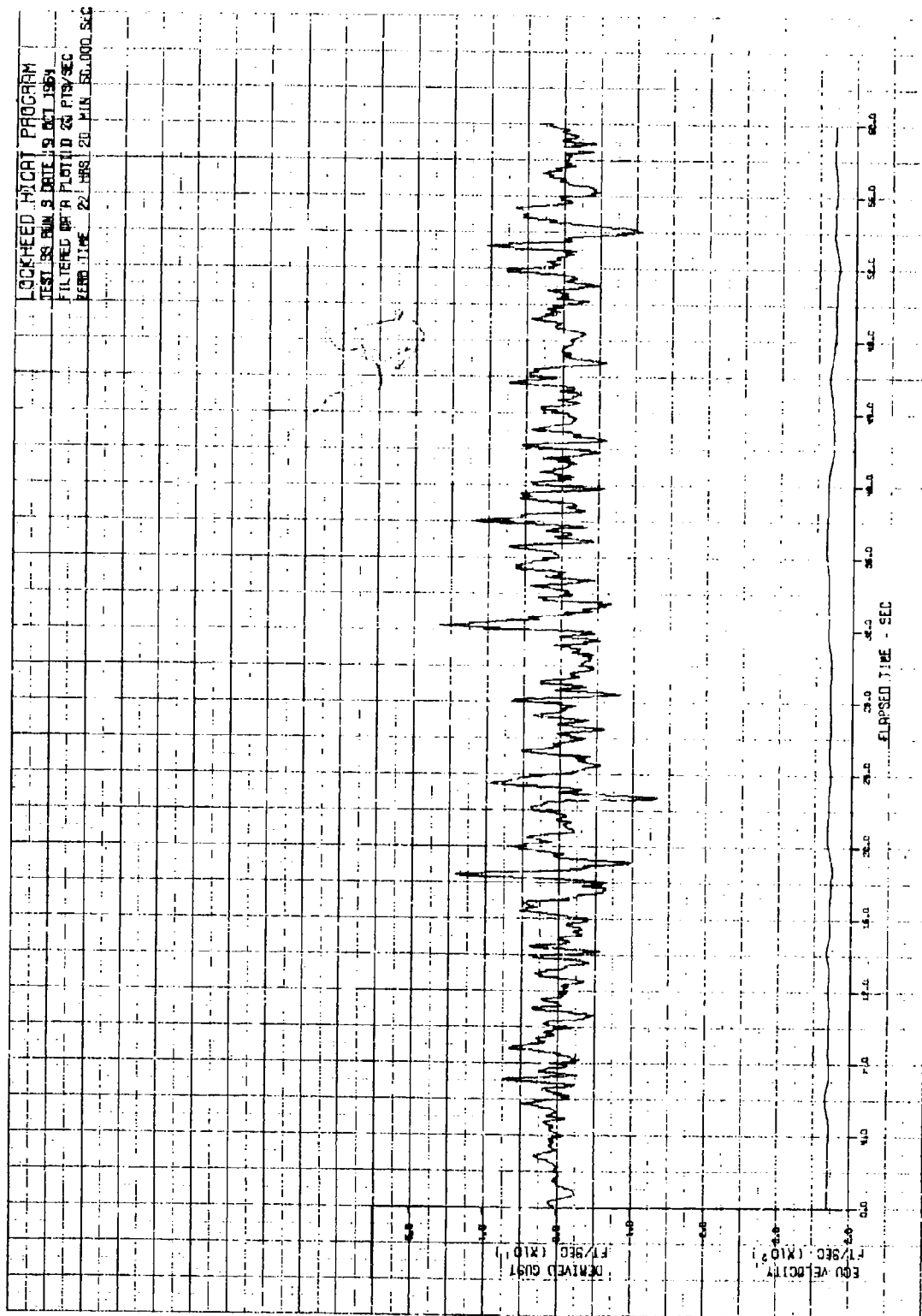


Figure 22. Time History of Derived Equivalent Gust Velocity (V_g) and Equivalent Velocity (V_a).
 Test 30, Run 5. 0 - 60 Sec.

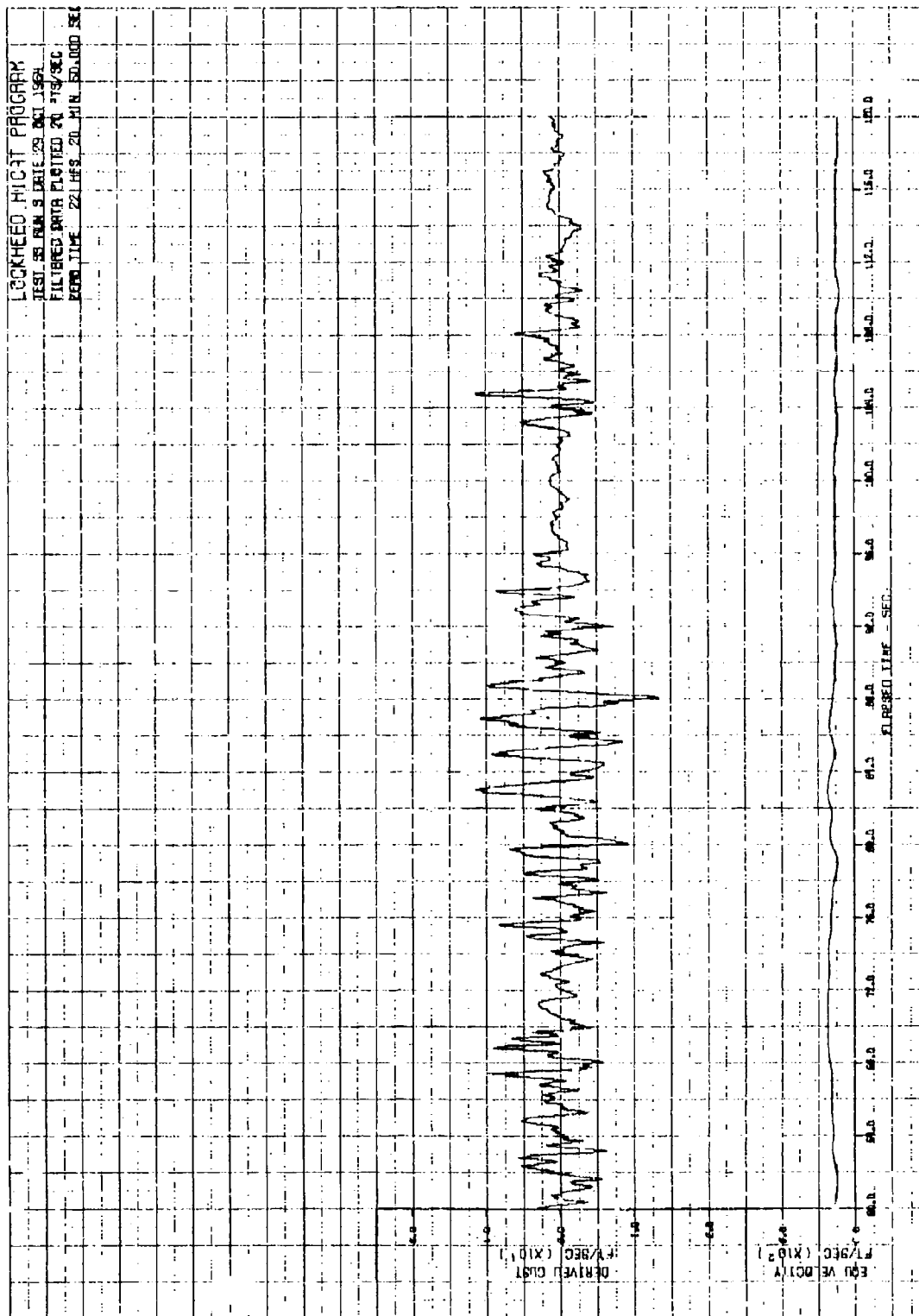


Figure 23. Time History of Derived Equivalent Gust Velocity (V_g) and Equivalent Velocity (V_{eq}).
 Test 33, Run 3. 60 - 120 Sec.

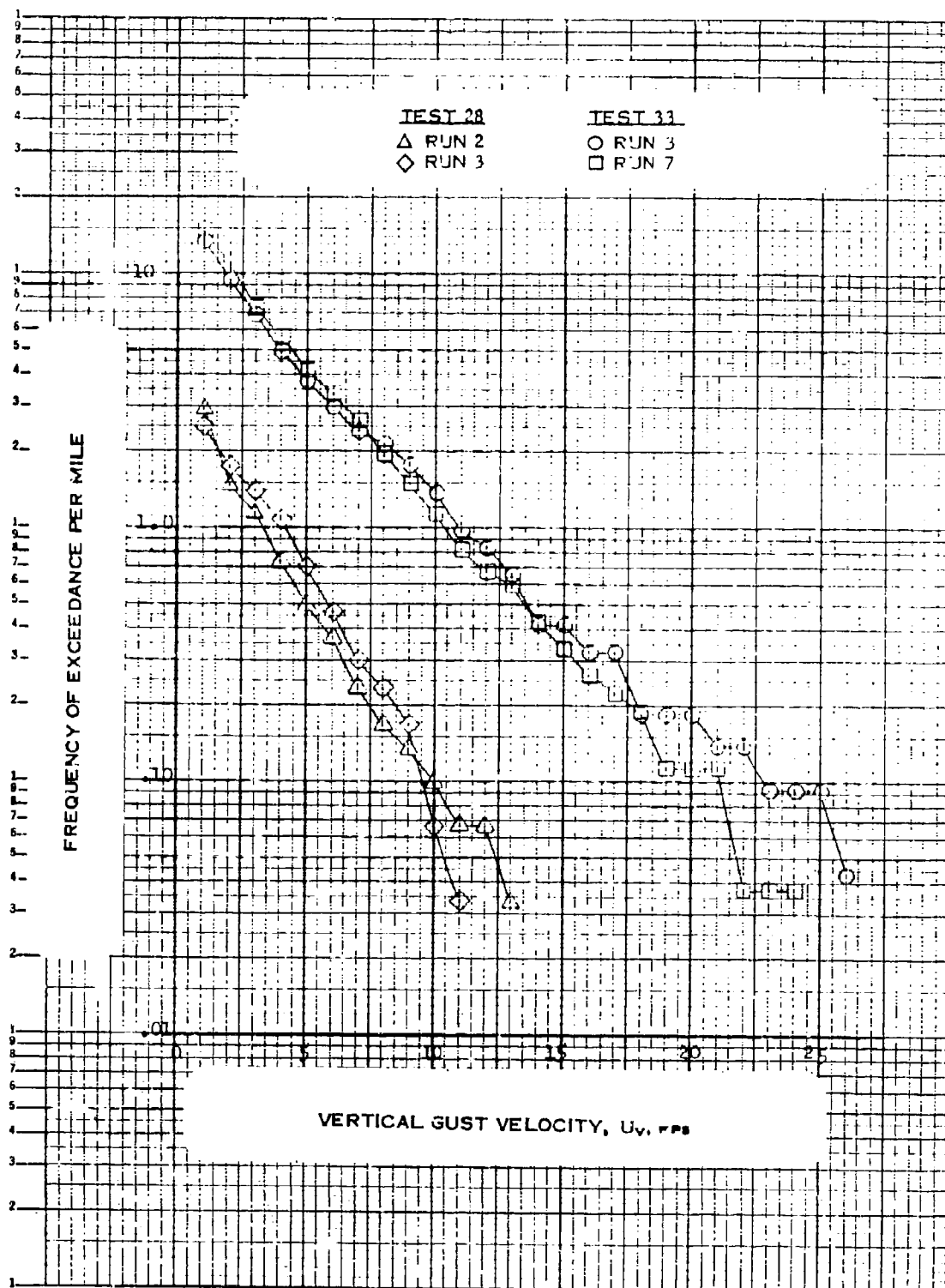


Figure 24. Frequency of Exceedance Per Mile of Vertical Gust Velocity, Tests 28 and 33

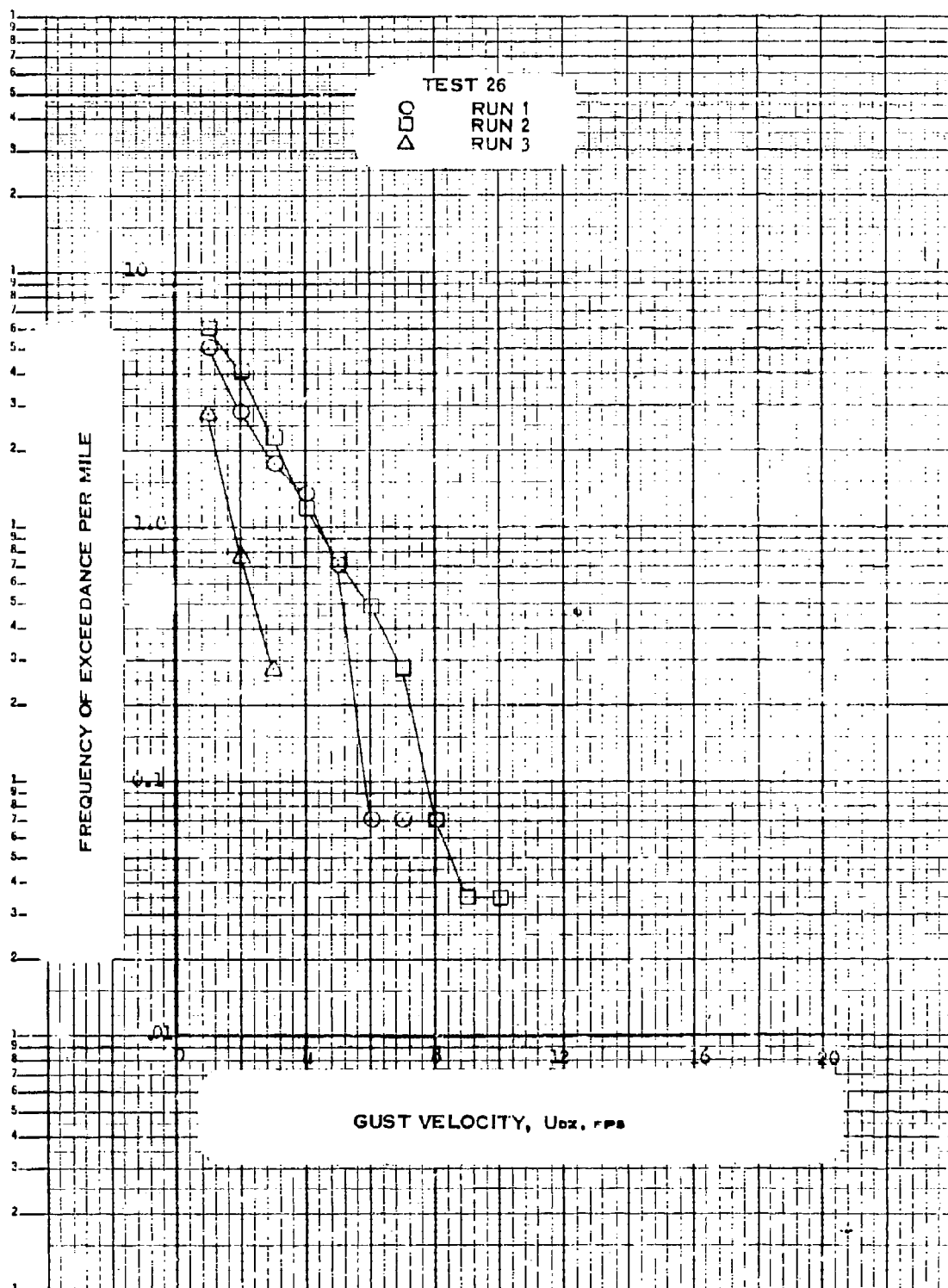


Figure 25. Frequency of Exceedance Per Mile of Derived Equivalent Gust Velocity, Test 26

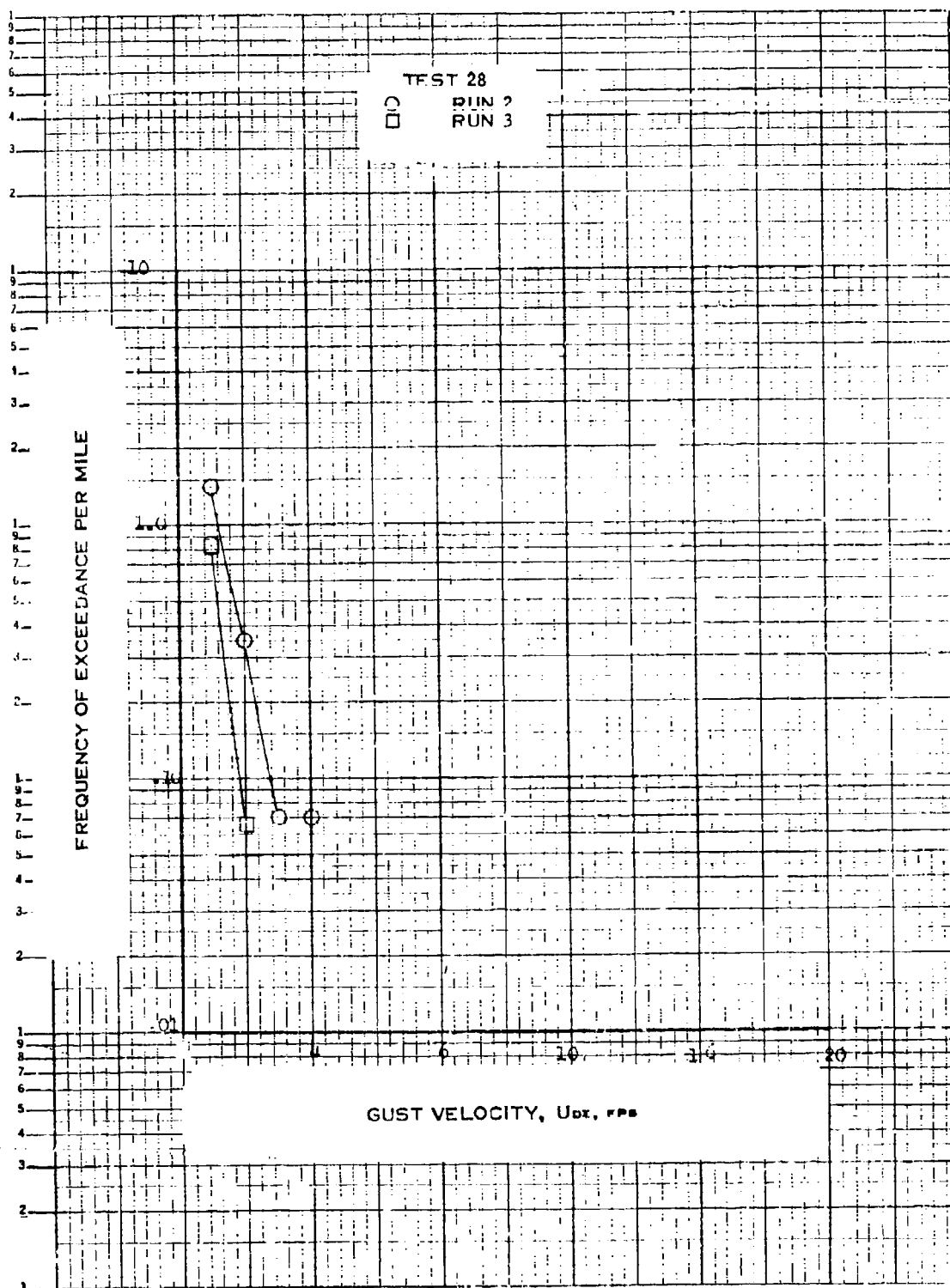


Figure 26. Frequency of Exceedance Per Mile of
 Derived Equivalent Gust Velocity, Test 28

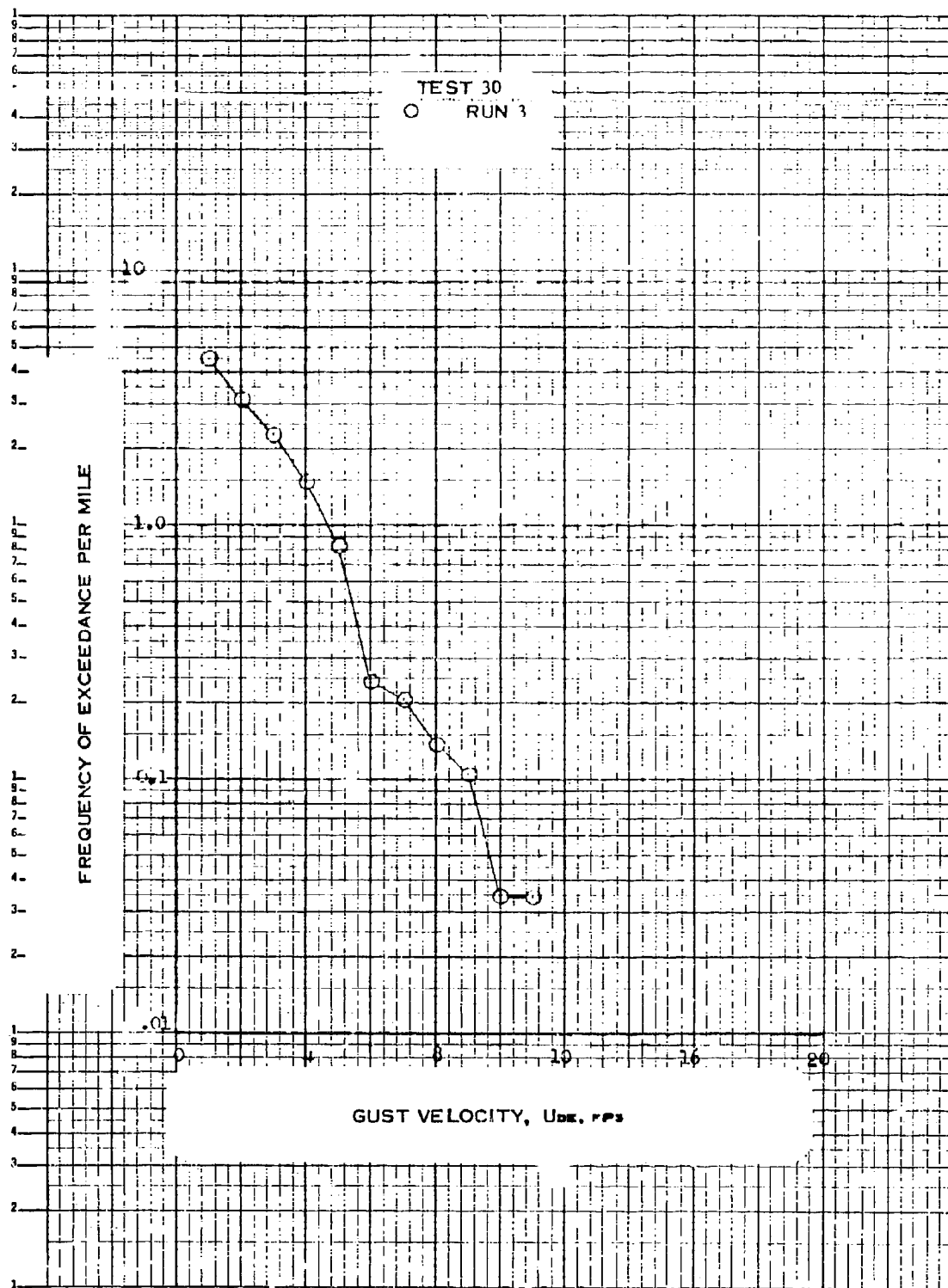


Figure 27. Frequency of Exceedance Per Mile of
Derived Equivalent Gust Velocity, Test 30

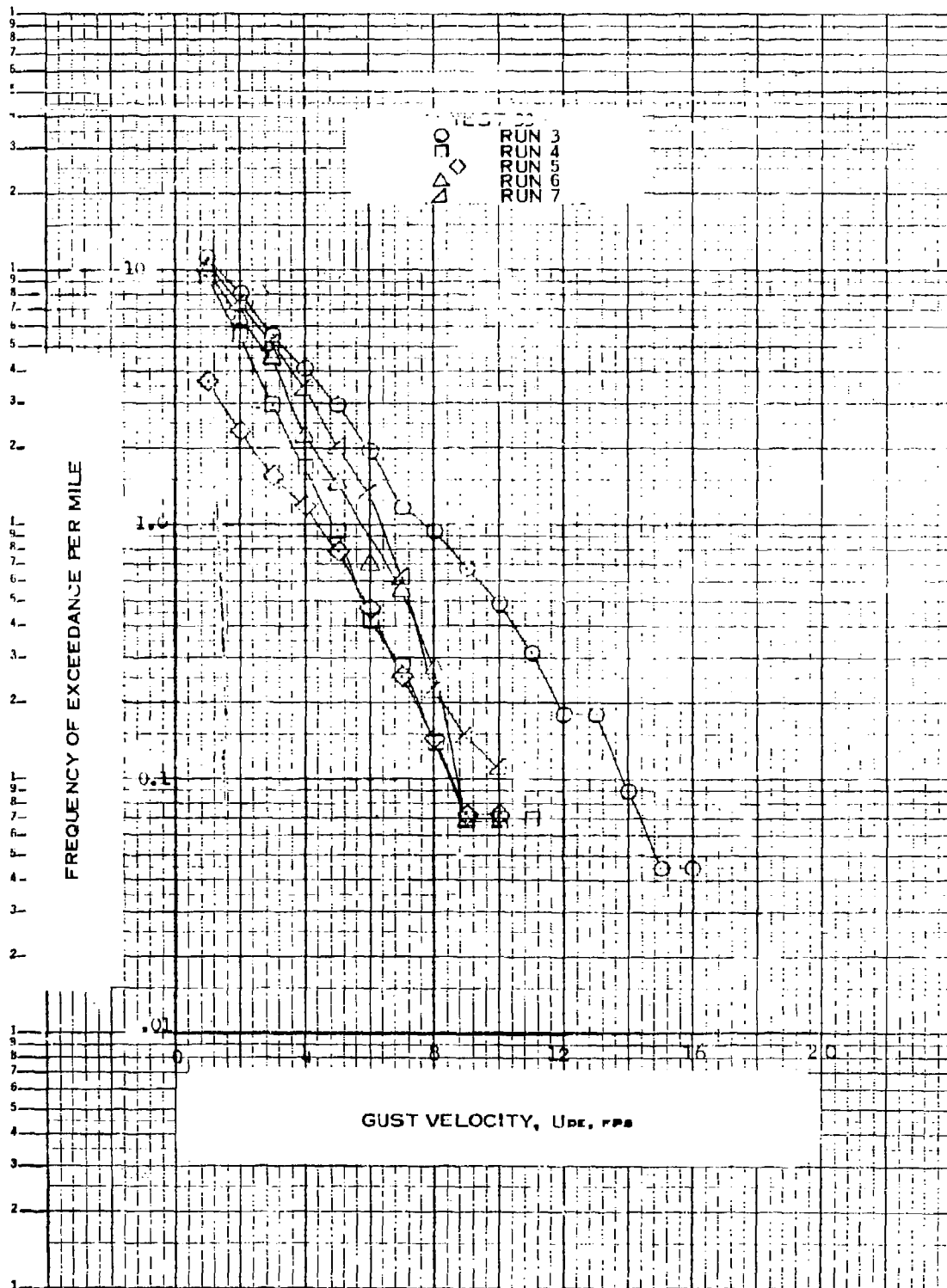


Figure 28. Frequency of Exceedance Per Mile of Derived Equivalent Gust Velocity, Test 33, Runs 3-7

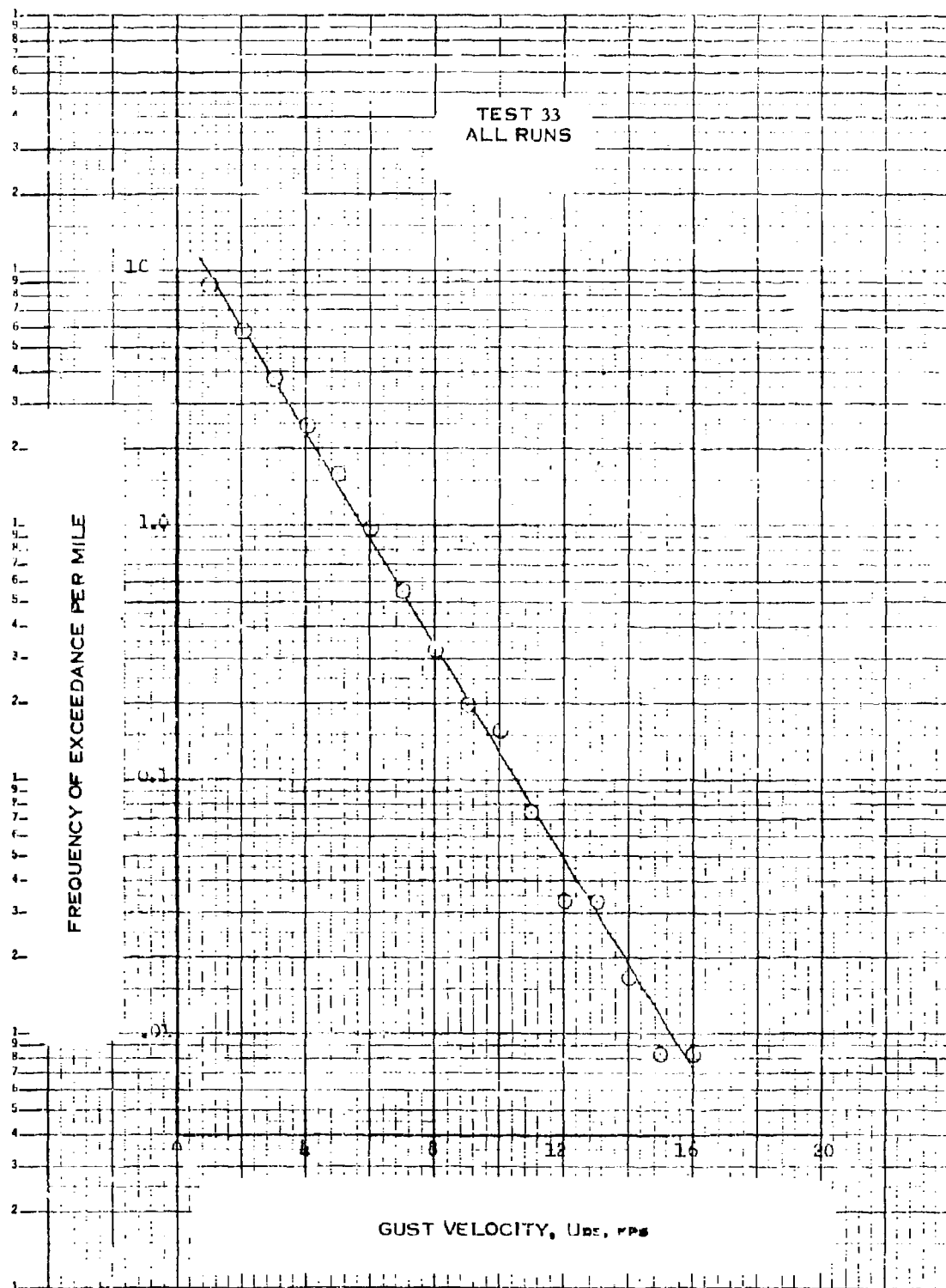


Figure 29. Frequency of Exceedance Per Mile of Derived Equivalent Gust Velocity, Test 33, All Runs Combined

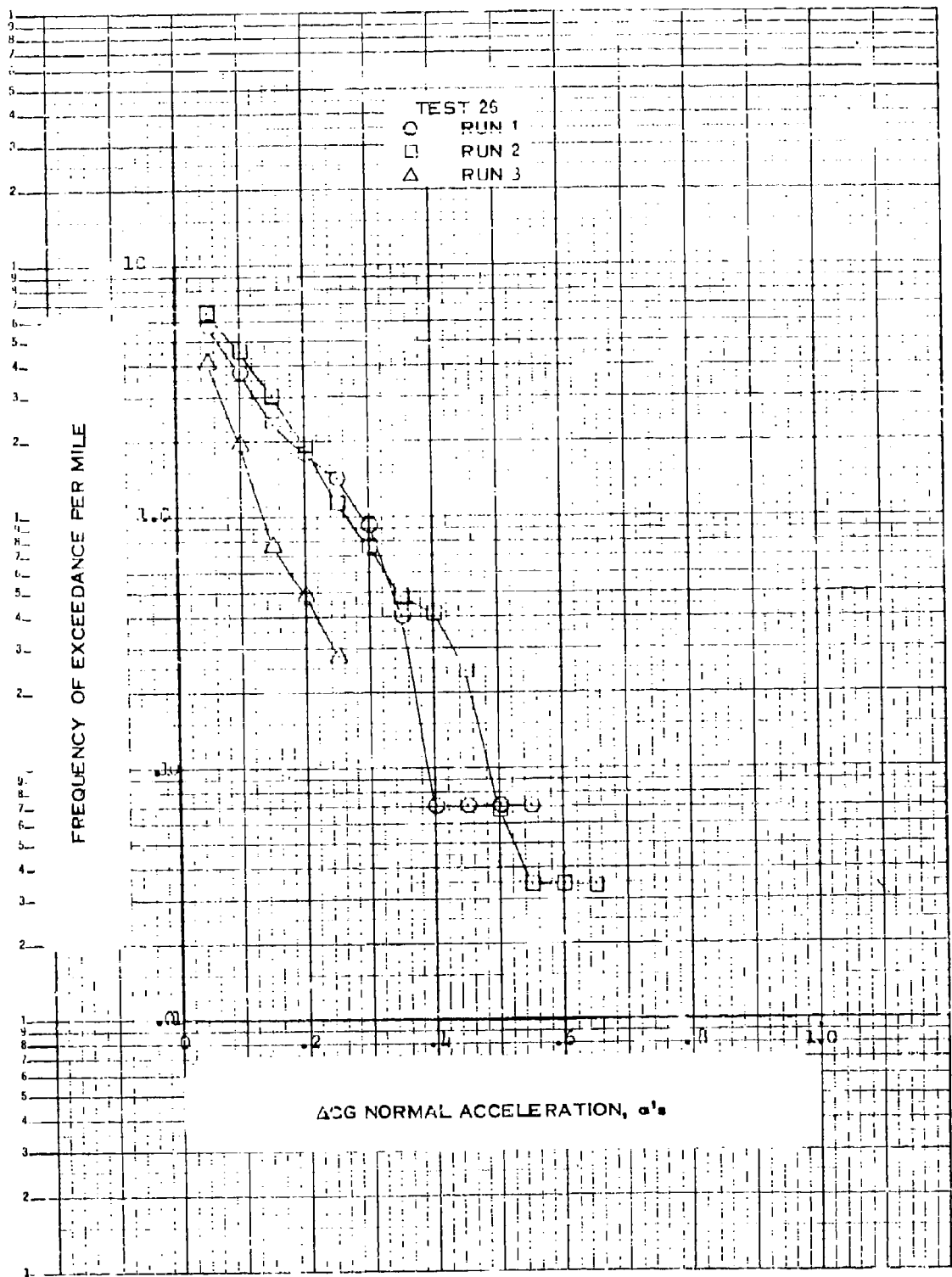


Figure 30. Frequency of Exceedance Per Mile of Incremental C.G. Normal Acceleration, Test 26

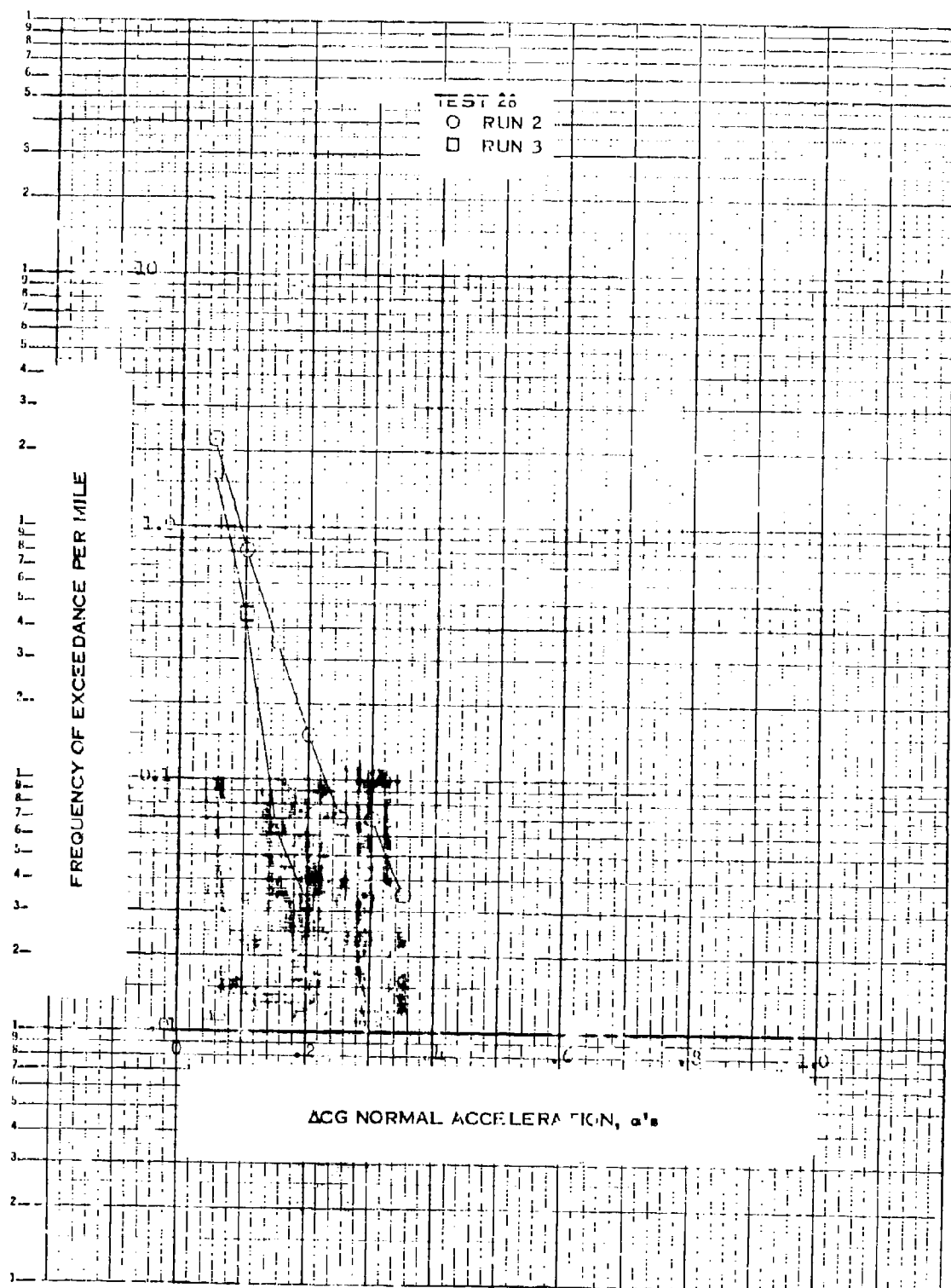


Figure 30. Frequency of Exceedance Per Mile of Incremental C.G. Normal Acceleration, Test 20

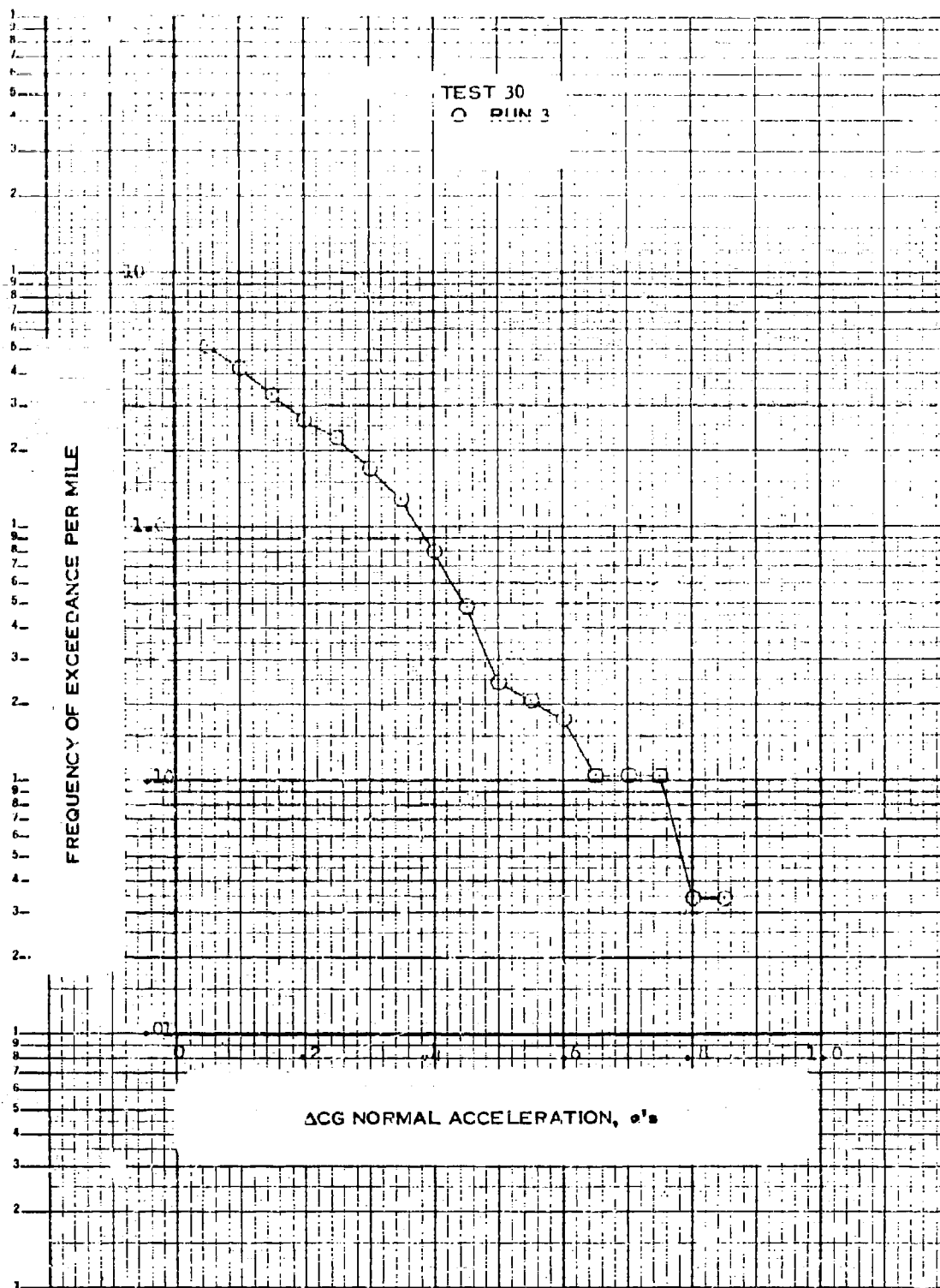


Figure 32. Frequency of Exceedance Per Mile of Incremental C.G. Normal Acceleration, Test 30

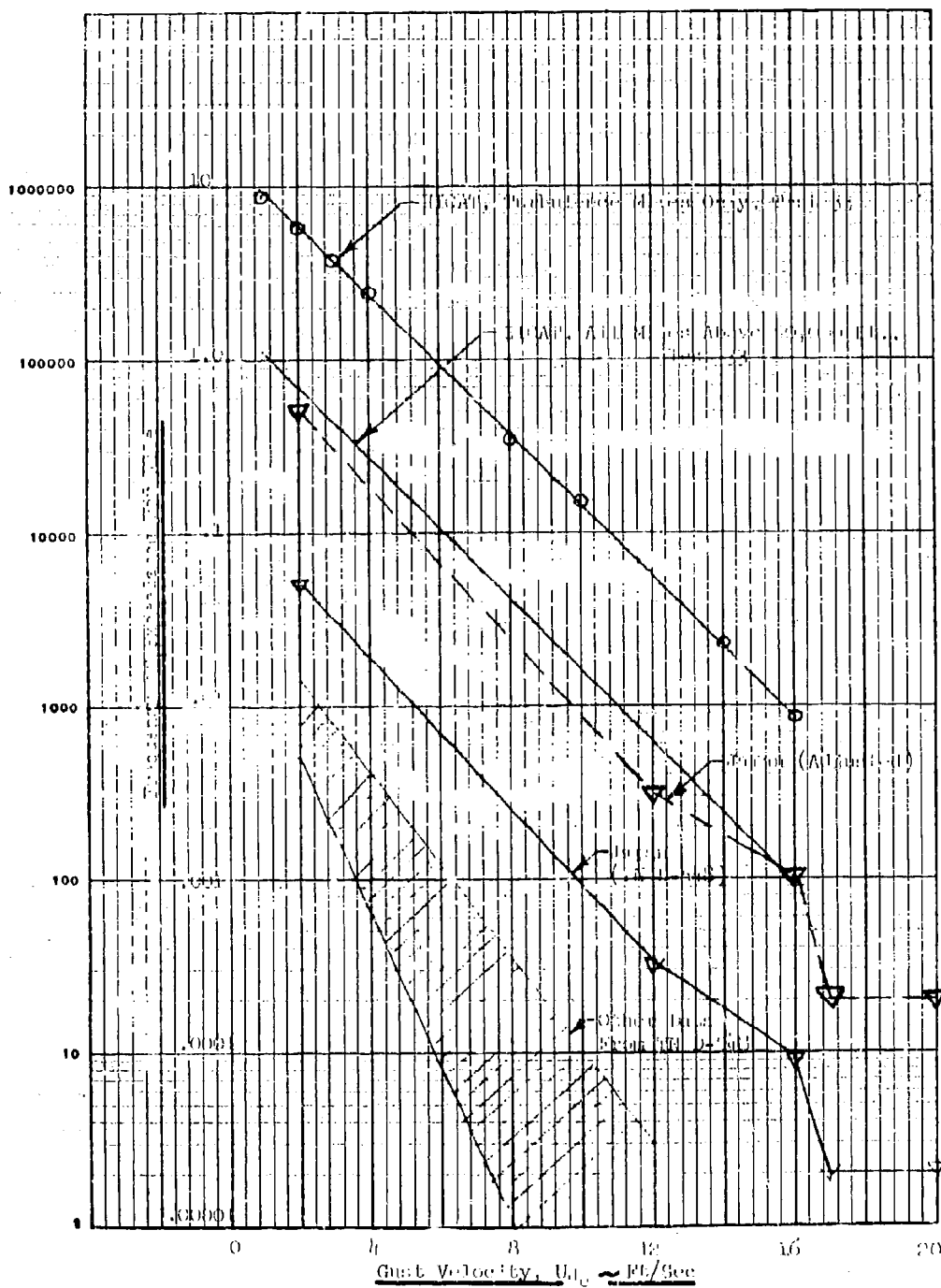


Figure 34. Comparison of HICAT Frequency of Exceedance of Gust Velocity per Mile of Flight with TN D-548

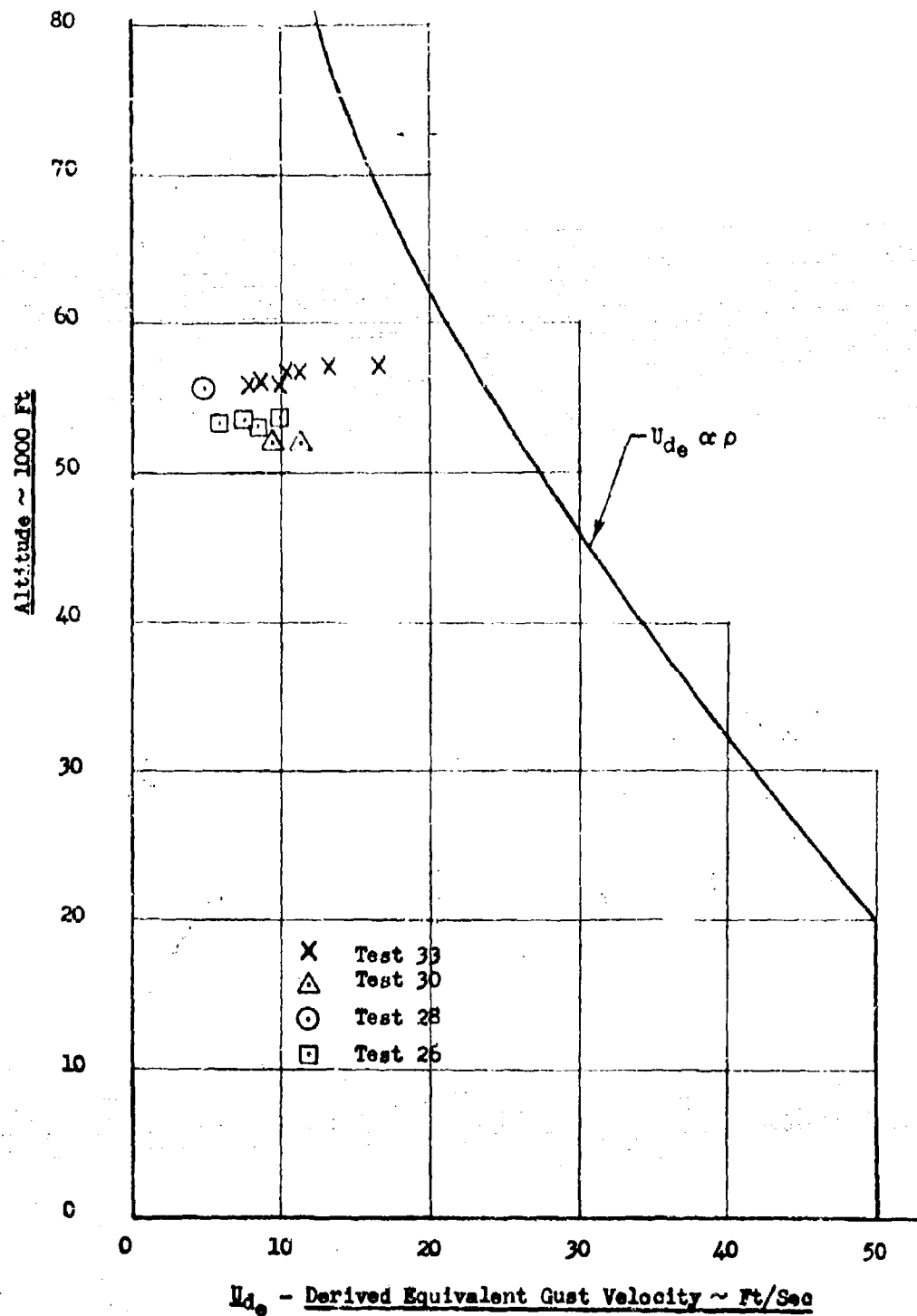


Figure 35. Comparison of HICAT Derived Equivalent Gust Velocities With U_{d_e} Design Envelope

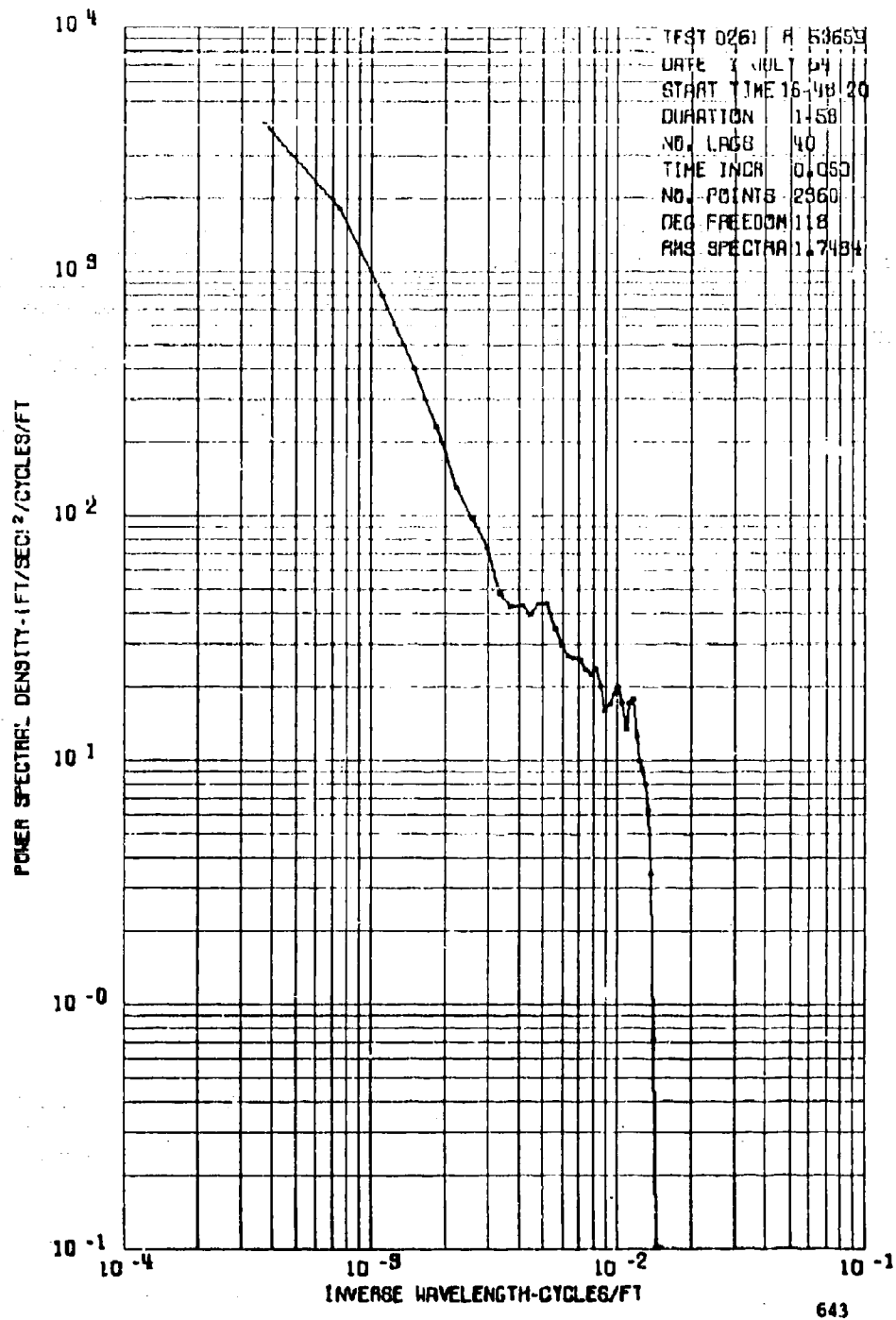
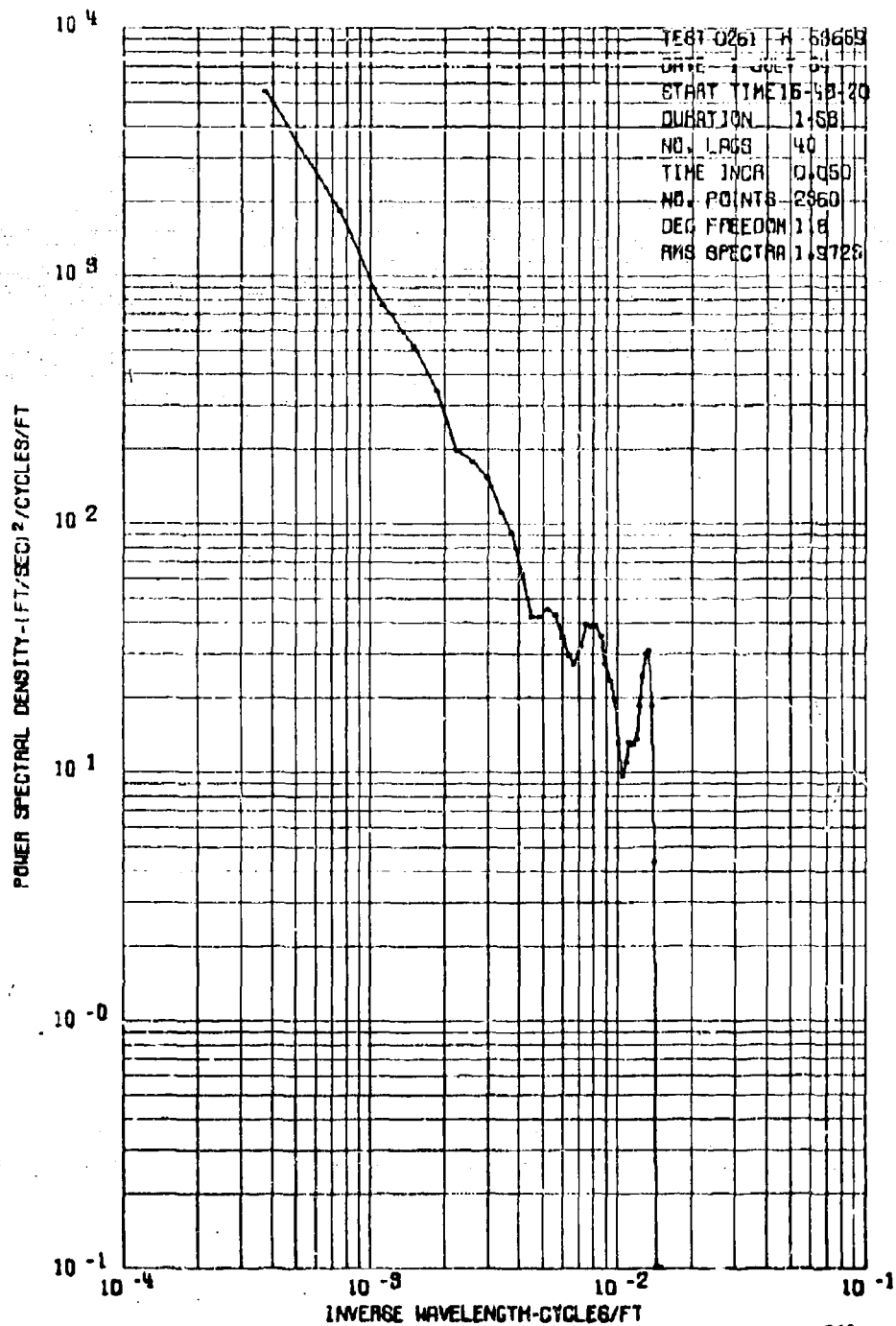


Figure 36. Power Spectrum of $V_T \Delta \alpha$, Test 26, Run 1



642

Figure 37. Power Spectrum of $V_T \Delta \beta$, Test 26, Run 1

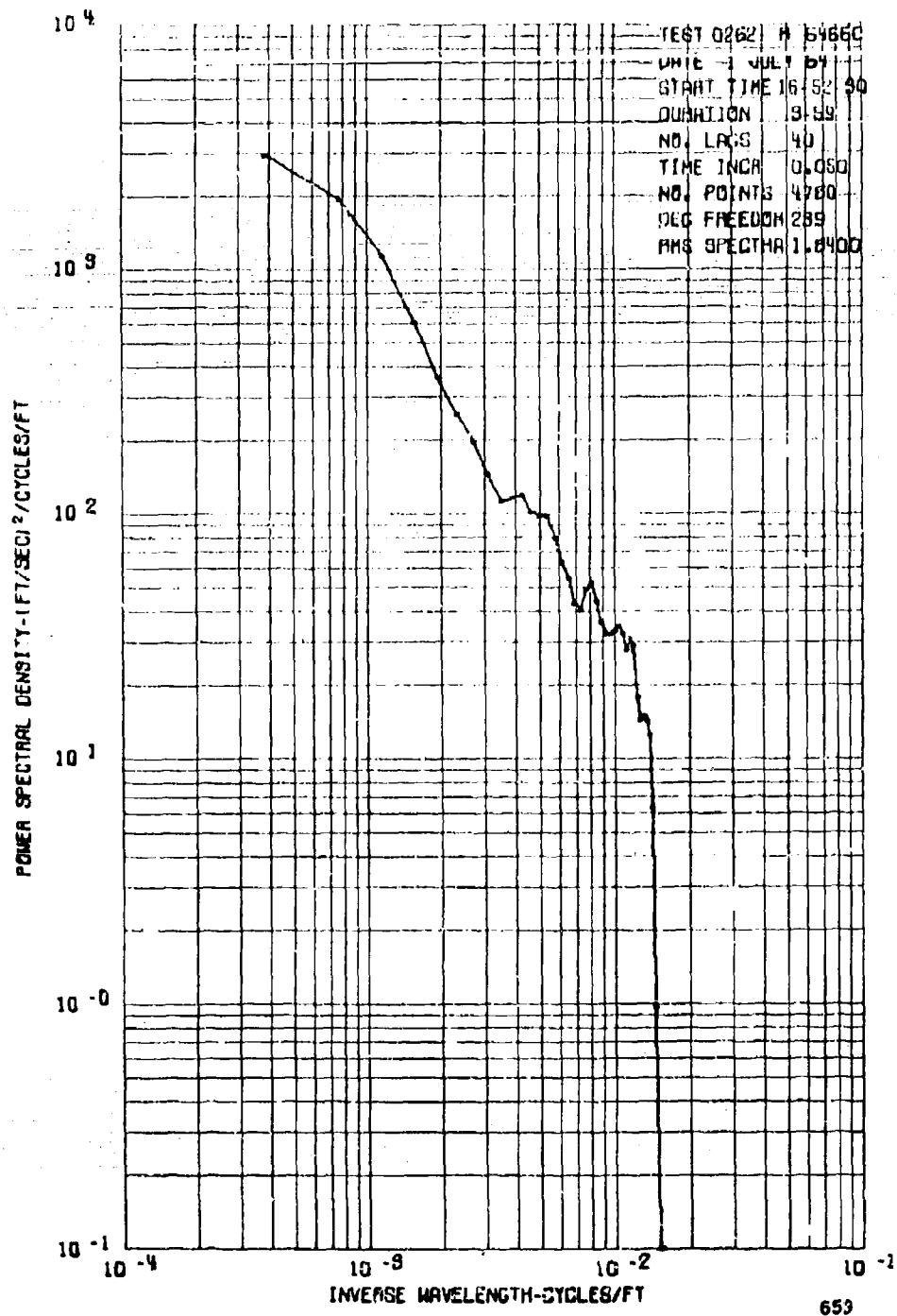


Figure 38. Power Spectrum of $V_T \Delta \alpha$, Test 26, Run 2

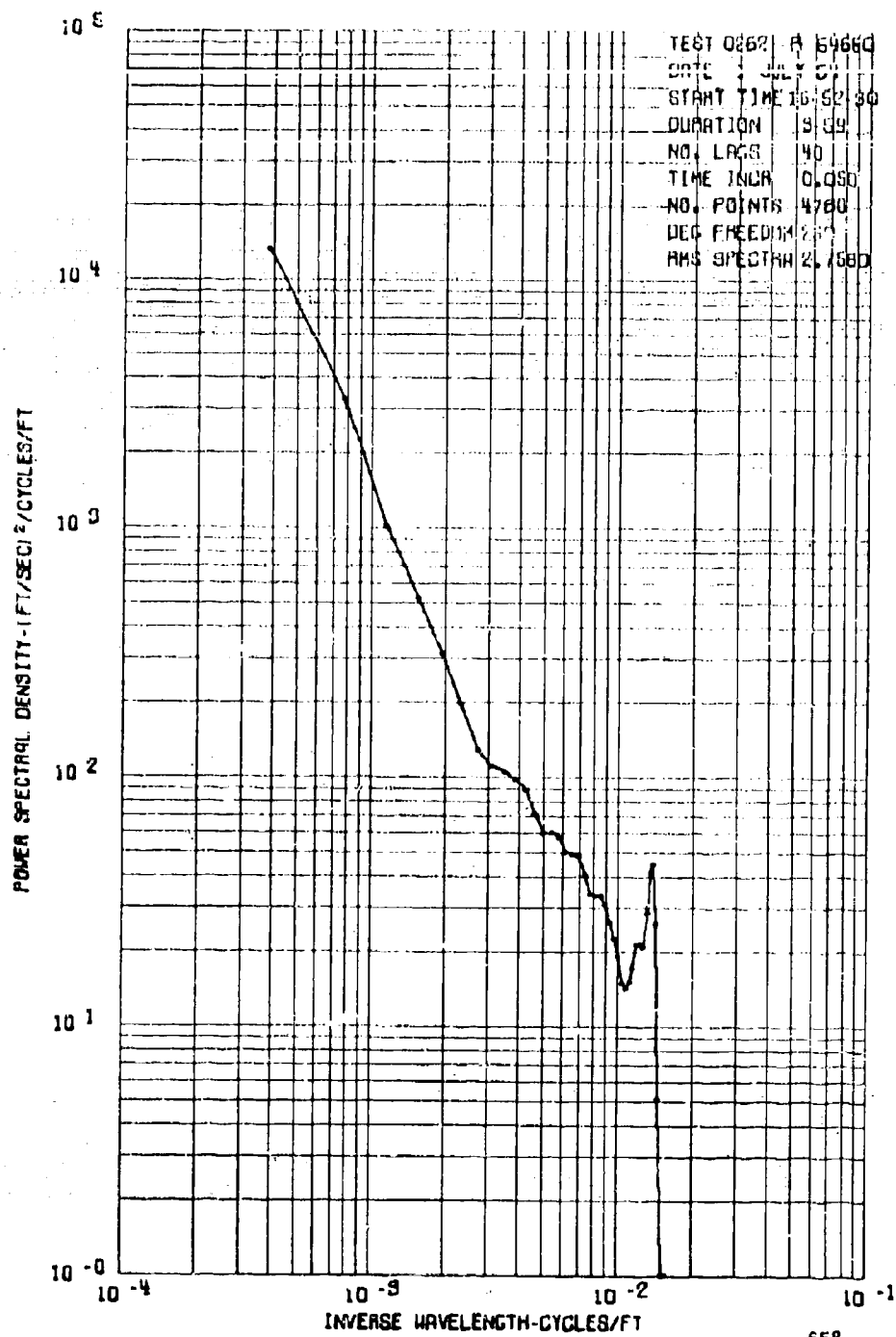


Figure 39. Power Spectrum of $V_T \Delta \beta$, Test 26, Run 2

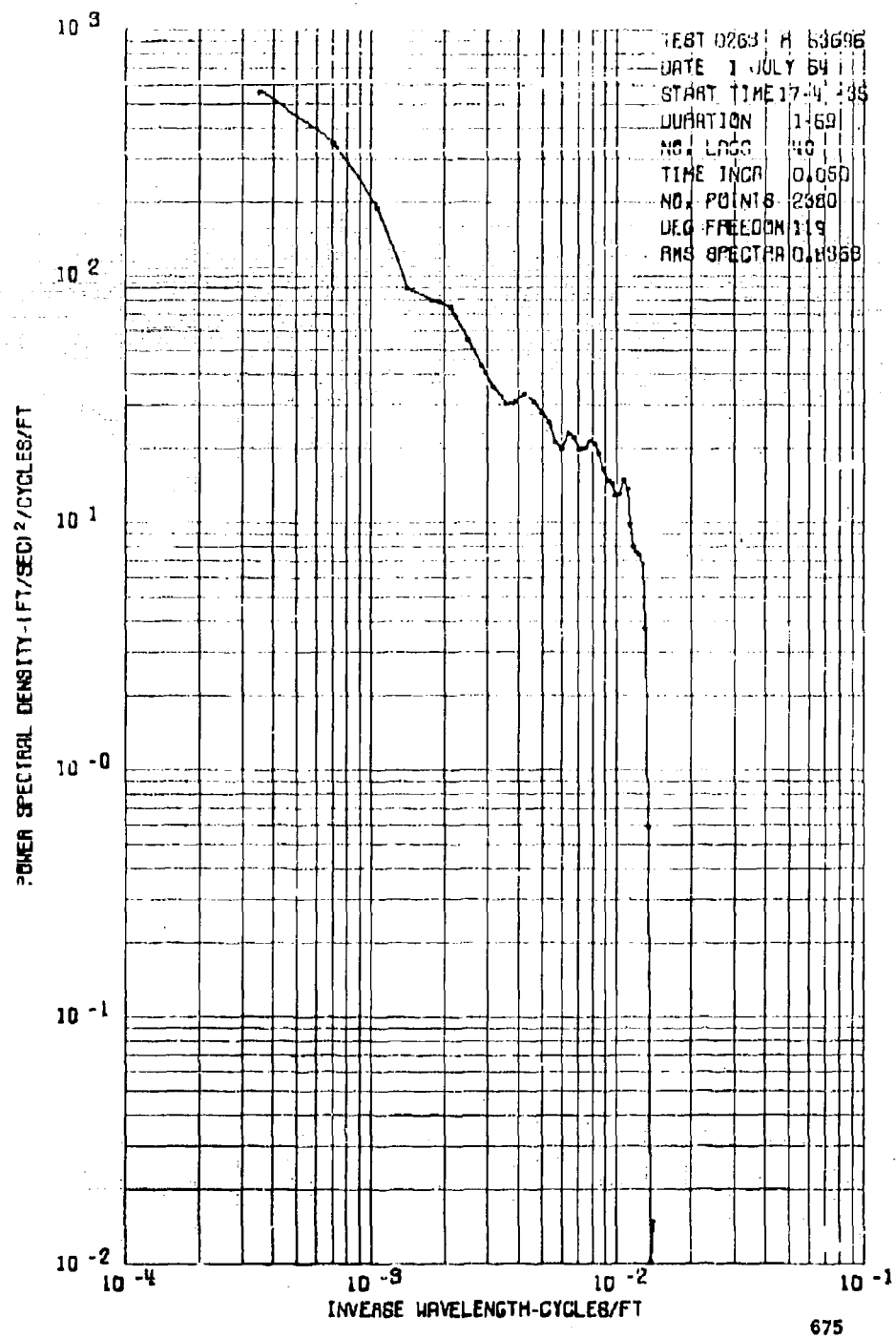
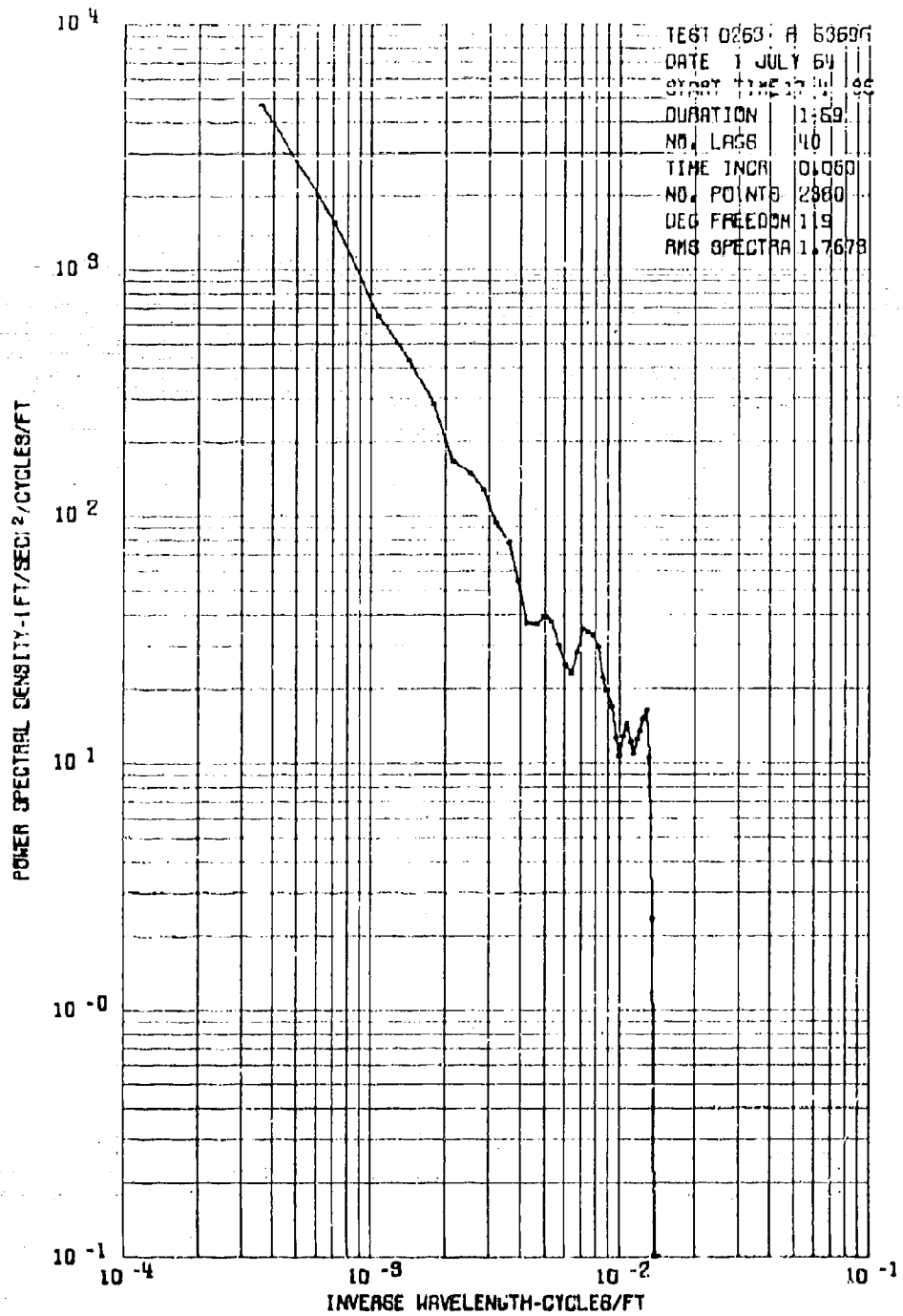


Figure 40. Power Spectrum of $V_T \Delta \alpha$, Test 26, Run 3



674

Figure 41. Power Spectrum of $V_T \Delta \beta$, Test 26, Run 3

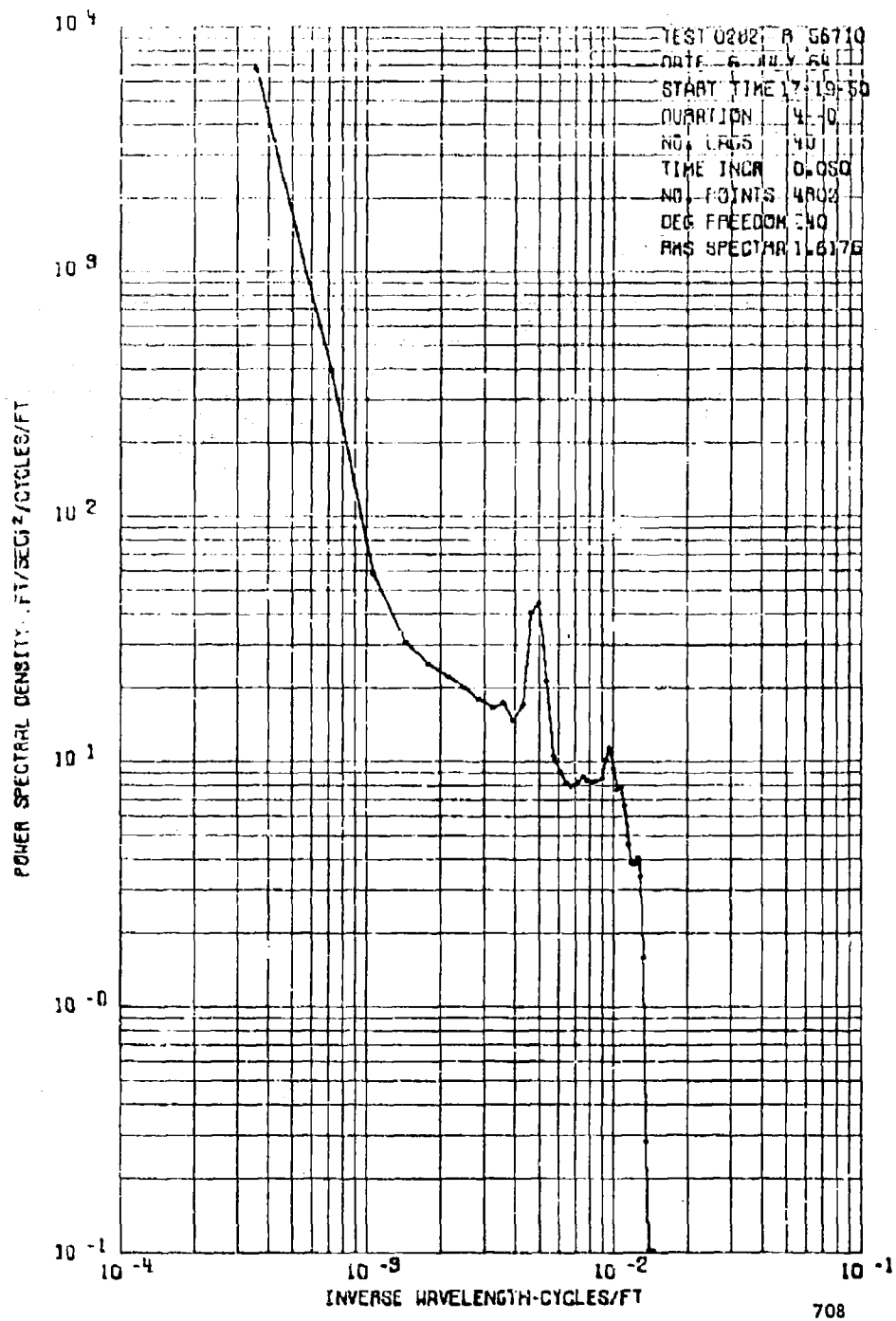


Figure 42. Power Spectrum of Vertical Gust Velocity, Test 28, Run 2

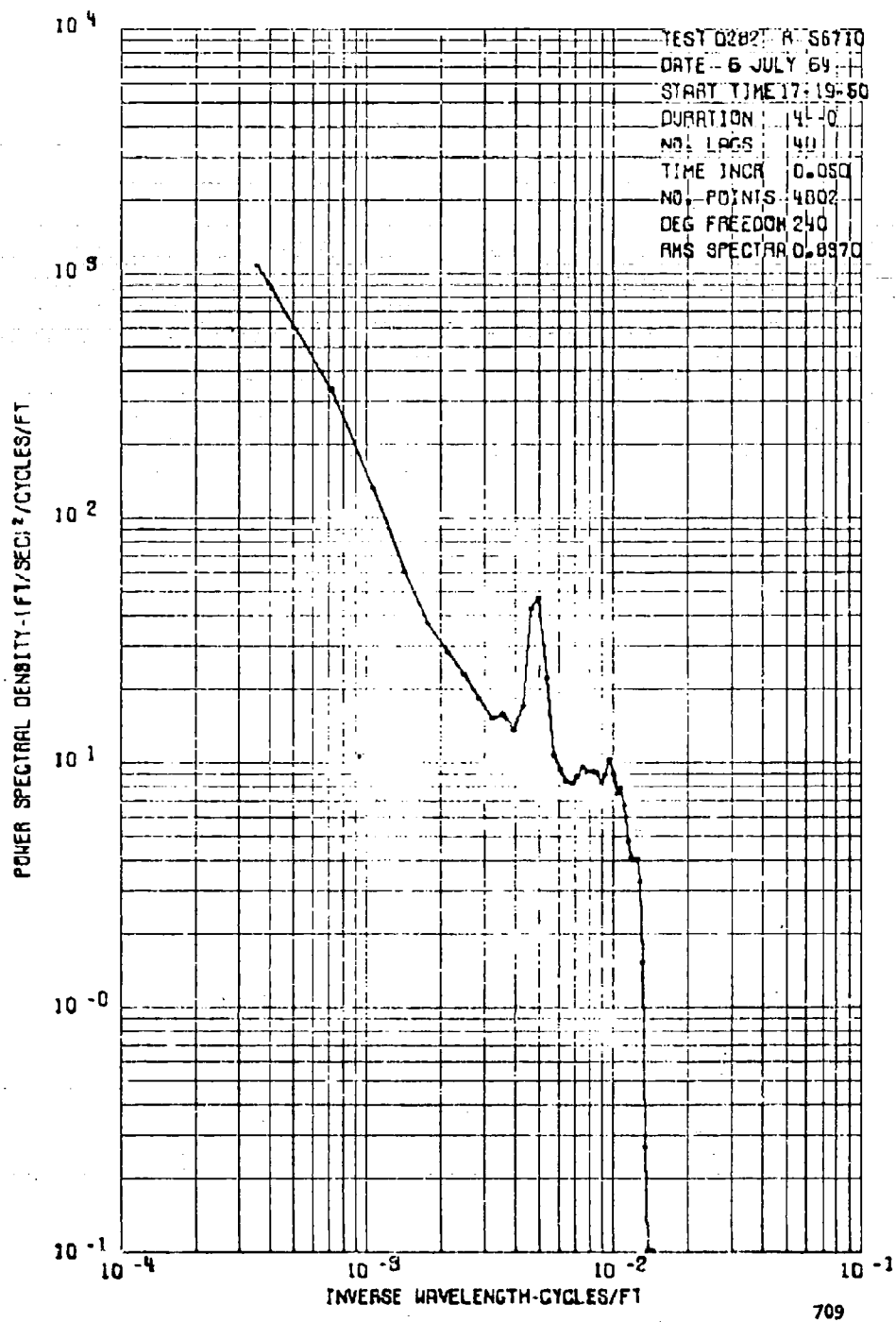


Figure 43. Power Spectrum of $V_T \Delta \alpha$, Test 28, Run 2

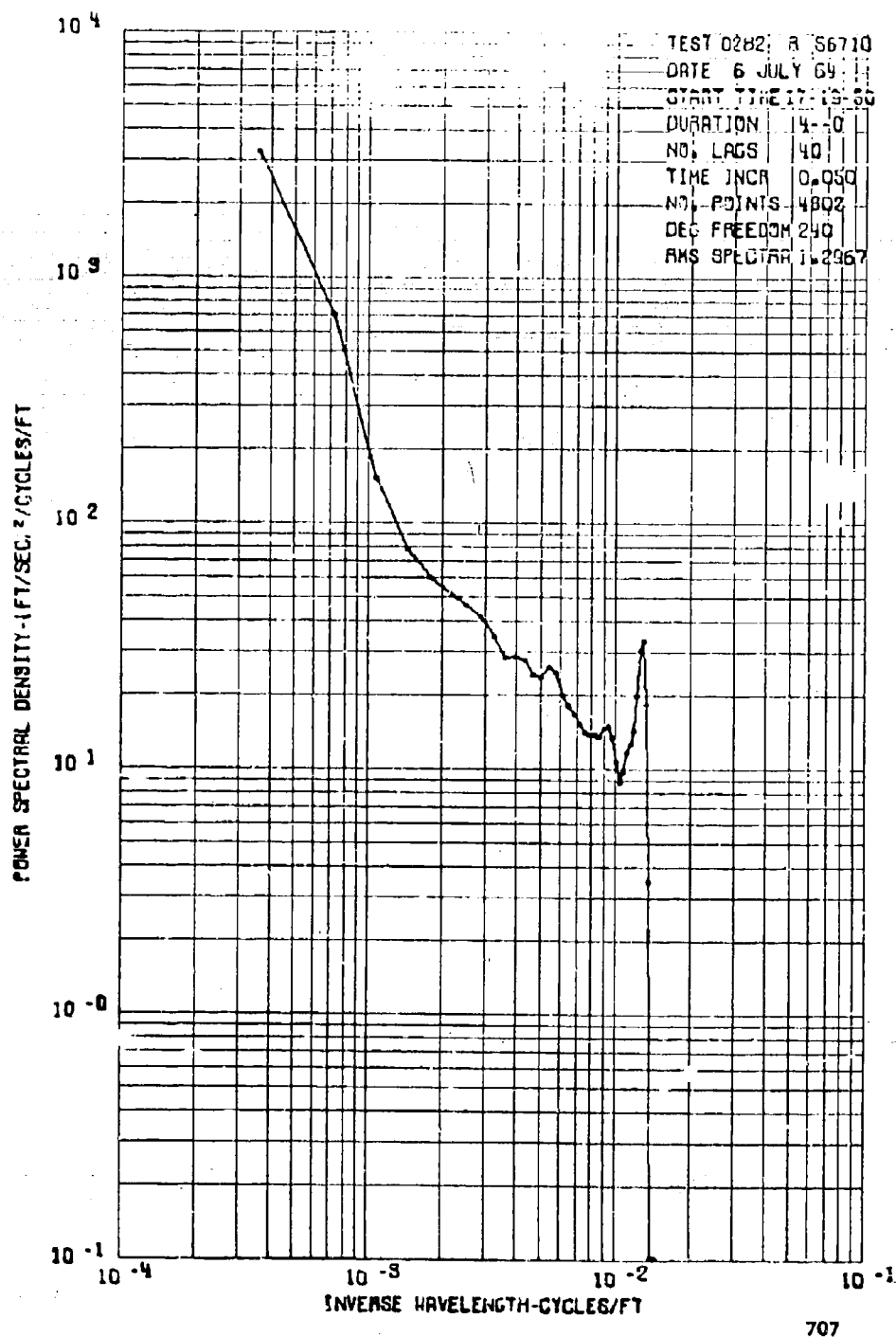
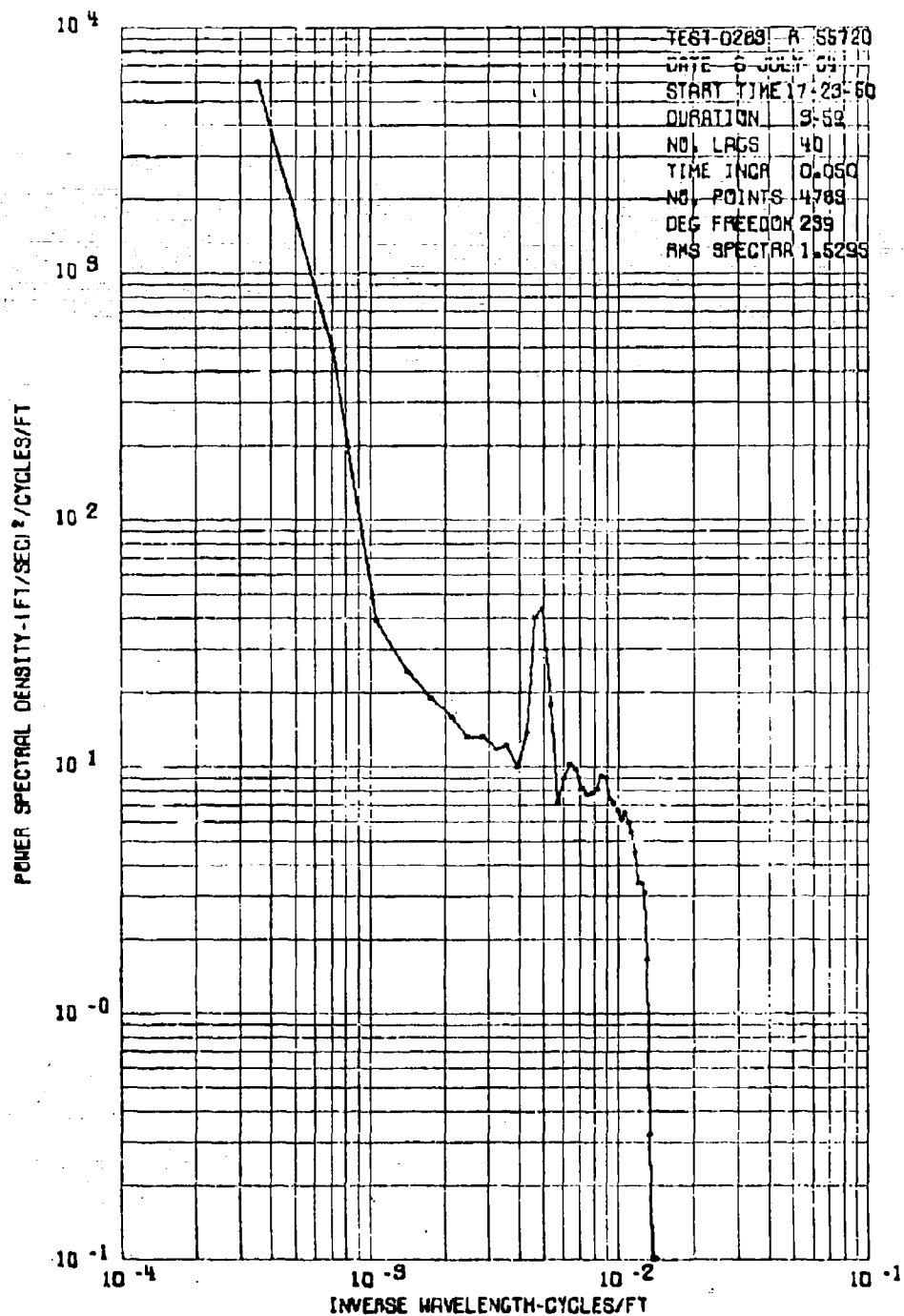


Figure 44. Power Spectrum of $V_{\eta} \Delta \beta$, Test 28, Run 2



732

Figure 45. Power Spectrum of Vertical Gust Velocity,
 Test 28, Run 3

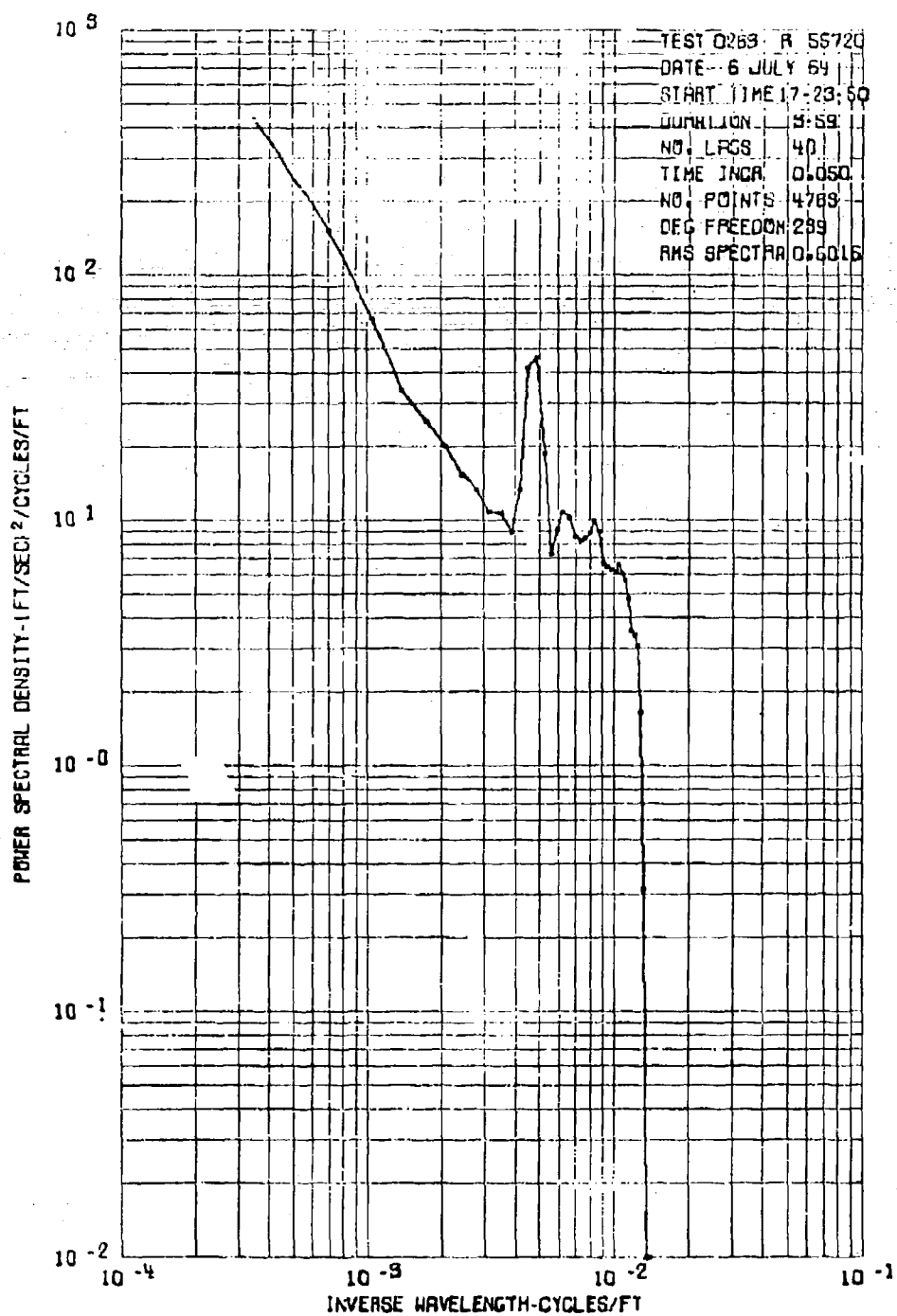
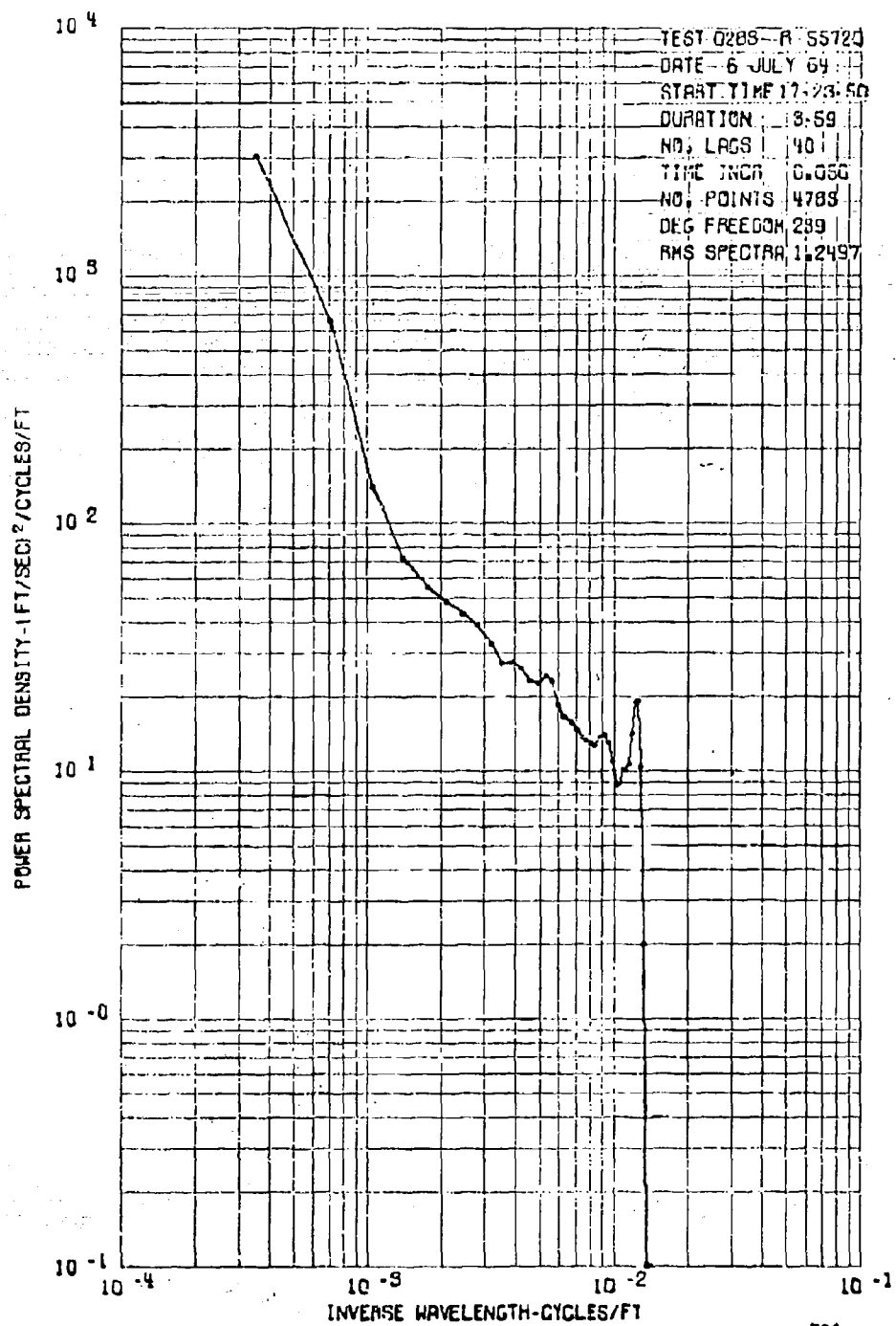


Figure 46. Power Spectrum of $V_T \Delta \alpha$, Test 28, Run 3



731

Figure 47. Power Spectrum of $V_T \Delta \beta$, Test 28, Run 3

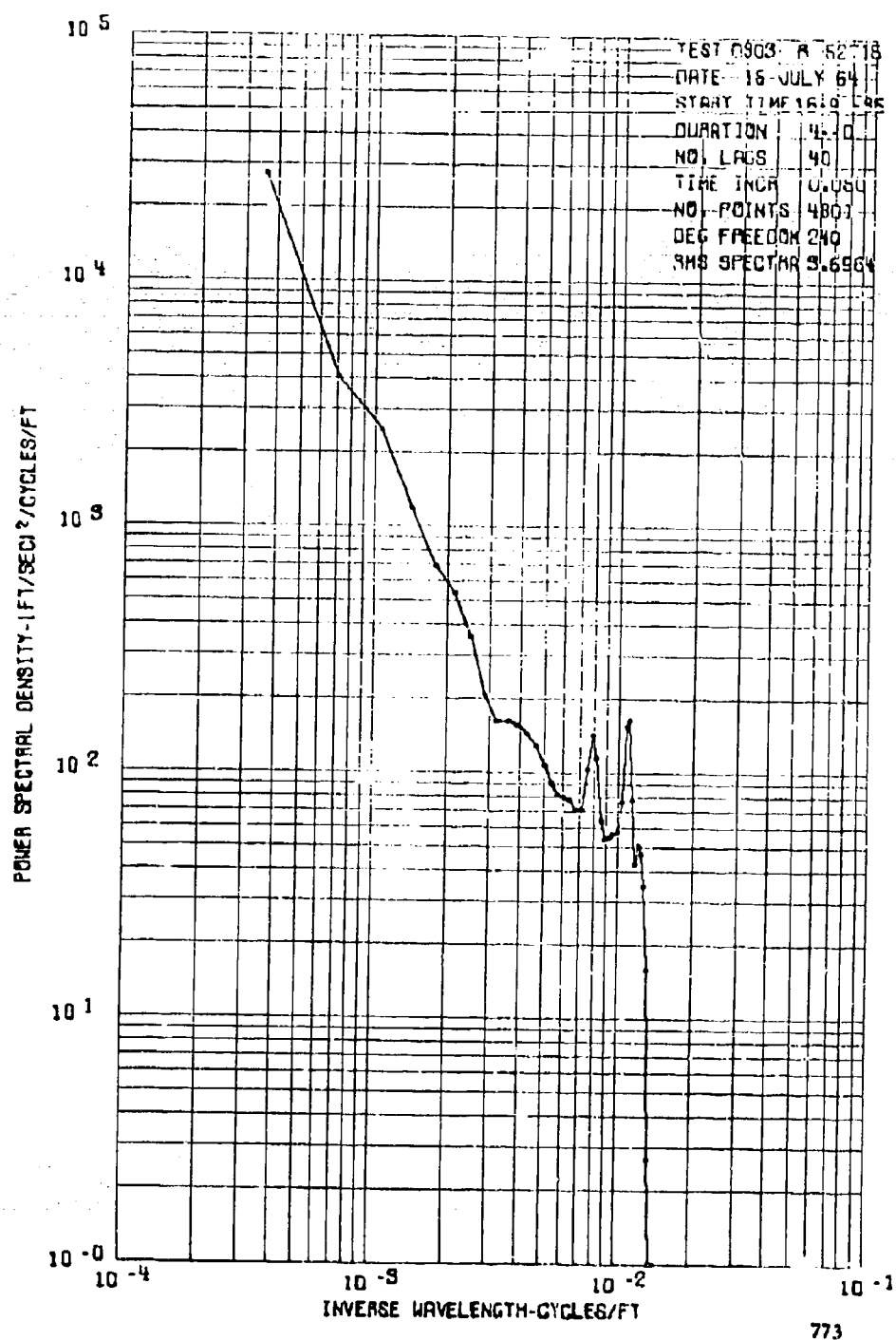
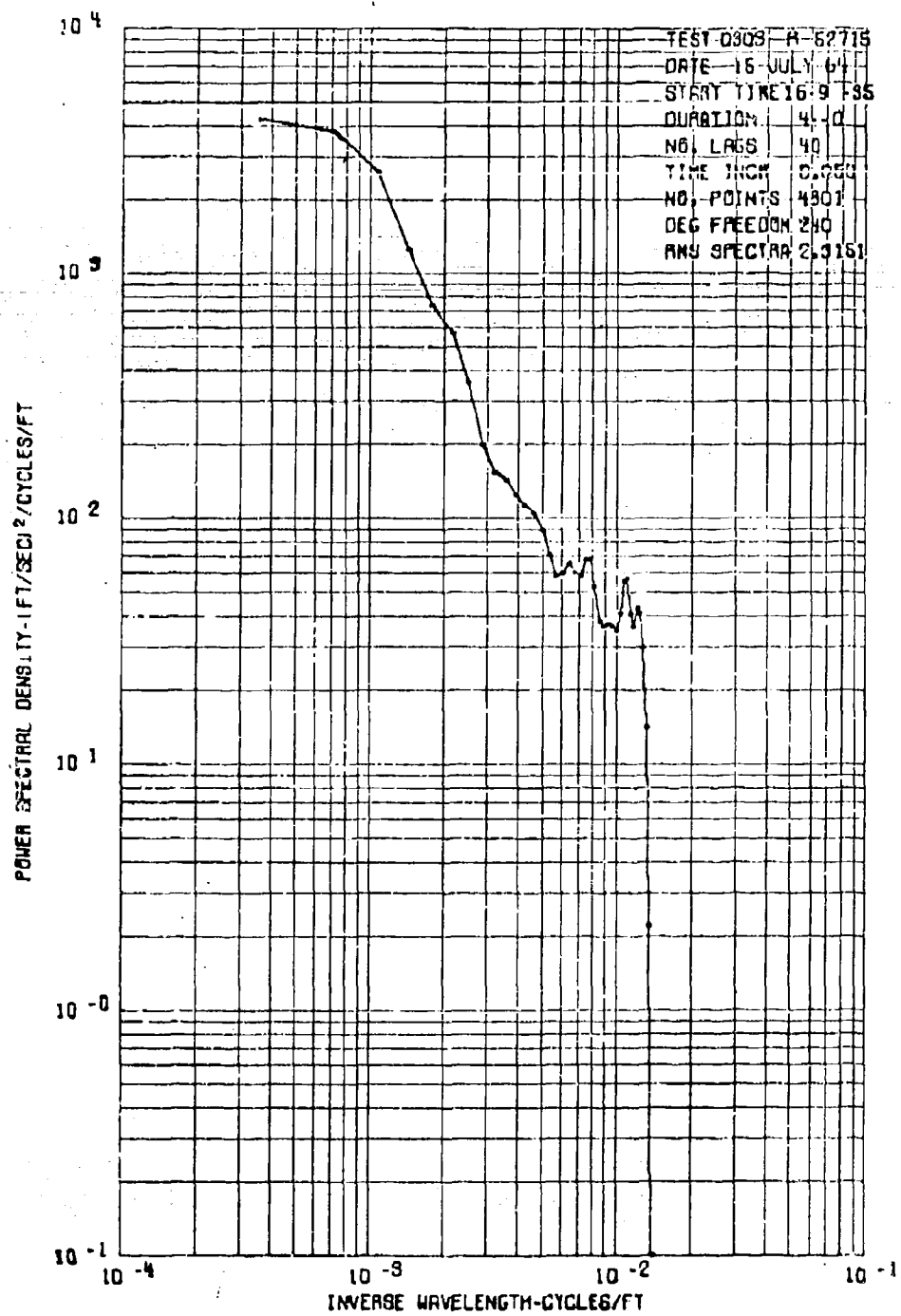
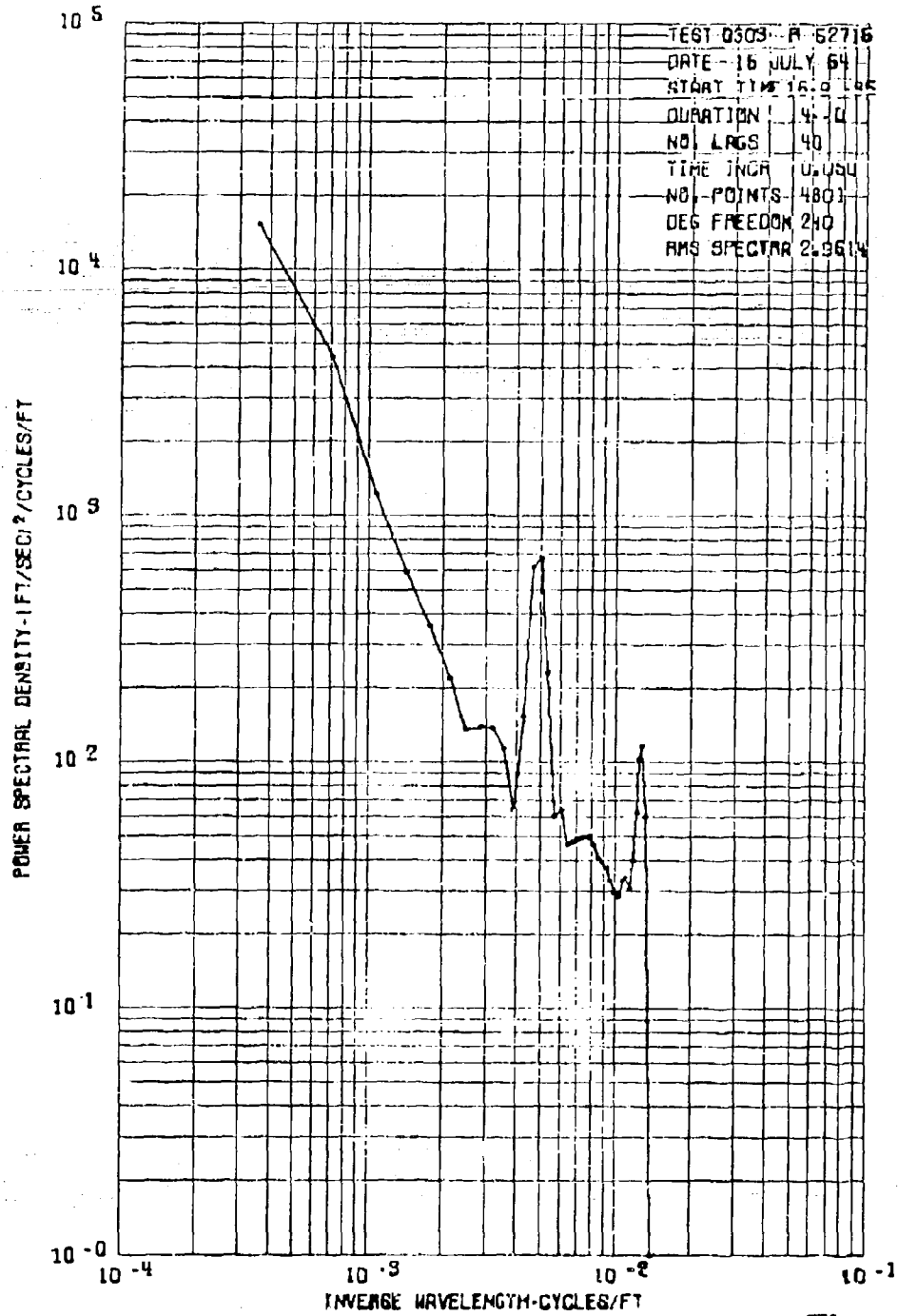


Figure 48. Power Spectrum of Vertical Gust Velocity, Test 30, Run 3



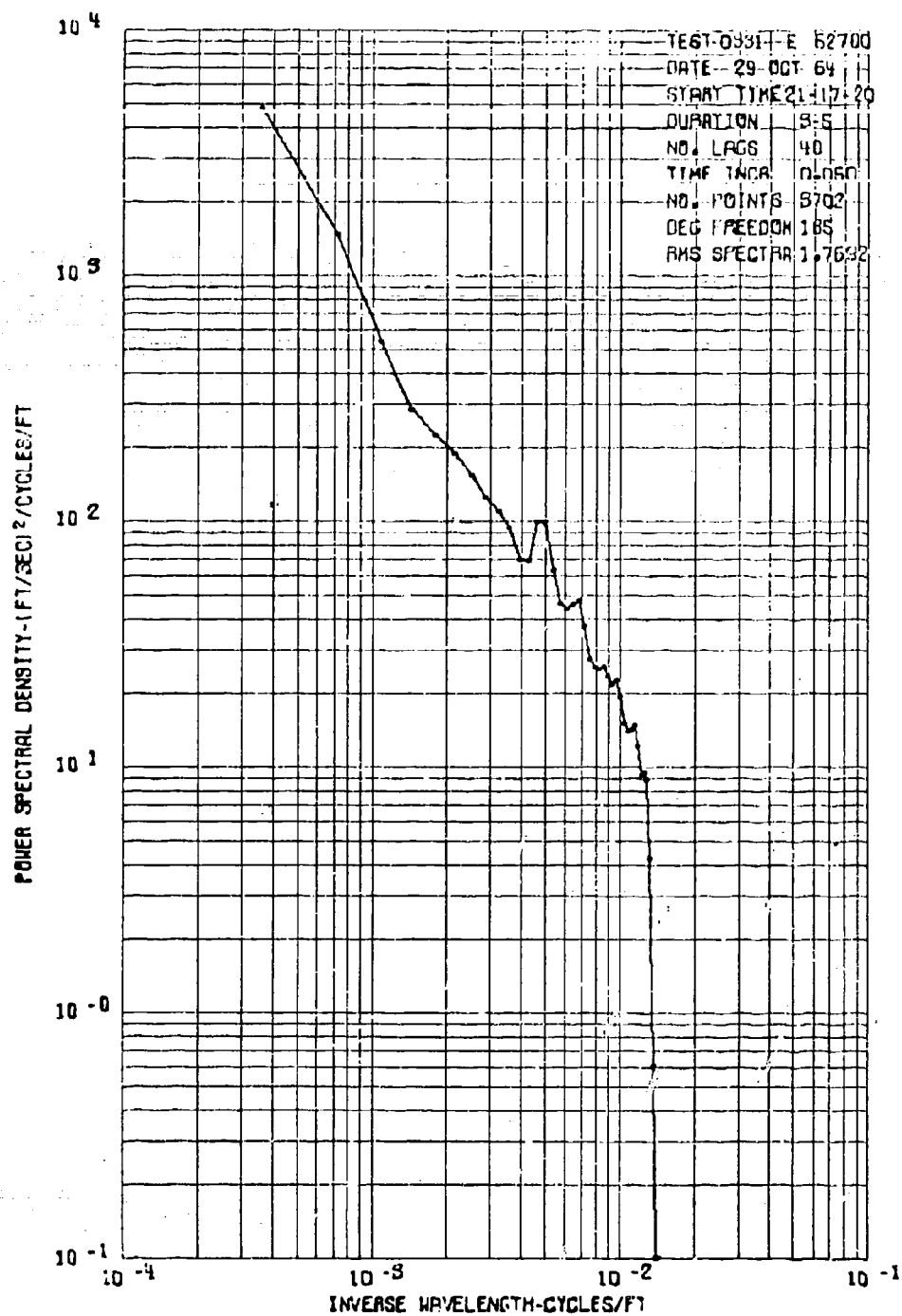
774

Figure 49. Power Spectrum of $V_T \Delta \alpha$, Test 30, Run 3



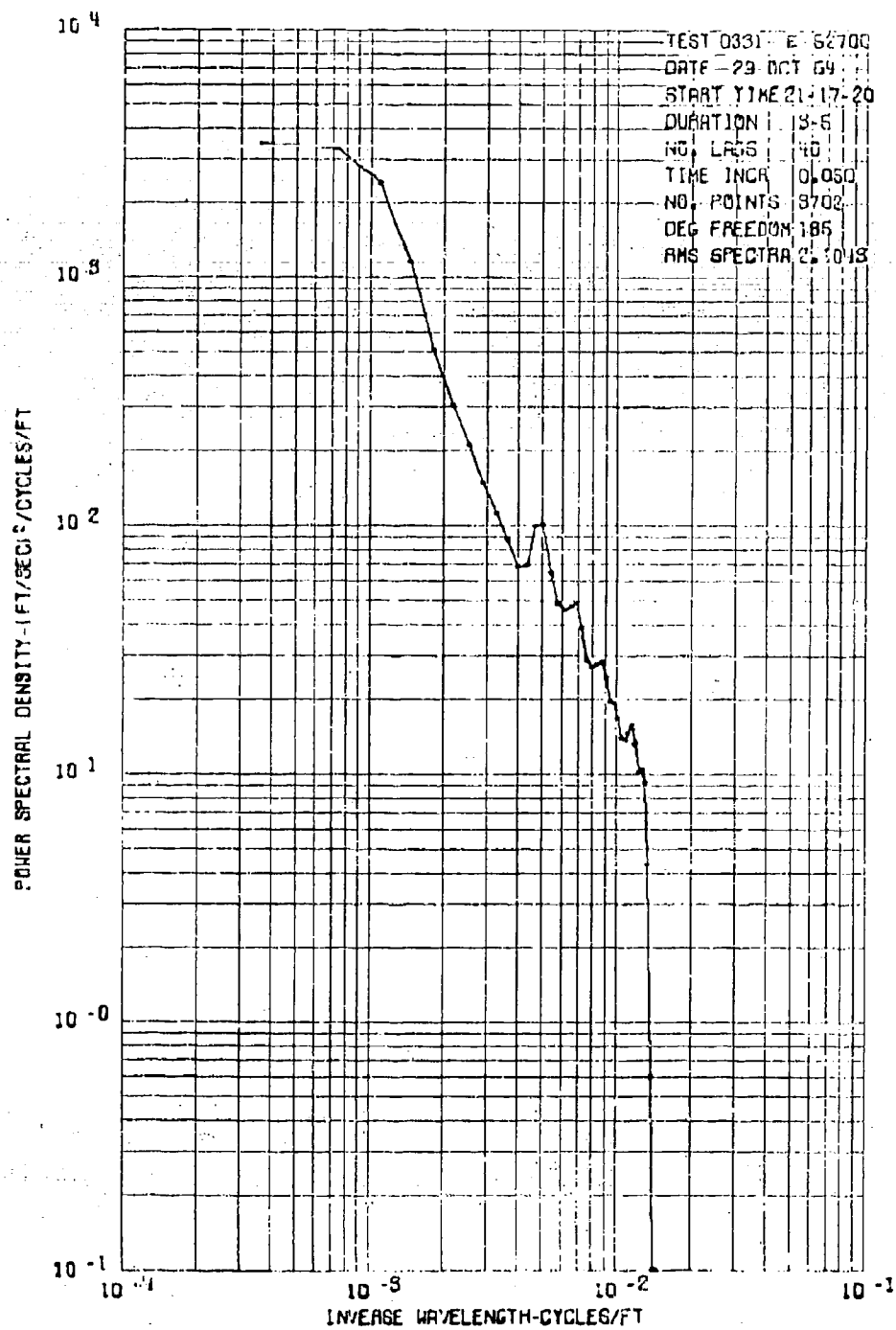
772

Figure 50. Power Spectrum of $V_T \Delta \beta$, Test 30, Run 3



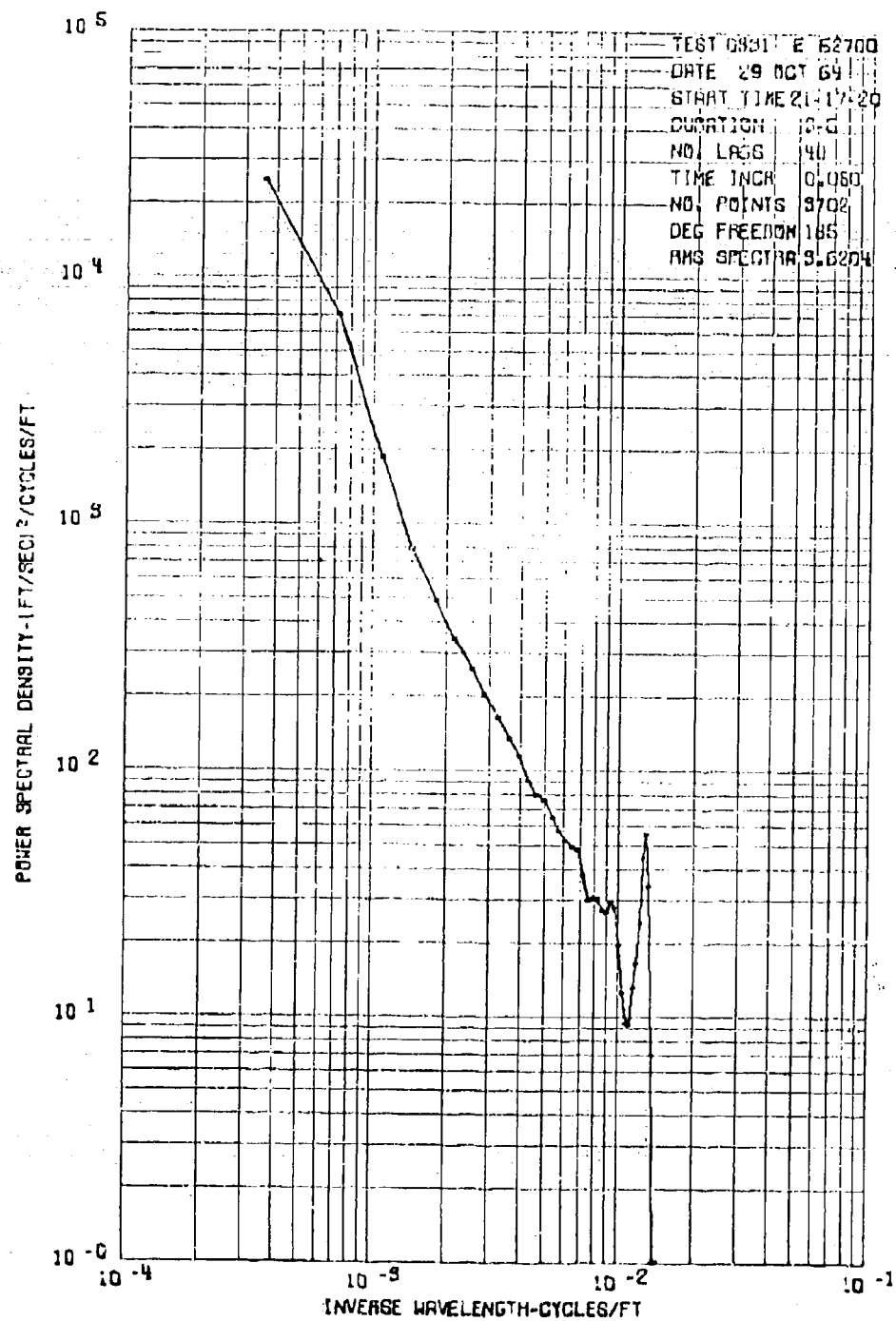
752

Figure 51. Power Spectrum of Vertical Gust Velocity, Test 33, Run 1



754

Figure 52. Power Spectrum of $V_T \Delta \alpha$, Test 33, Run 1



753

Figure 53. Power Spectrum of $V_T \Delta \beta$, Test 33, Run 1

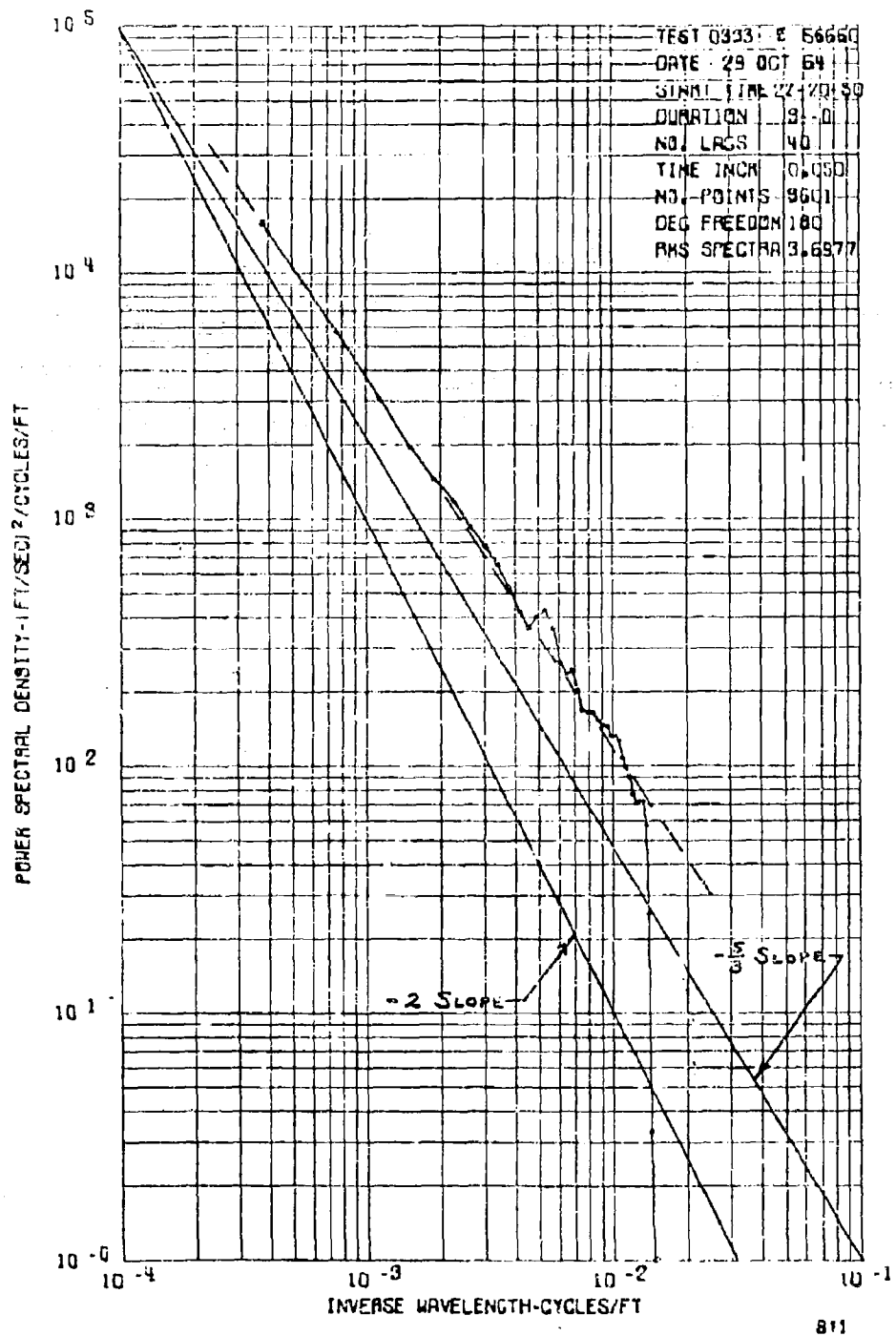
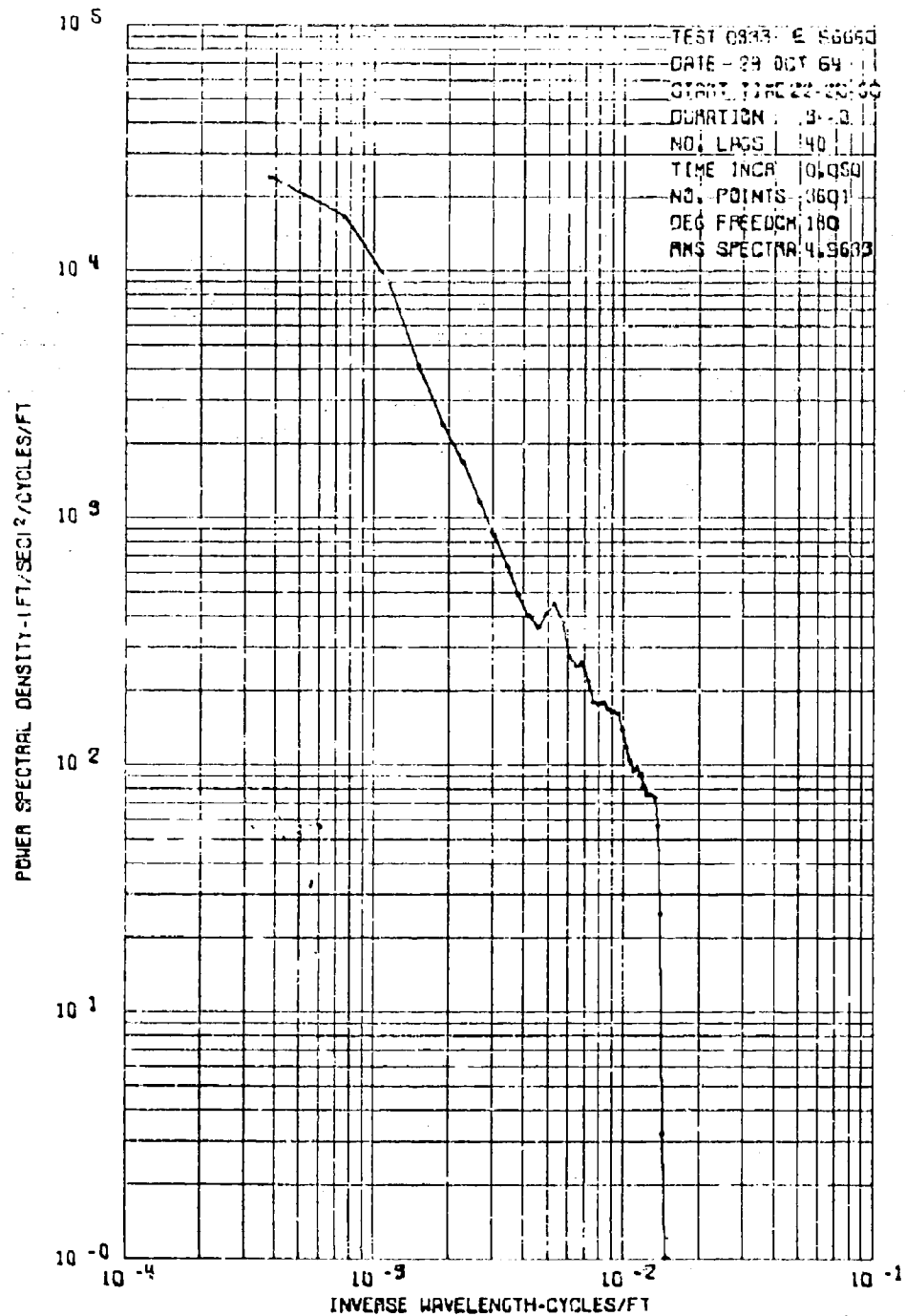
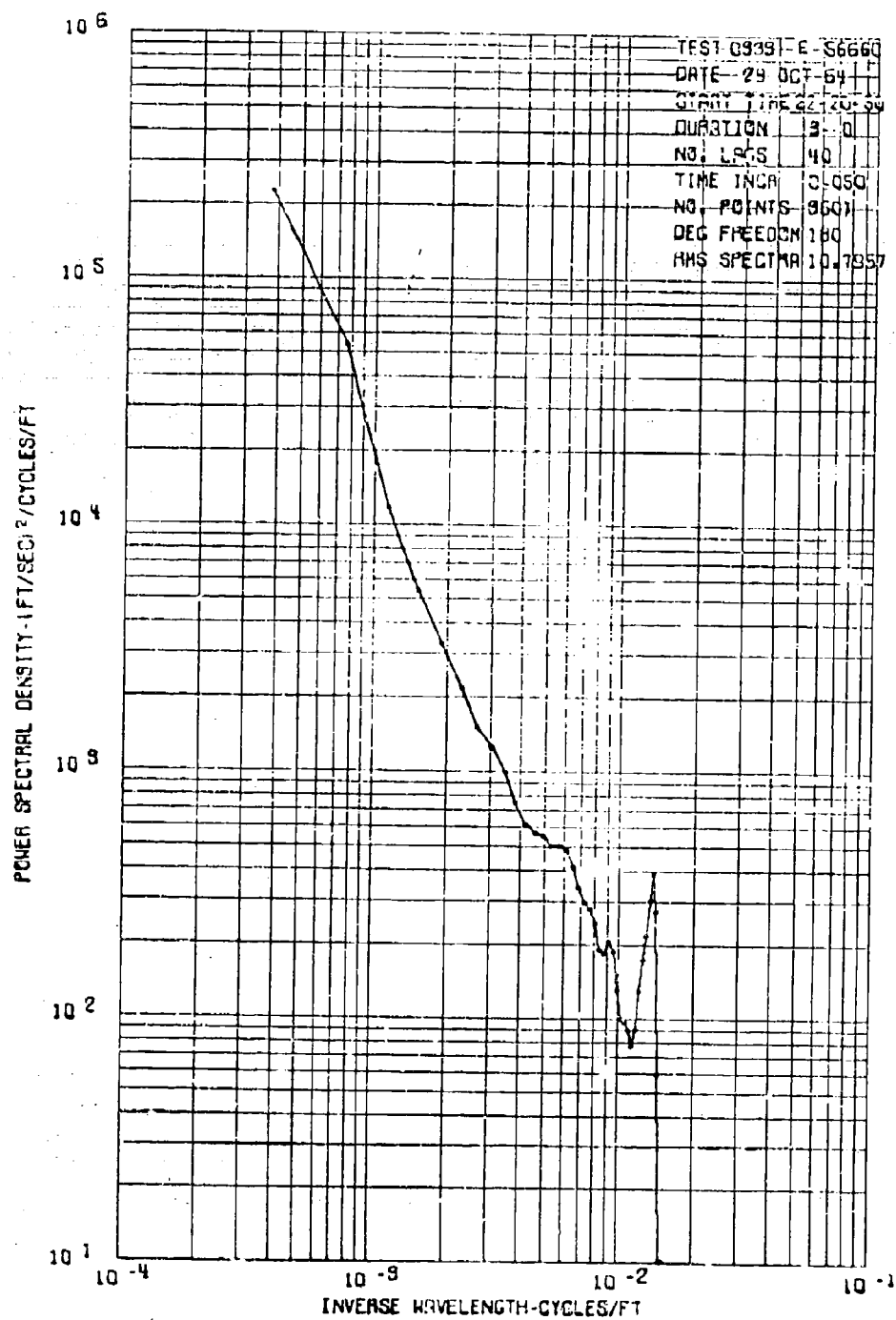


Figure 54. Power Spectrum of Vertical Gust Velocity, Test 33, Run 3



812

Figure 55. Power Spectrum of $V_T \Delta \alpha$, Test 33, Run 3



810

Figure 56. Power Spectrum of $V_{\text{IT}} \Delta \beta$, Test 33, Run 3

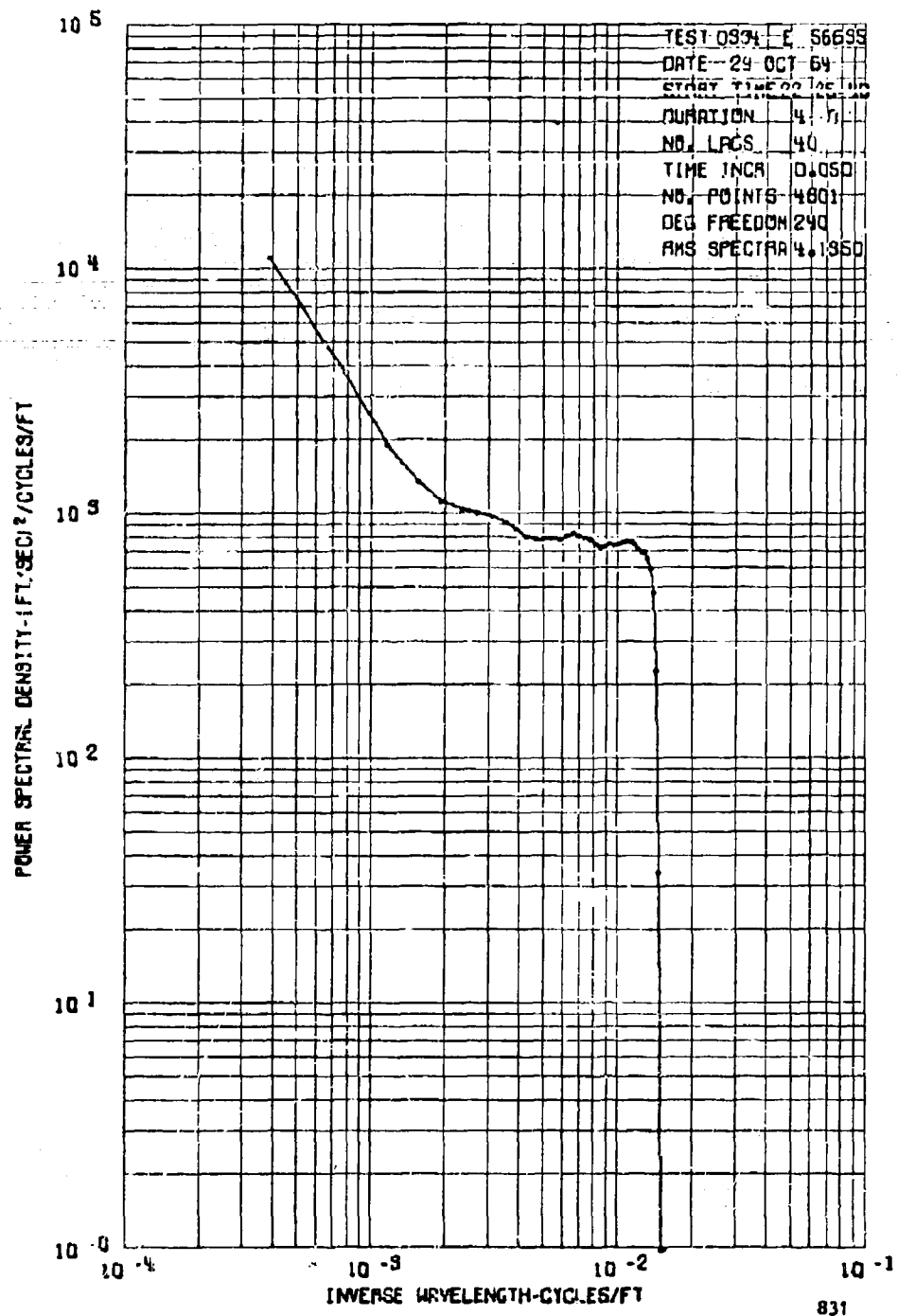
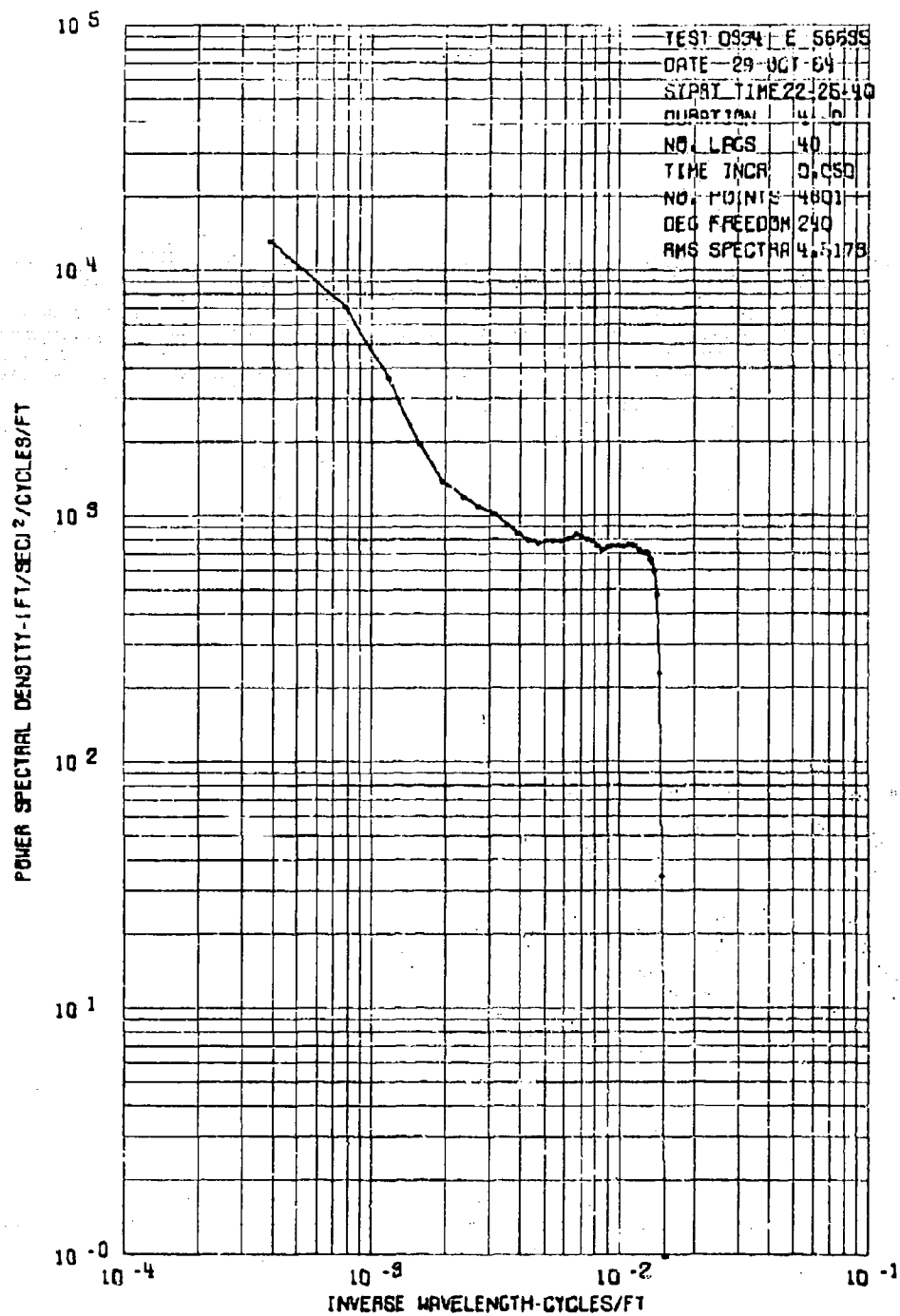


Figure 57. Power Spectrum of Vertical Gust Velocity, Test 33, Run 4



132

Figure 58. Power Spectrum of $V_T \Delta \alpha$, Test 33, Run 4

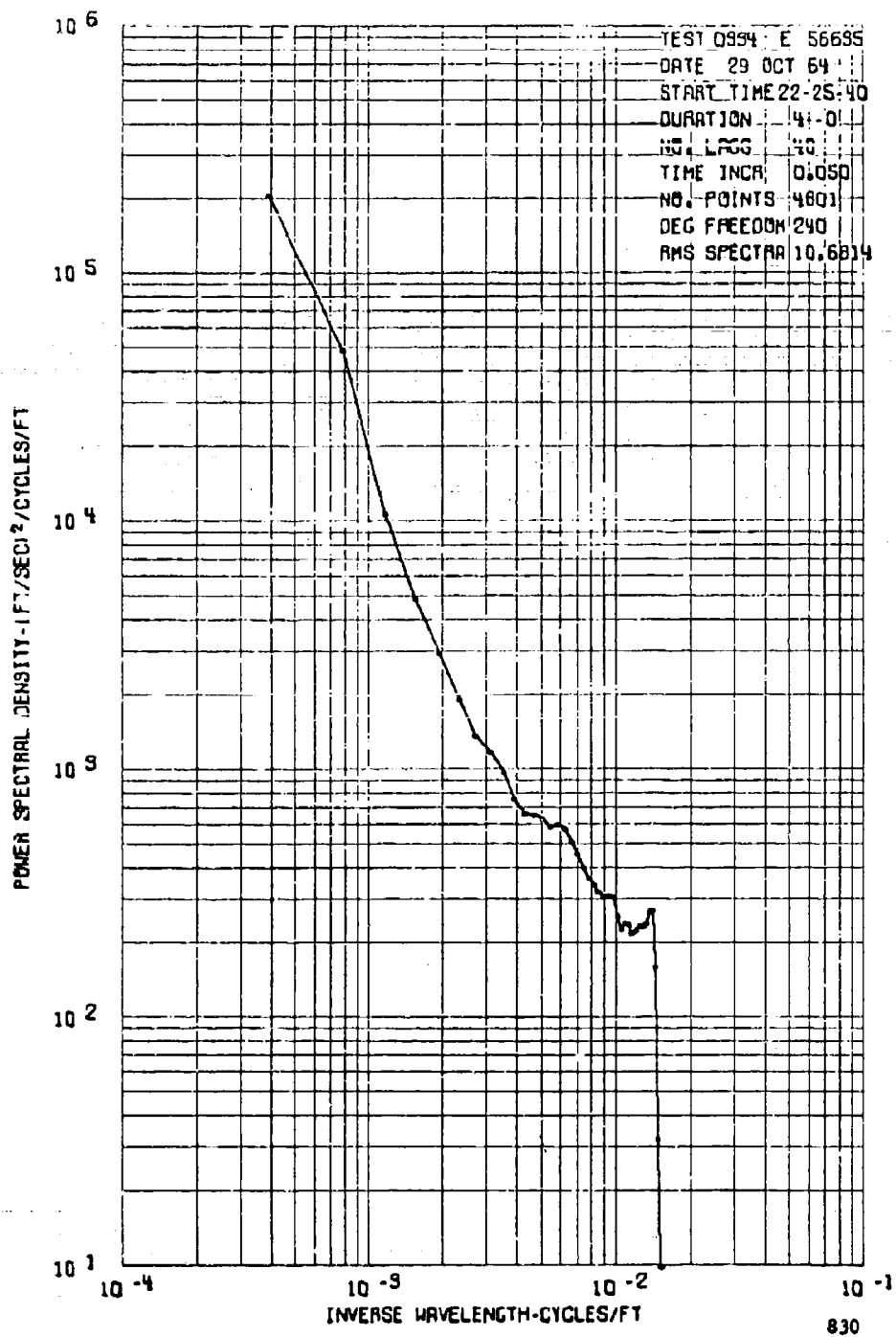


Figure 59. Power Spectrum of $V_T \Delta \beta$, Test 33, Run 4

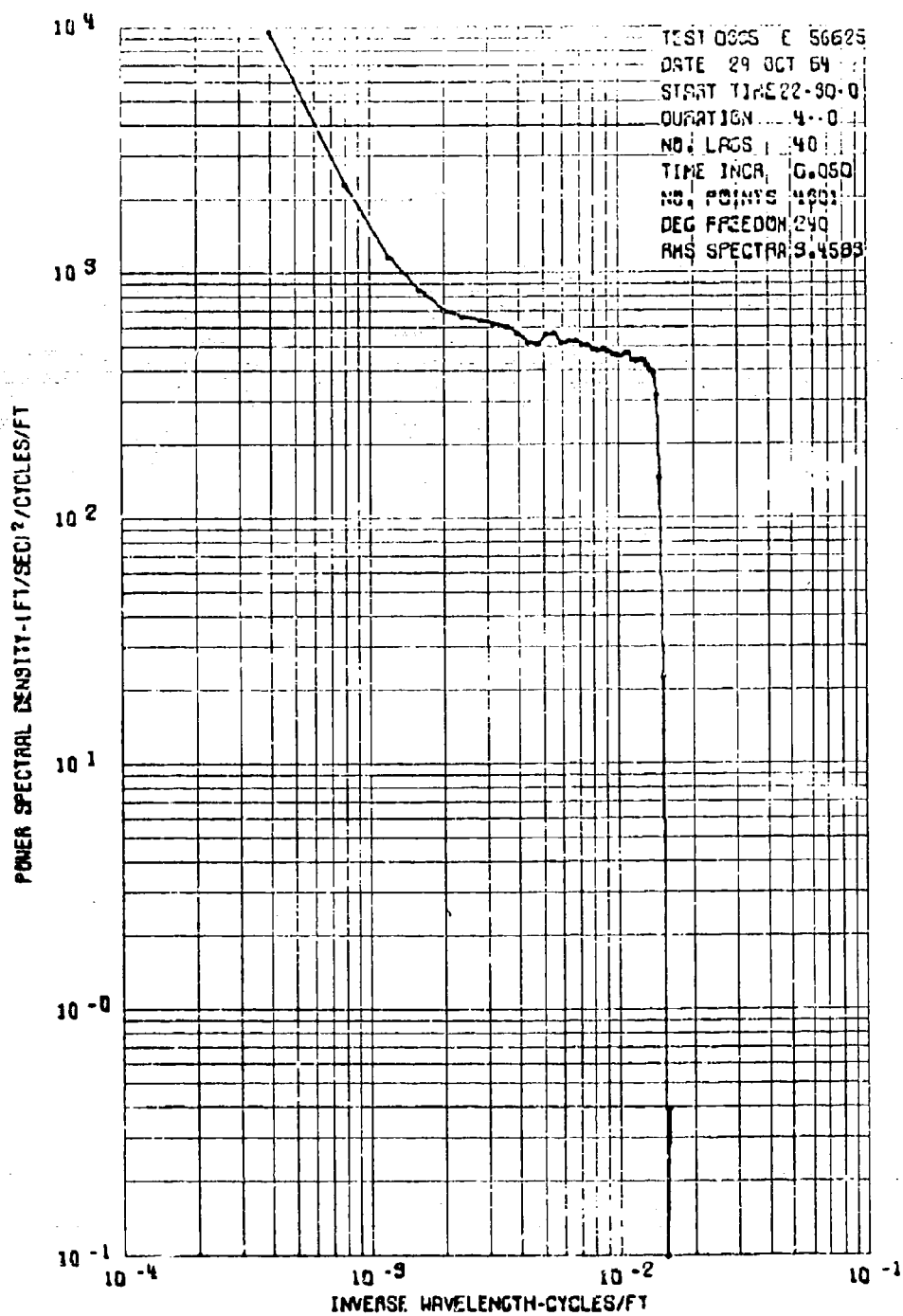
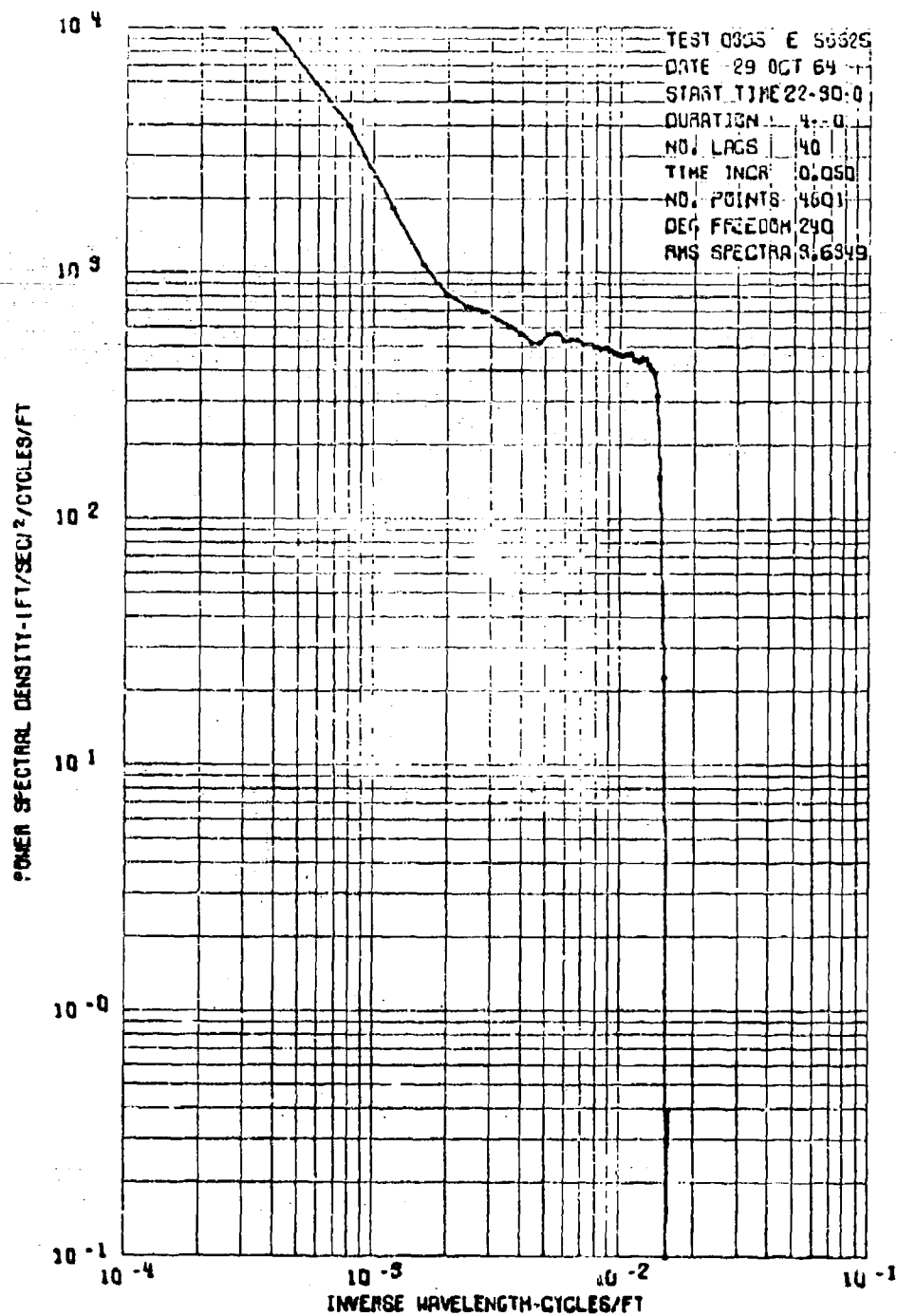


Figure 60. Power Spectrum of Vertical Gust Velocity, Test 33, Run 5



852

Figure 61. Power Spectra of $V_T \Lambda \alpha$, Test 33, Run 5

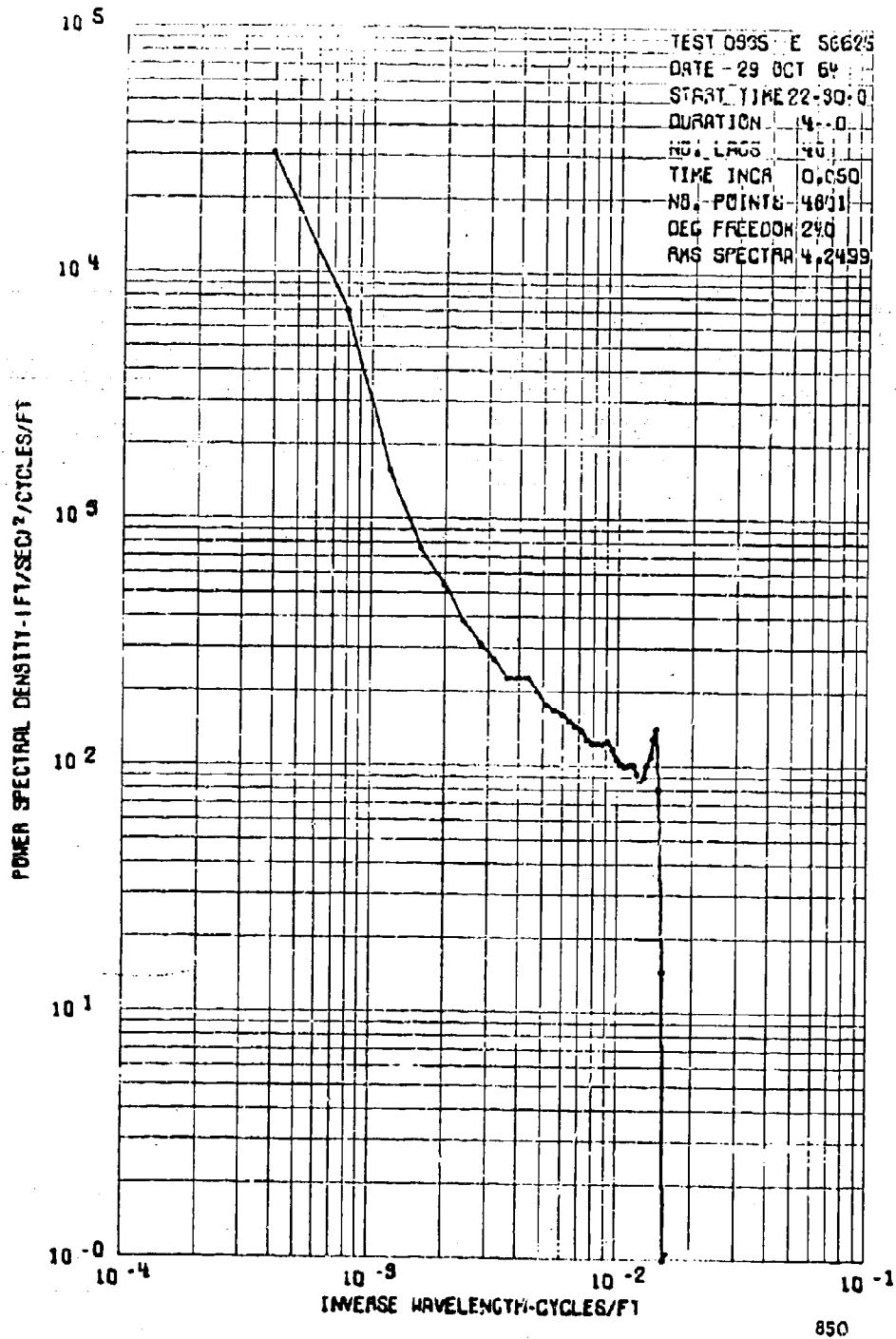
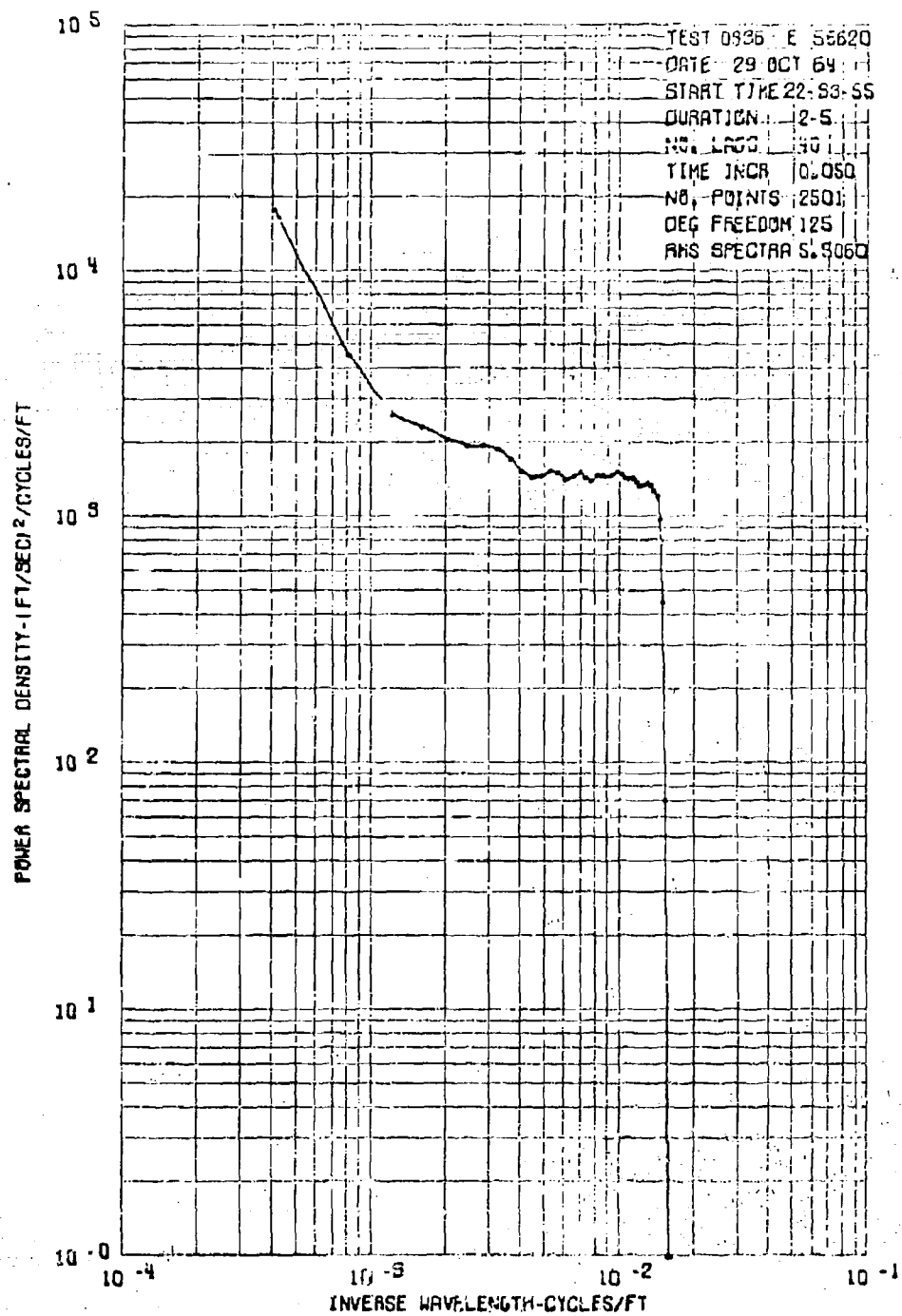


Figure 62. Power Spectrum of $V_{\eta} \Delta \beta$, Test 33, Run 5



871

Figure 63. Power Spectrum of Vertical Gust Velocity, Test 33, Run 6

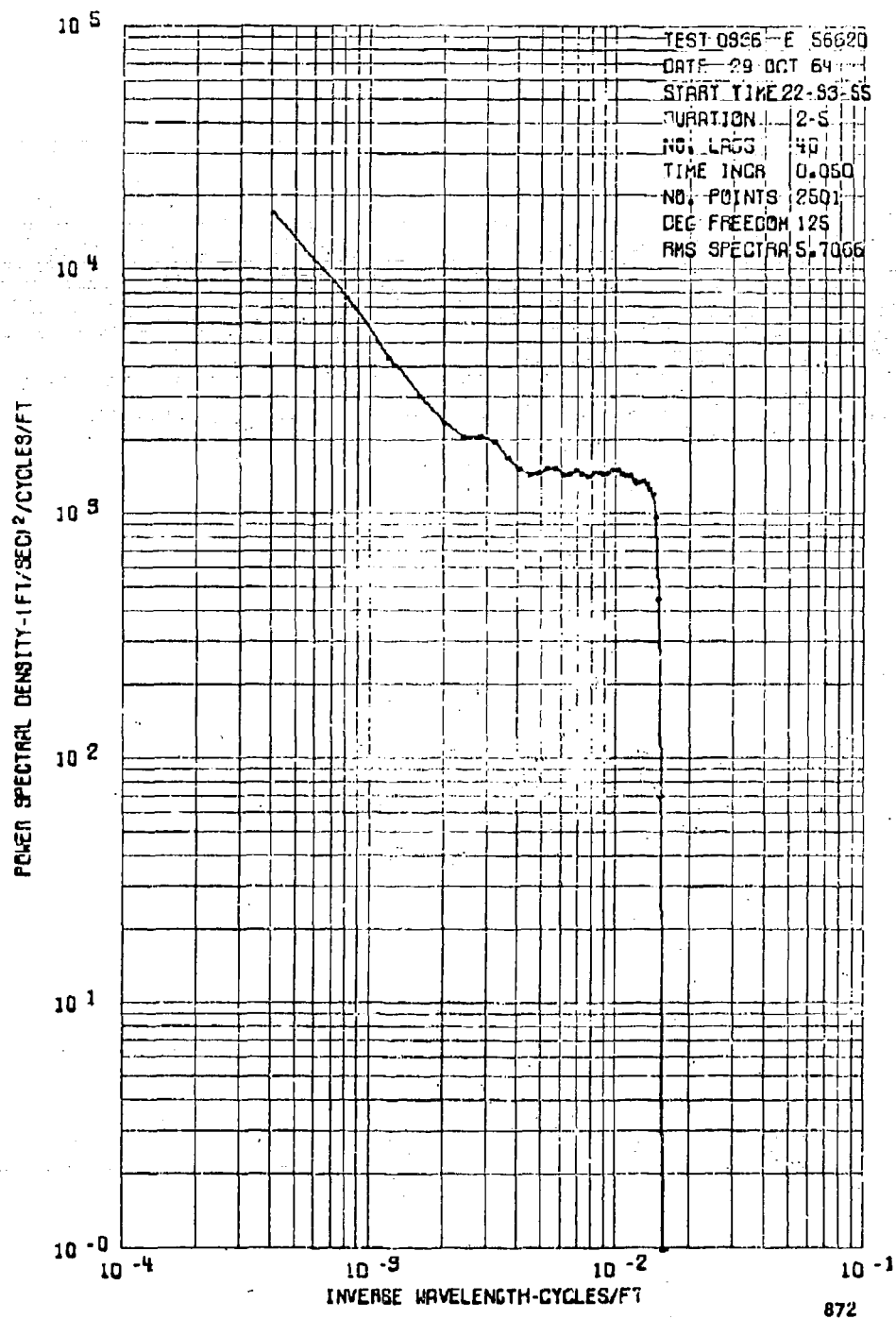
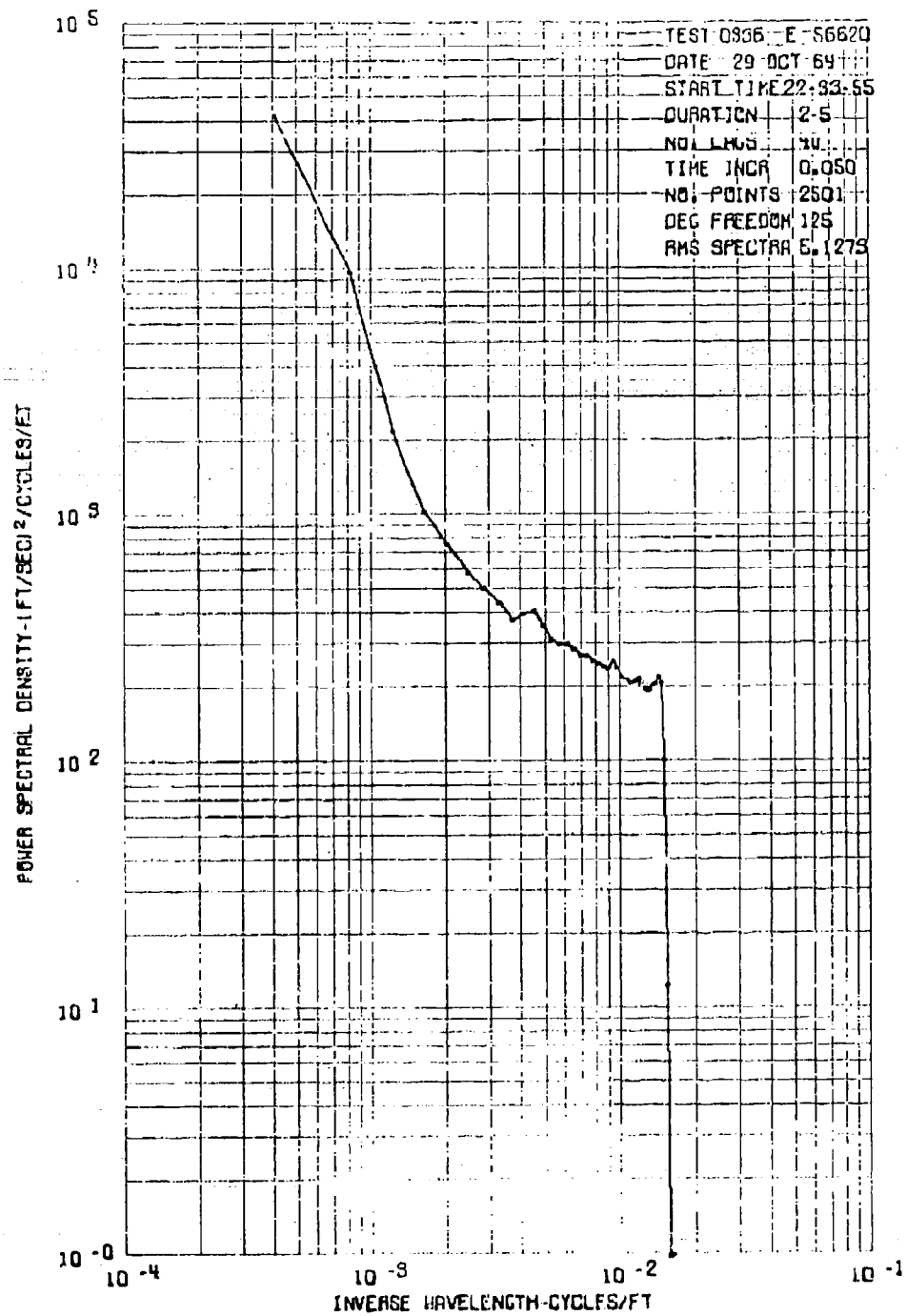
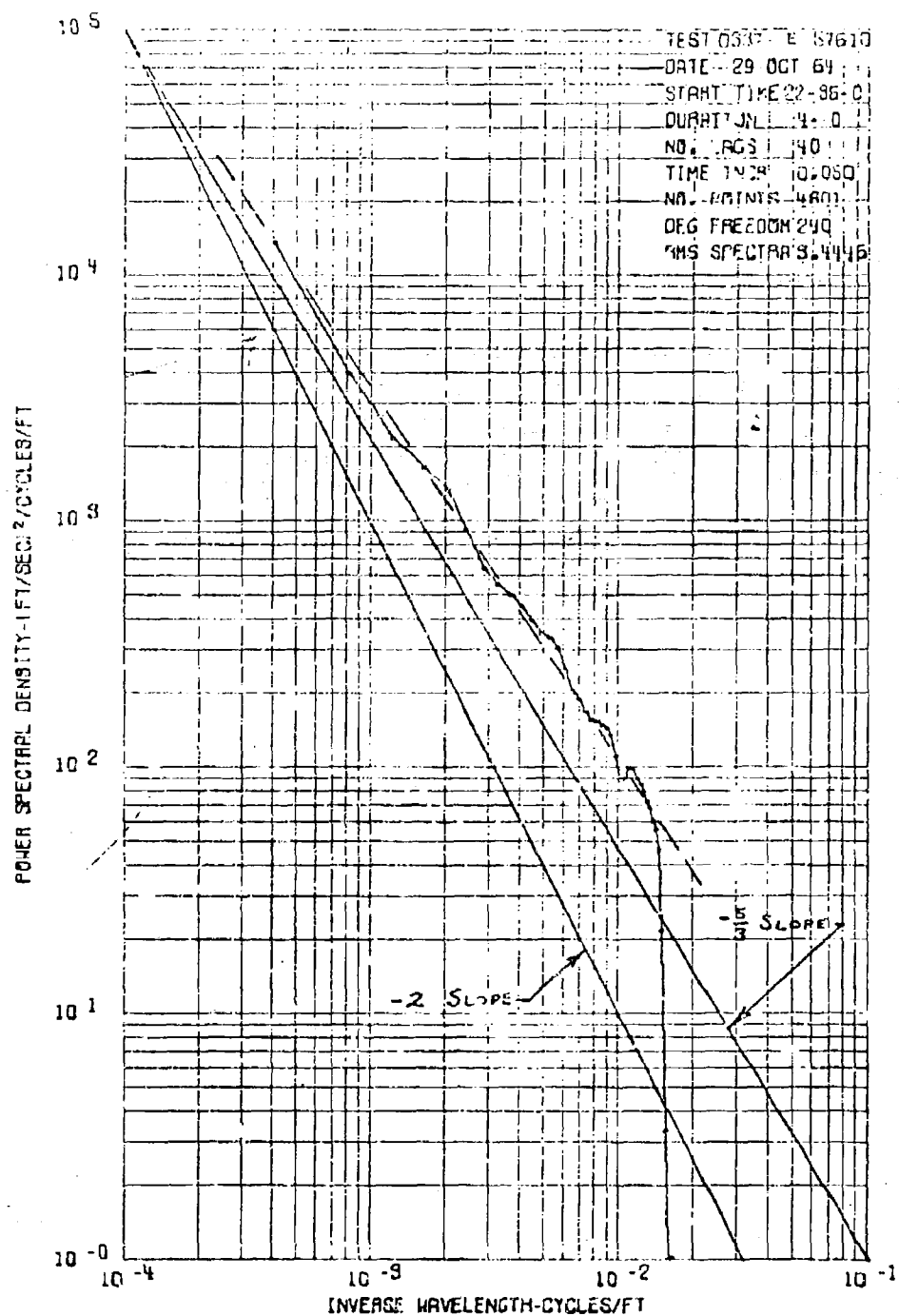


Figure 64. Power Spectrum of $V_T \Delta \alpha$, Test 33, Run 6



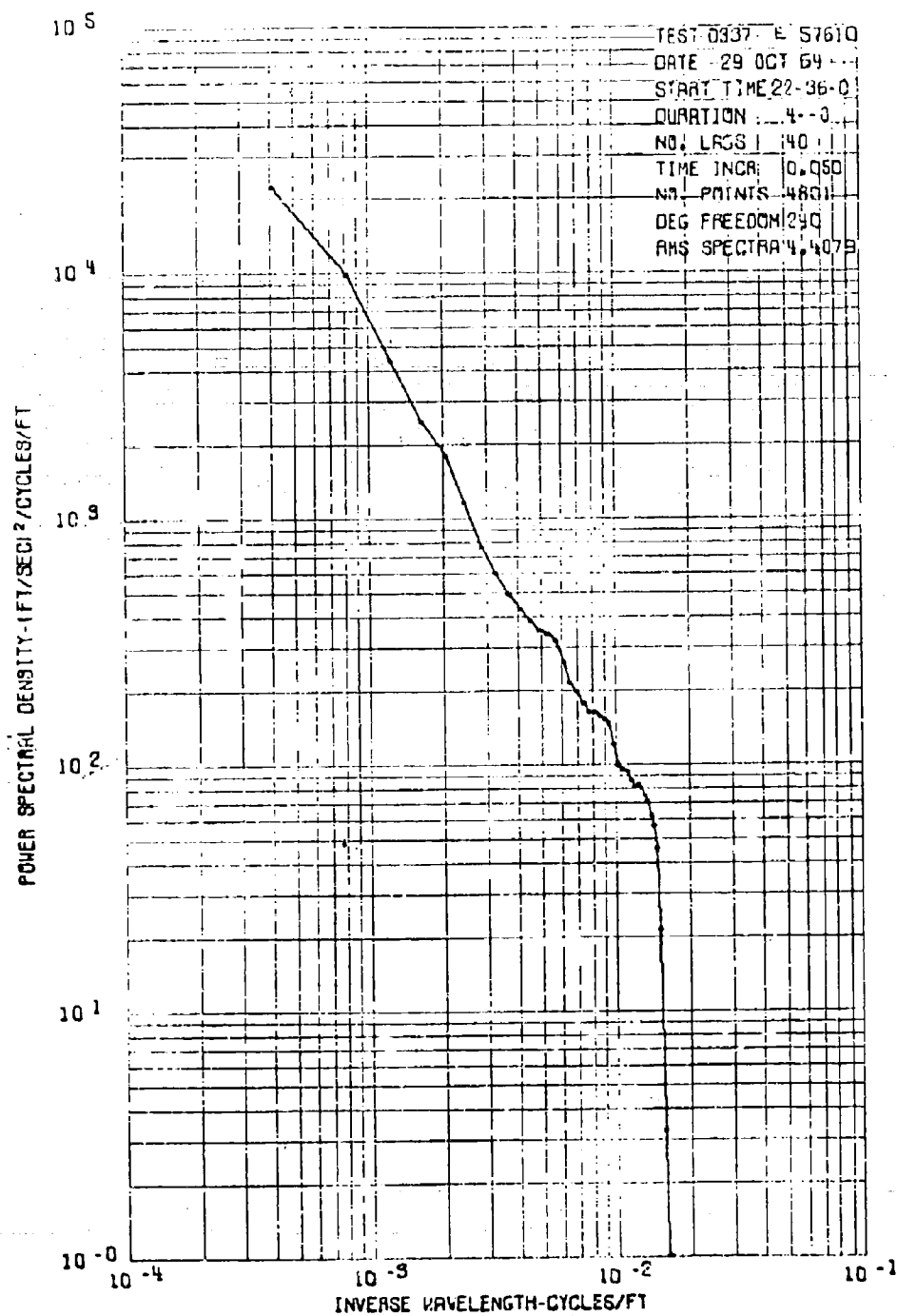
870

Figure 65. Power Spectrum of $V_T \Delta \beta$, Test 33, Run 6



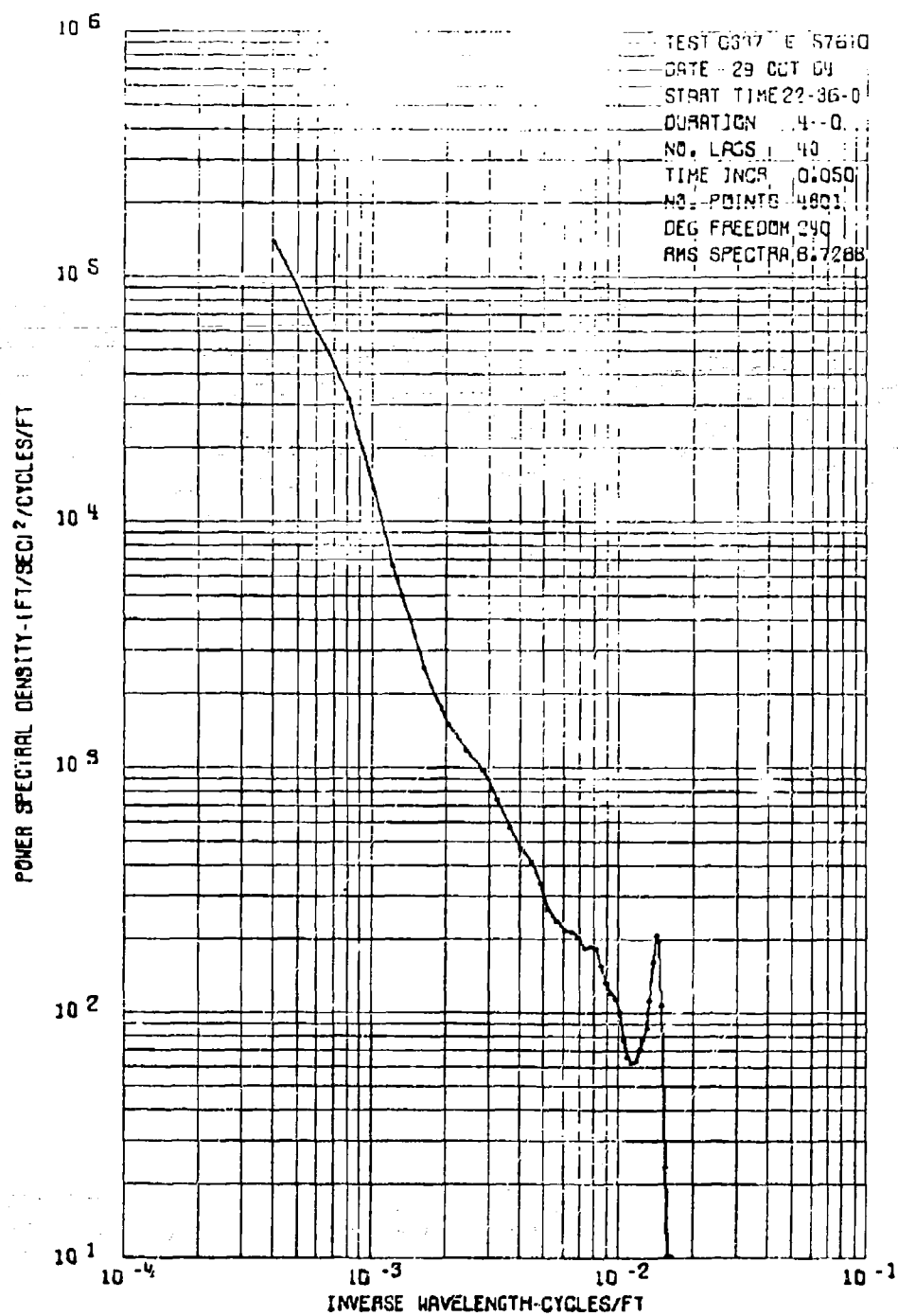
837

Figure 66. Power Spectrum of Vertical Gust Velocity, Test 33, Run 7



886

Figure 67. Power Spectrum of $V_T \Delta \alpha$, Test 33, Run 7



888

Figure 68. Power Spectrum of $V_T \Delta \beta$, Test 33, Run 7

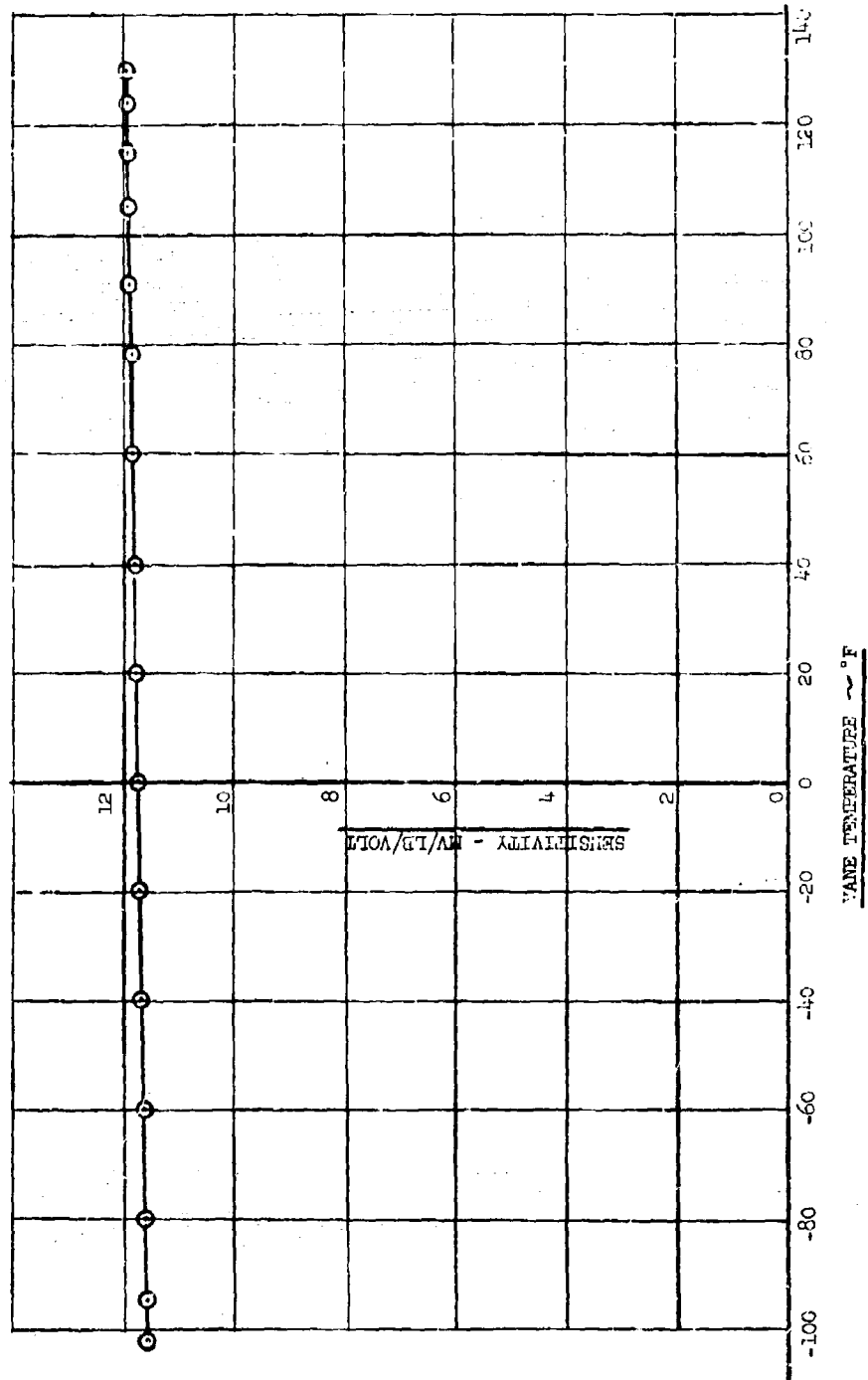


Figure 69. Sensitivity Versus Vane Temperature for Semi-Conductor Cage System

Room Temp. Properties Under Load Conditions Show:
All Loads applied by dead wt.

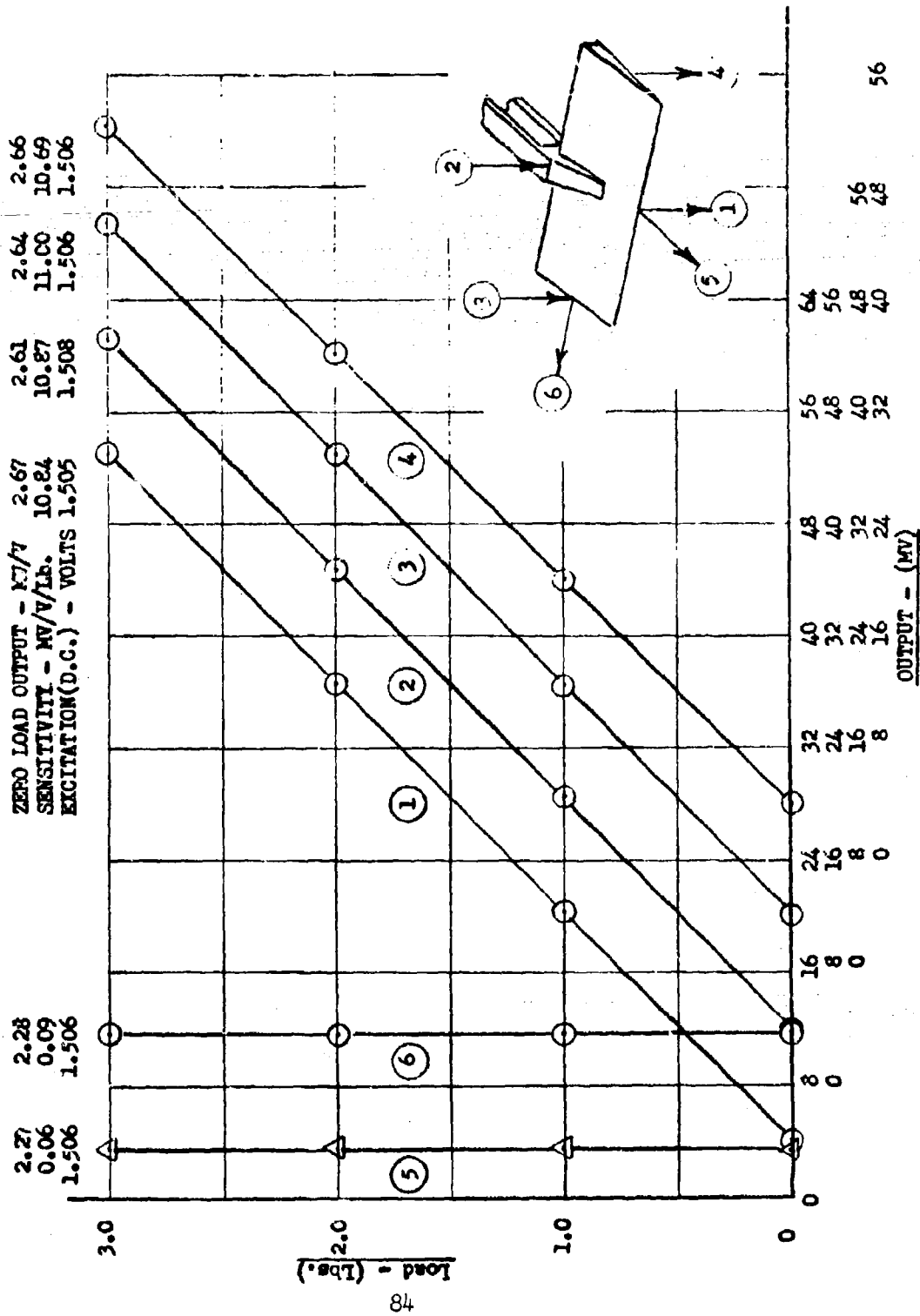


Figure 70. HICAT Gust Sensor Load Calibration ~ Vane #

APPENDIX I

HICAT GUST SENSOR SPECIFICATIONS AND CALIBRATIONS

Laboratory tests of the HICAT gust sensor have demonstrated the following capabilities:

Range:	± 12 lb
Sensitivity:	11.8 MV/LB/VOLT (DC or RMS AC) @ 78°F
Thermal Sensitivity Shift:	$+0.00154(\text{MV/LB})/^{\circ}\text{F}$ @ 1 volt or $+1.3\%/100^{\circ}\text{F}$
Thermal Zero Shift:	$.025 \text{ MV/VOLT}/^{\circ}\text{F}$ or 1.8% Full Scale/ 100°F
Test Temperature Range:	-102°F to $+130^{\circ}\text{F}$
Natural Frequency (Undamped):	170 cps
Sensor Weight Ahead of Gages:	0.0365 lb
Overall Sensor Weight:	0.25 lb

The sensor temperature and load calibration data are presented in Figures 69 and 70. The sensor load calibration responses for various combinations of loading are shown in Table IV, page 86.

TABLE IV

HICAT GUST SENSOR LOAD CALIBRATION RESPONSES

Load Condi- tion	Sensor Response (MV/V/lb.)						Deviation from Load Cond. 1 (percent)						Percent of Load Condition 1					
	Vane #3	Vane #4	Vane #5	Vane #6	Vane #3	Vane #4	Vane #5	Vane #6	Vane #3	Vane #4	Vane #5	Vane #6	Vane #3	Vane #4	Vane #5	Vane #6	Vane #3	Vane #6
1	10.85	10.84	10.71	11.84	0	0	0	0	100.00	100.00	100.00	100.00	100.00	100.00	100.00	100.00	100.00	100.00
2	10.86	10.87	10.68	11.84	0.09	0.28	-0.28	0.00	100.09	100.28	99.72	100.00	100.09	100.28	99.72	100.00	100.09	100.00
3	10.86	11.00	10.82	12.02	0.09	1.48	1.03	1.52	100.09	101.48	101.03	101.52	100.09	101.48	101.03	101.52	100.09	101.52
4	10.94	10.69	10.57	11.72	0.83	-1.38	-1.31	-1.01	100.83	98.62	98.69	98.99	100.83	98.62	98.69	98.99	100.83	98.99
5	0.10	0.06	-0.03	-0.02	-	-	-	-	0.92	0.55	-0.28	-0.17	0.92	0.55	-0.28	-0.17	0.92	-0.17
6	0.00	0.09	0.21	0.00	-	-	-	-	0.00	0.83	1.96	0.00	0.00	0.83	1.96	0.00	0.00	0.00

Note: 1,2 Vertical Load ~ Moment Arm Varied
 3,4 Torsion Load ~ Torque Direction Varied
 5 Fore-and-Aft Load
 6 Side Load
 — See loading diagram in Figure 70.

APPENDIX II

HICAT FLIGHT TEST LOG
AND TRACK MAPS

TABLE V

HICAT FLIGHT TEST LOG

TEST*	DATE	PILOT	PURPOSE	FLIGHT TIME (Hr:Min)(Hr:Min)	REMARKS
1	2-20-64	Capt. R. B. Lovell	Engine Functional Check. Gust Probe Instrumentation Check.	1:55 0	Gust probe varies and boom accelerations satisfactory. Pilots altimeter malfunctioned.
2	2-27-64	Lt. Col. H. Andonian	Engine Functional Check. Gust Probe Instrumentation Check.	1:40 0	Gust probe causes airspeed fluctuations several times larger than normal in yawing maneuvers.
3	3-13-64	Capt. W. H. Shawler	Airspeed System Check (Gust Probe Removed).	1:05 0	Airspeed fluctuations in yawing maneuvers less than with probe on.
4	3-17-64	Capt. W. H. Shawler	Airspeed System Check. Low Altitude Gust Penetration.	2:20 0	Comment for T-2 confirmed. C.G. accelerometer malfunction.
5	3-20-64	Capt. W. H. Shawler	Stick and Rudder Pulses. Roller Coaster Maneuvers	1:00 0	Stick and rudder pulses o.k. Roller coaster too abrupt, N.J.
6	3-31-64	Capt. R. B. Lovell	Stick and Rudder Pulses. Roller Coaster Maneuvers.	1:15 0	Alpha-vane force circuit failure. Maneuvers appear satisfactory.
7	4-03-64	Capt. R. B. Lovell	HICAT Search #1 (Altitude Above 50,000')	5:00 0:30	Found light turbulence over White Mountains in Nevada. Pilot reported C.G. acceleration: Max/Min = 1.0 + .5% Oscillator power supply failed near end of flight.
Subtotal:	7			14:15 0:30	
Subtotal:	1			5:00 0:30	

* Test numbers correspond to those flights by Ship No. 65722 for which HICAT Instrumentation Package was installed and a tape recording made.

TABLE V. HICAT FLIGHT TEST LOG (Cont'd.)

TEST#	DATE	PILOT	PURPOSE	FLIGHT HICAT TIME		REMARKS
				(H:MM)	(EST:MM)	
8	4-10-64	Capt. R. B. Lowell	HICAT Search #2	3:00	0:15	Encountered light turbulence at 60,000'. Used B-47 as chase and turbulence scout.
9	4-15-64	Capt. R. B. Lowell	Checkout new fuel control - HICAT roller coaster maneuvers	1:30	0	Mainly a fuel control test flight.
10	4-21-64	Capt. R. B. Lowell	HICAT Search #3	3:20	0:25	Local area flight, some light turbulence over Ely, Nevada.
11	4-24-64	Capt. W. H. Shawler	HICAT Search #4	2:35	0**	Jetstream activity near Edwards AFB. Connector failed such that both vanes and tape speed compensation inoperative. No useable data.
12	4-29-64	Lt. Col. E. Andonian	HICAT Search #5	2:10	0:37	Local area flight. Light turbulence encountered at 65,000'. Last flight before aircraft periodic inspection.
Subtotal	12			26:50	1:43	
Subtotal Searches only)	5			16:05	1:43	

* Test numbers correspond to those flights by Ship No. 66722 for which HICAT Instrumentation Package was installed and a tape recording was made.

** Gust velocities permanently lost; however, VGH data may be recoverable with special processing.

TABLE V. HICAT FLIGHT TEST LOG (Cont'd.)

TEST*	DATE	PILOT	PURPOSE	FLIGHT TIME (Hr:Min)	HICAT TIME (Hr:Min)	REMARKS
13	5-12-64	Lt. Col. H. Andonian	Functional Check	2:00	0	Slight local turbulence over Mono Lake.
14	5-15-64	Lt. Col. H. Andonian	Armed Forces Day Air Show Rehearsal	1:15	0	Instrumentation exercise, no calibration.
15	5-16-64	Lt. Col. H. Andonian	Armed Forces Day Air Show	1:20	0	Instrumentation exercise, no calibration.
16	5-18-64	Capt. R. E. Lovell	Transcontinental Ferry Flight Edwards AFB, Calif. to Patrick AFB, Fla.	5:10	0	Smooth, no turbulence.
17	5-21-64	Capt. R. B. Lovell	HICAT Search #6 (from PAFB)	3:40	0:12	Some slight turbulence at 51,000 ft. over the Bahamas.
18	5-28-64	Capt. R. B. Lovell	HICAT Search #7 (from PAFB)	3:15	0:24	Light turbulence over the Bahamas. C. G. accelerometer failure due to water (condensate) in connector.
19	6-04-64	Capt. R. B. Lovell	HICAT Search #8 (from PAFB)	3:15	0	No significant turbulence encountered.
20	6-08-64	Capt. R. B. Lovell	HICAT Search #9 (from PAFB)	4:00	0:32	Light turbulence over Florida and Gulf. Max. MC = +.5 g. Evon accelerometer circuit failed near end of flight.
Subtotal				50:45	2:56	
Subtotal				30:15	2:56	
Searches only)						

* Test numbers correspond to those flights by Ship No. 66722 for which HICAT Instrumentation Package was installed and a tape recording made.

TABLE V. HICAT FLIGHT TEST LOG (Cont'd.)

TEST#	DATE	PILOT	PURPOSE	FLIGHT TIME (hr:min)	HICAT TIME (hr:min)	REMARKS
21	6-15-64	Capt. R.B. Lowell	Overseas Ferry Flight Patrick AFB, Fla. to Ramey AFB, Puerto Rico	2:45	0:11	Light turbulence at 50,000 ft. Approx. $\pm 3g$ max C.G. accel.
22	6-18-64	Capt. R.B. Lowell	HICAT Search #10 (from Ramey AFB)	3:05	0:08	Very light turbulence near Guadeloupe at 50 and 58,000 ft. ($\pm 2g$ max). No clouds.
23	6-19-64	Capt. V. E. Shawler	HICAT Search #11 (from Ramey AFB)	2:10	0	No turbulence encountered. Ot- side air temp. probe failed.
24	6-23-64	Capt. R. B. Lowell	HICAT Search #12 (from Ramey AFB)	2:45	0	No turbulence encountered. Yaw attitude gyro failed.
25	6-26-64	Capt. R.B. Lowell	HICAT Search #13 (from Ramey AFB)	3:25	0:49	Light to moderate turbulence en- countered ($\pm 3g$ at 50,000 ft.) for about half hour.
26	7-1-64	Lt. Col. H. Andonian	HICAT Search #14 (from Ramey AFB)	3:45	0:44	Light to moderate turbulence at 51,000 ft. associated with storm cloud buildup near St. Martin ($\pm 5g$) New OAT probe installed.
27	7-2-64	Capt. W. H. Shawler	HICAT Search #15 (from Ramey AFB)	4:00	0:58	Moderate turbulence ($\pm 3g$ to $\pm 7g$) encountered south of Hispaniola above clouds.
28	7-6-64	Lt. Col. H. Andonian	HICAT Search #16 (from Ramey AFB)	3:30	0:25	Very light turbulence south of Puerto Rico near high altitude inversion ($\pm 2g$). Gust vane load sensitivity increased to ± 2 lb and new pitch and roll attitude gyro installed.
Subtotal 28				7:10	6:11	
Subtotal 16 (Searches only)				52:55	6:00	

* Test numbers correspond to those flights by Ship No. 66722 for which HICAT Instrumentation Package was installed and a tape recording made.

TABLE V. HICAT FLIGHT TEST LOG (Cont'd.)

TEST*	DATE	PILOT	PURPOSE	FLIGHT TIME (H:Min)(H:Min)	REMARKS
29	7-7-64	Capt. V. H. Shawler	HICAT Search #17 (from Ramey AFB)	4:35 0	No significant turbulence.
30	7-15-64	Capt. V. H. Shawler	HICAT Search #18 (from Ramey AFB)	3:05 0:08	Local flight, light turbulence
31	7-16-64	Capt. R. B. Lovell	Overseas Ferry Flight Ramey AFB, Puerto Rico to Patrick AFB, Florida	2:50 0:34	Light turbulence.
32	7-17-64	Capt. R. B. Lovell	Transcontinental Ferry Flight, Patrick AFB, Florida to Edwards AFB, California	5:00 0	No turbulence.
33	10-29-64	Capt. V. H. Shawler	Engine and HICAT Calibrator Functional Check	2:45 0:33	Calibrator actuated at 15 minute intervals throughout flight. Moderate turbulence encountered above 50,000 ft in Sierra Nevada. Electrical power failure near end of flight.
Subtotal 33				94:25 7:26	
Subtotal 18 (Searches only)				60:35 6:08	

* Test numbers correspond to those flights by Ship No. 66722 for which HICAT Instrumentation Package was installed and a tape recording made.

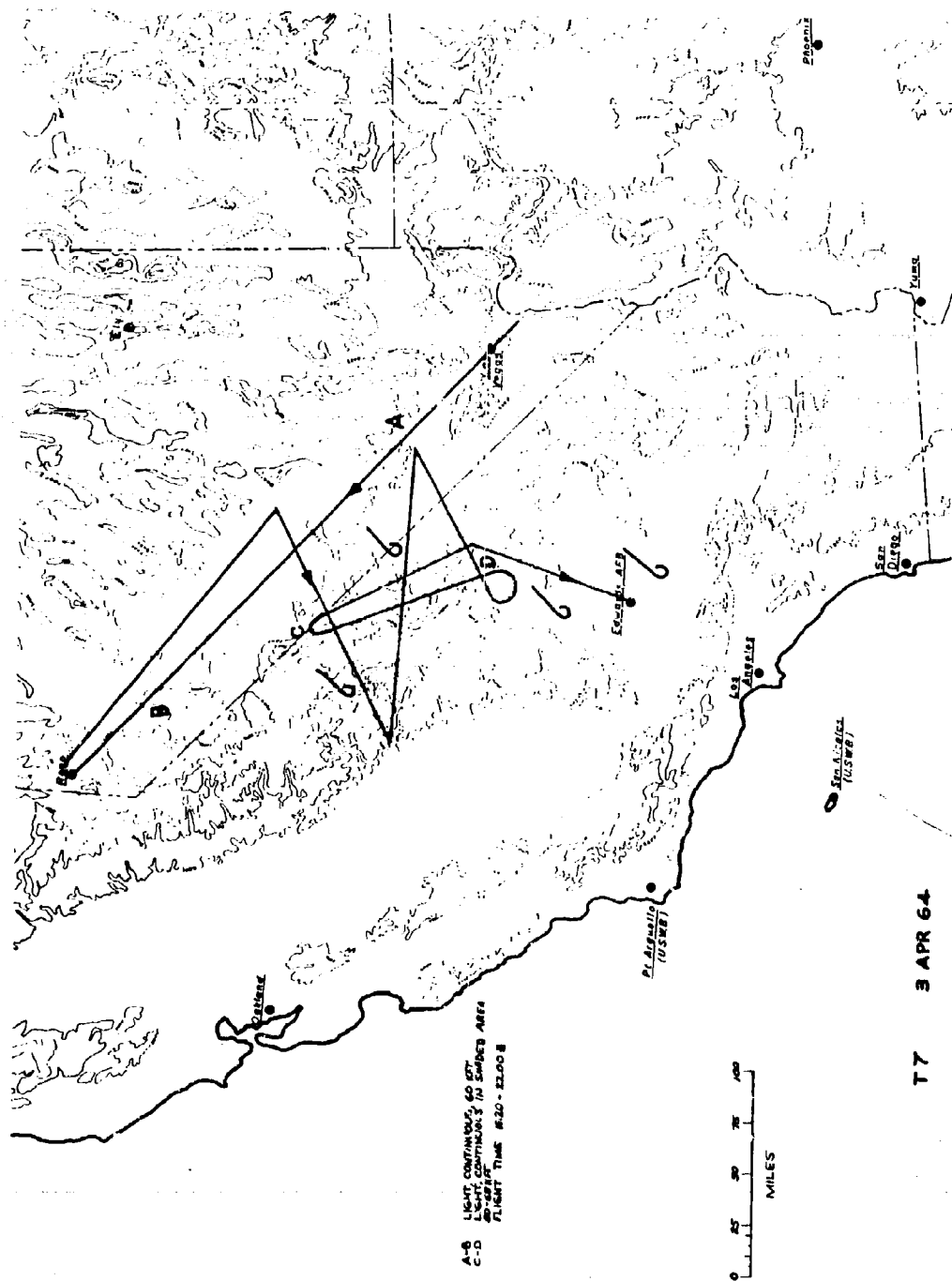


Figure 7. HICAT Track Map, Test 7

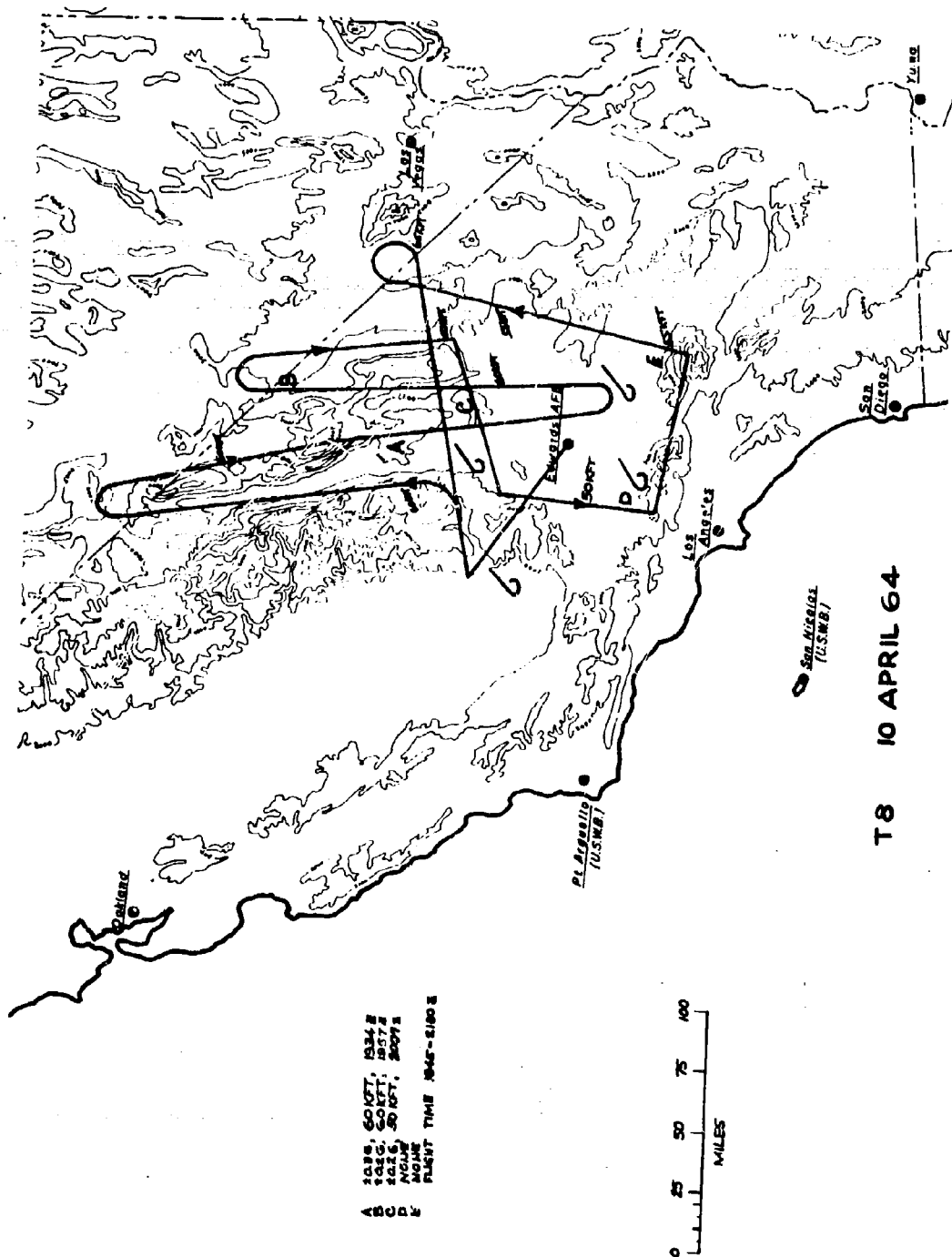


Figure 72. HICAT Track Map, Test 8

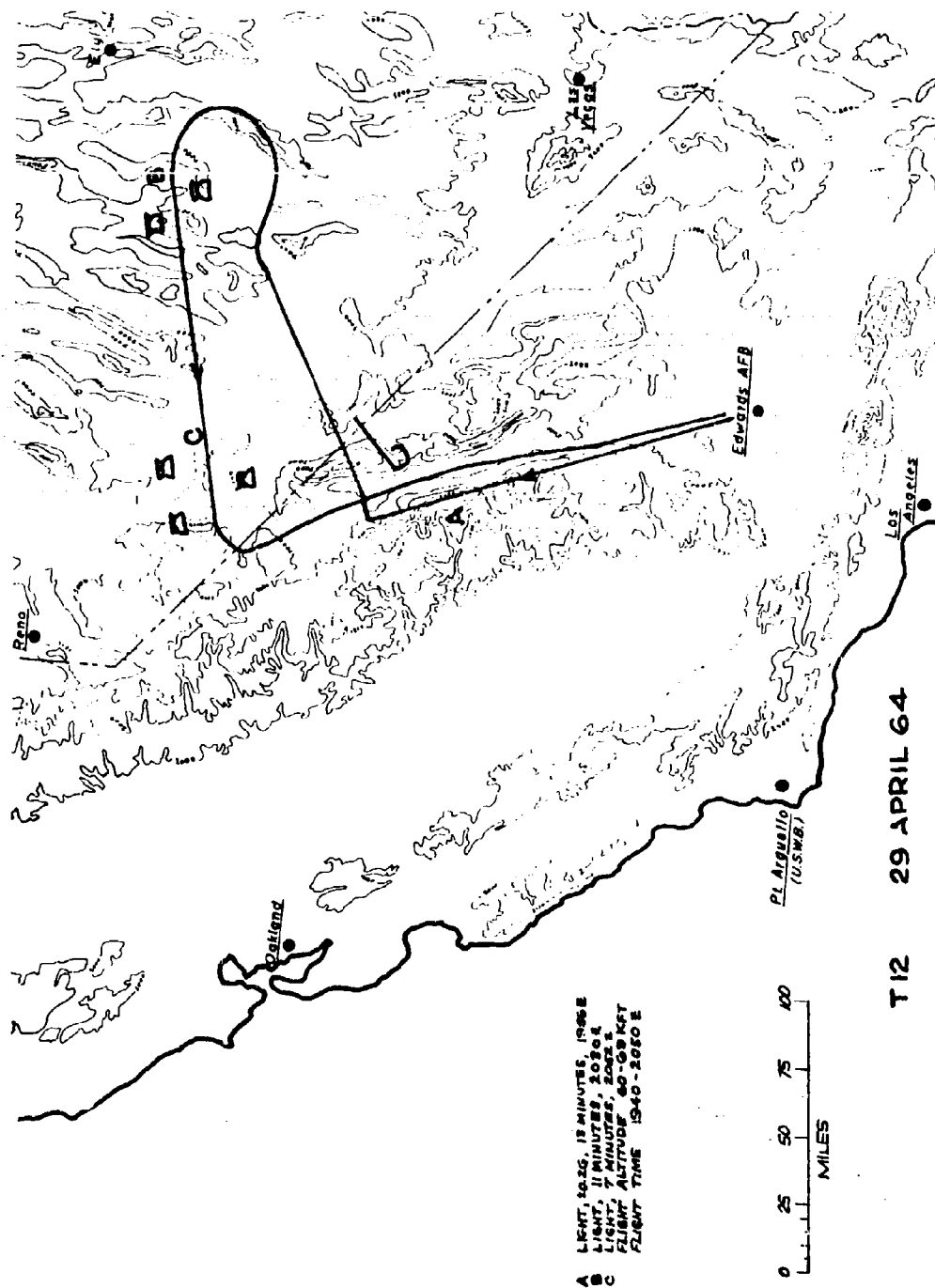


Figure 75. HICAT Track Map, Test 12

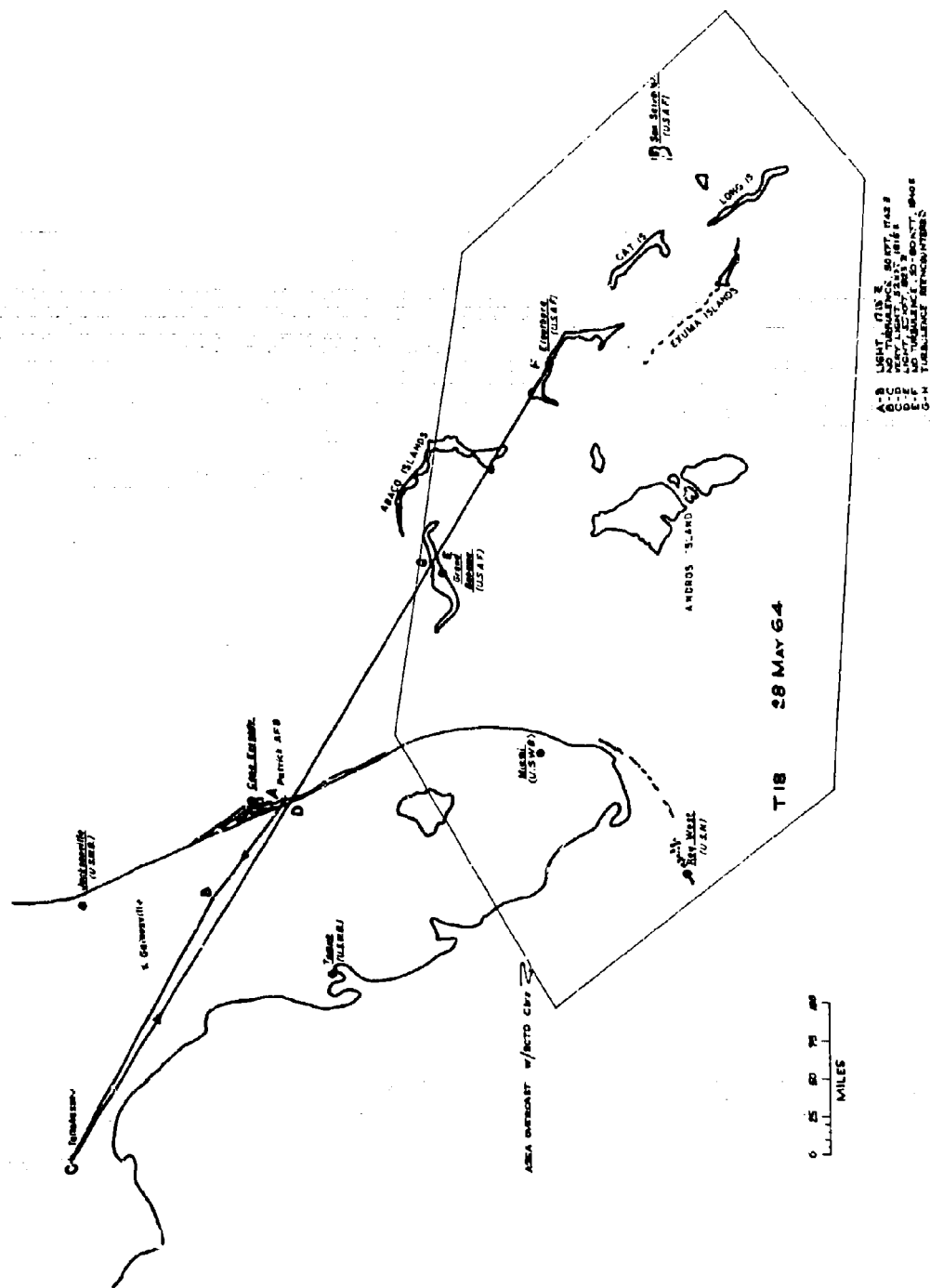


Figure 77. HICAT Track Map, Test 18

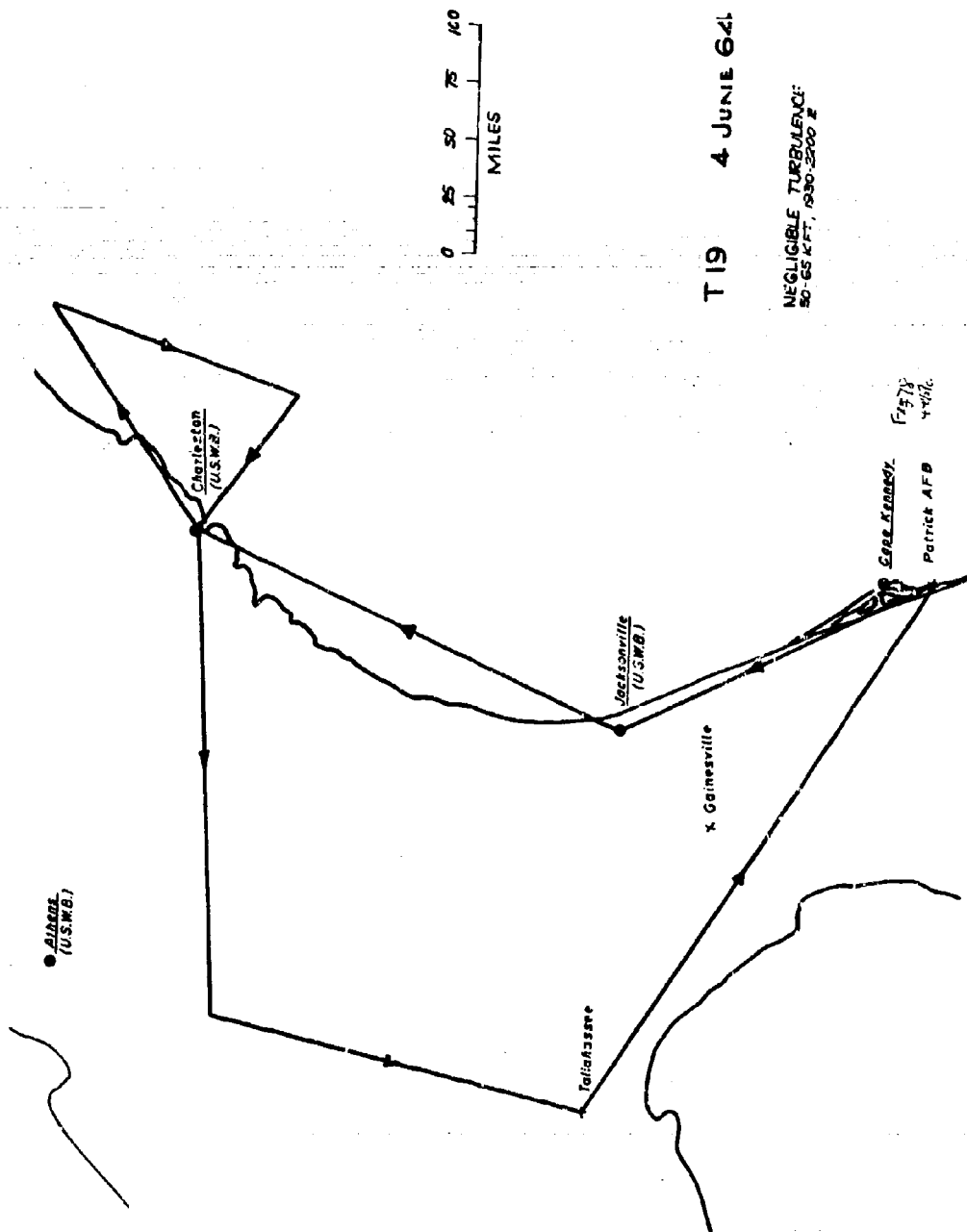
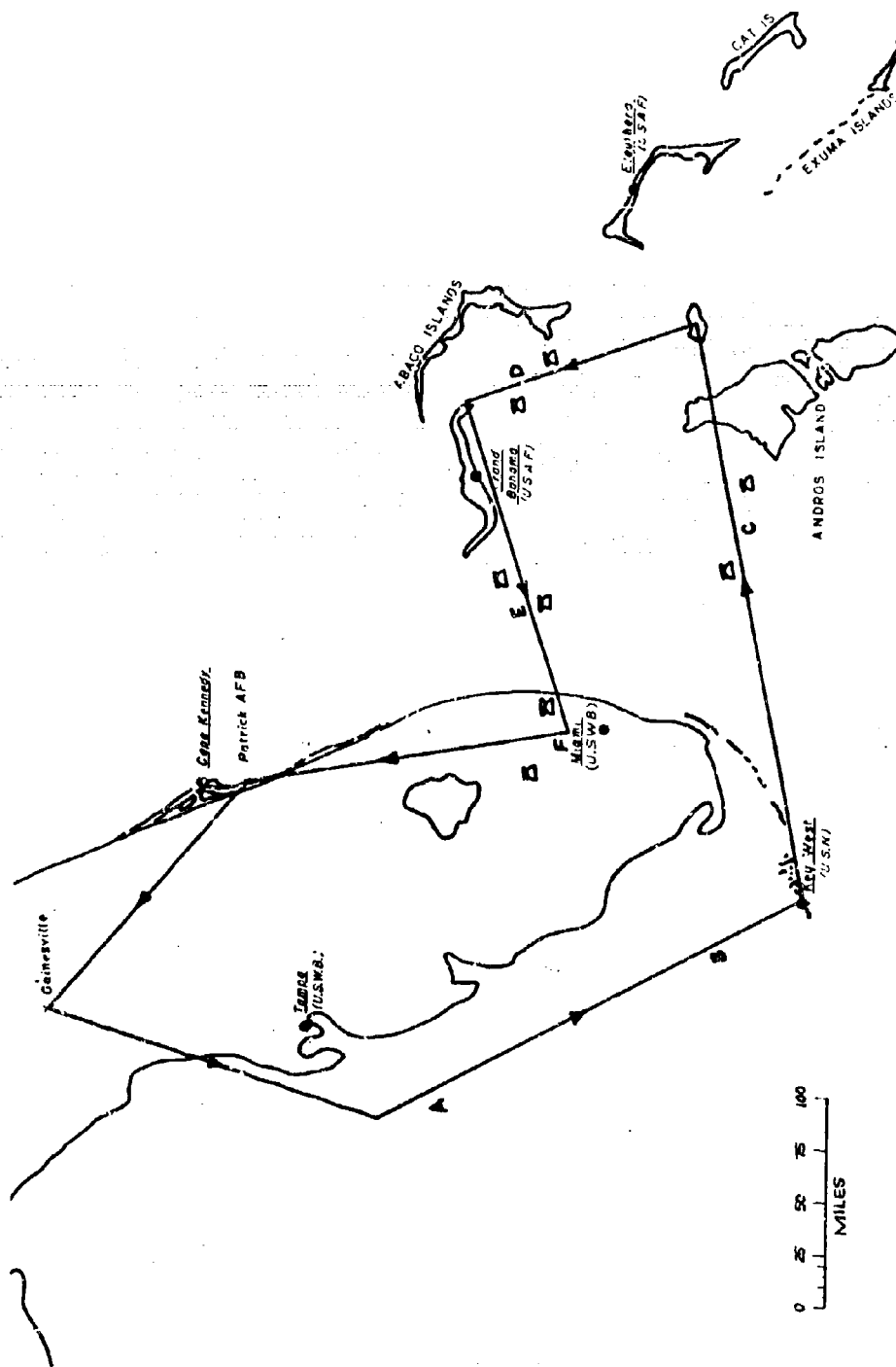


Figure 78. HICAT Track Map, Test 19



T20 8 JUNE 64
Figure 79. HICAT Track Map, Test 20

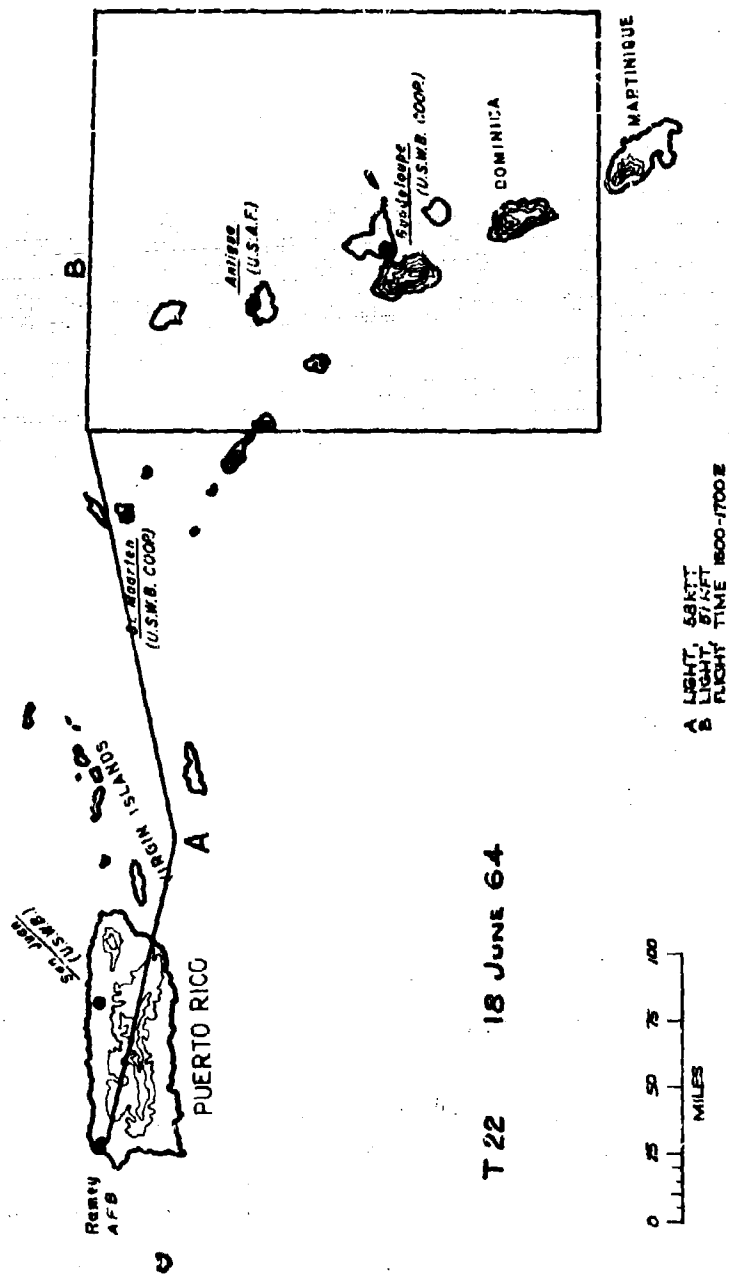


Figure 80. HICAT Track Map, Test 22

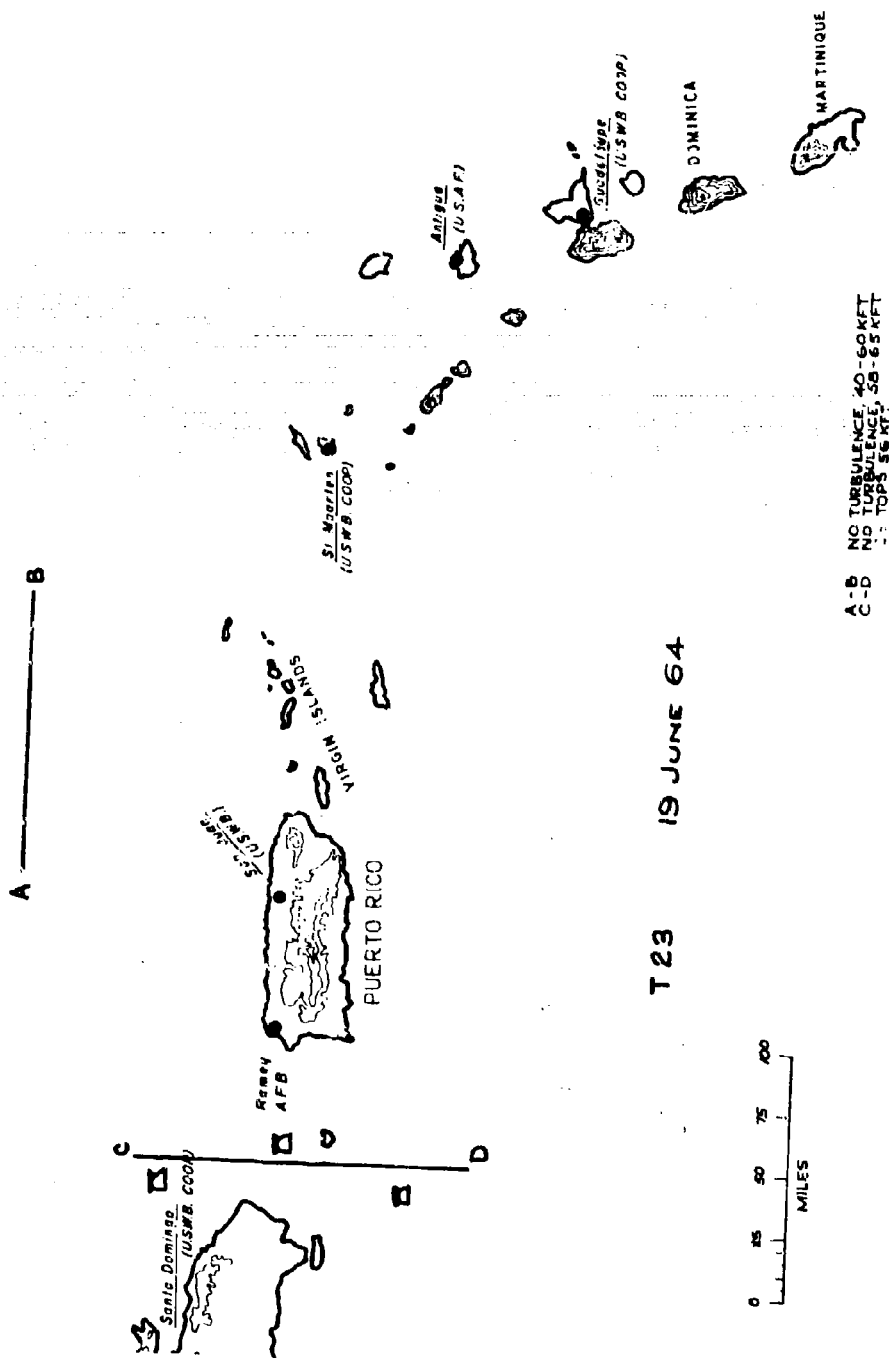
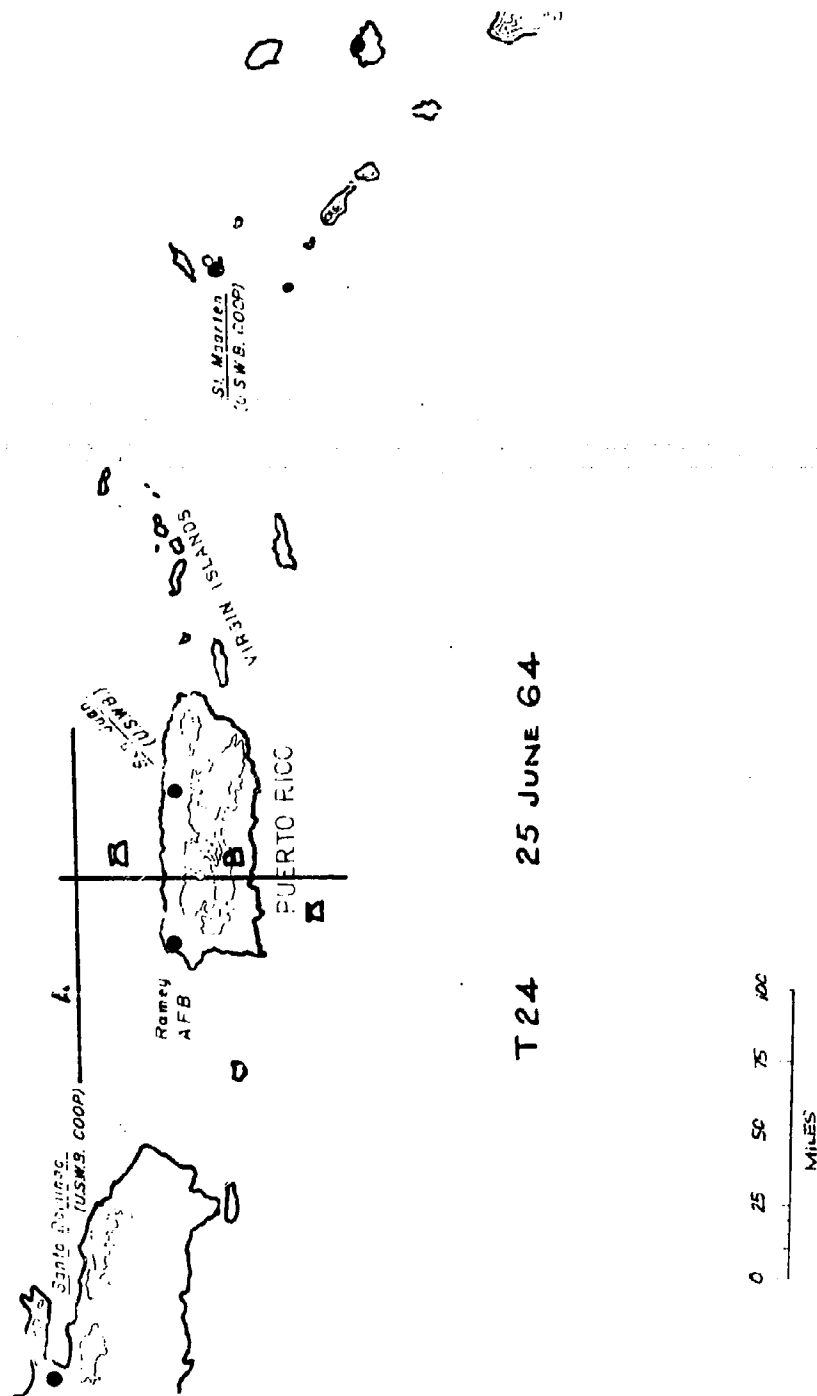


Figure 81. HICAT Track Map, Test 23



A LIGHT, CONTINUOUS, 59 KFT, CLEAR
 B LIGHT, CONTINUOUS, 54 KFT, CB ACTIVITY, 1130Z

Figure 2a. HICAT Track Map, Test 24

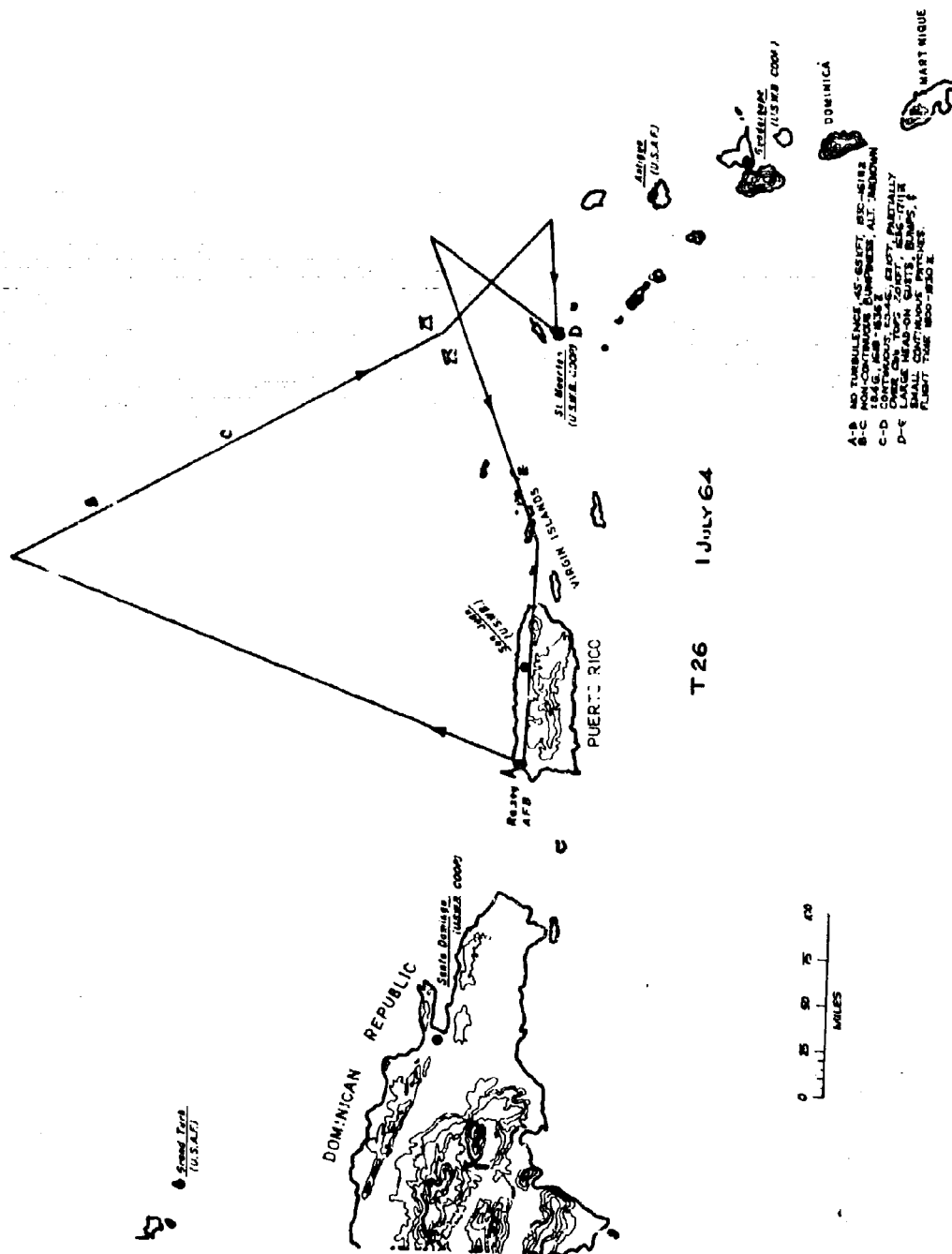


Figure 84. HICAT Track Map, Test 26

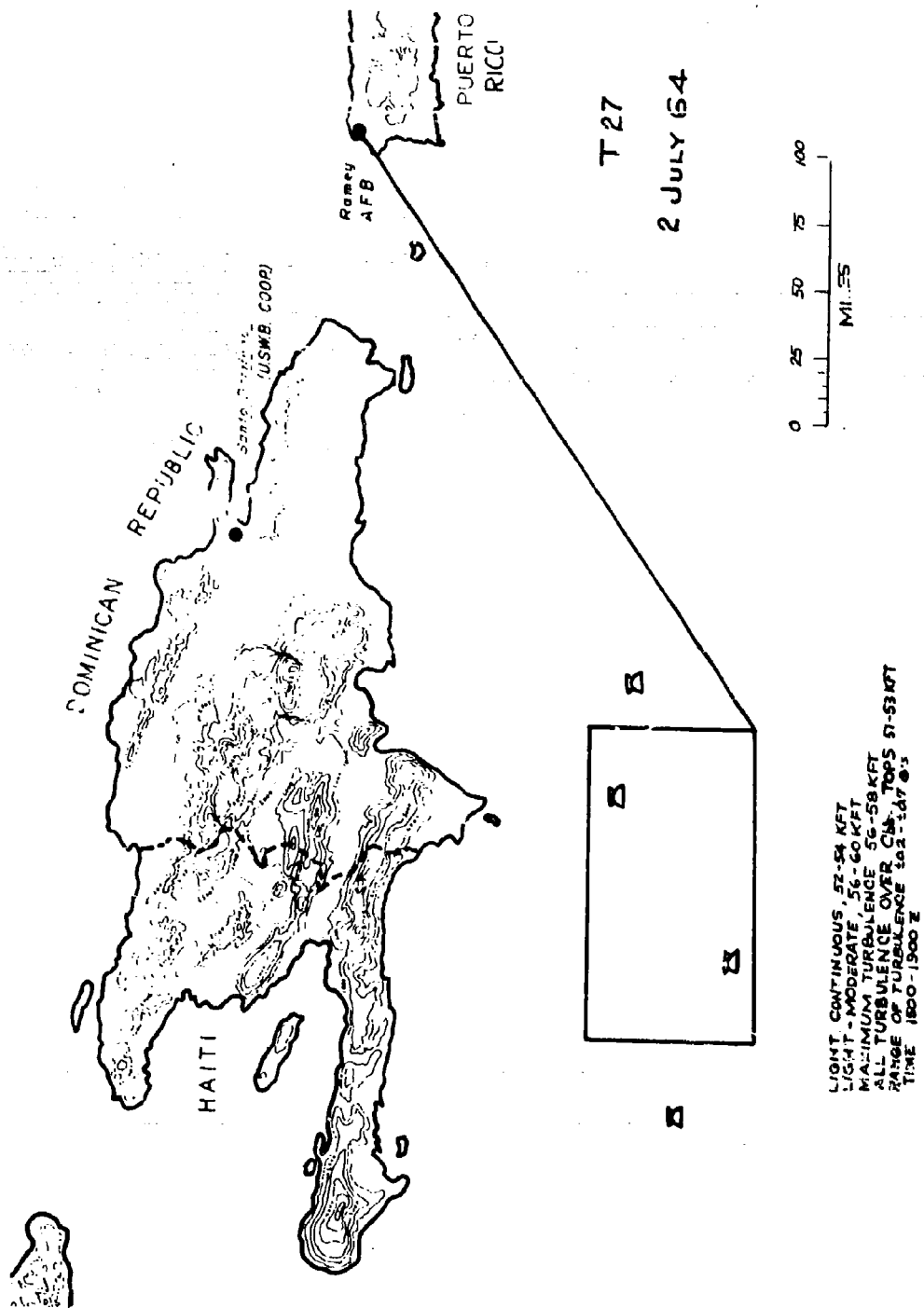


Figure 85. HICAT Track Map, Test 27

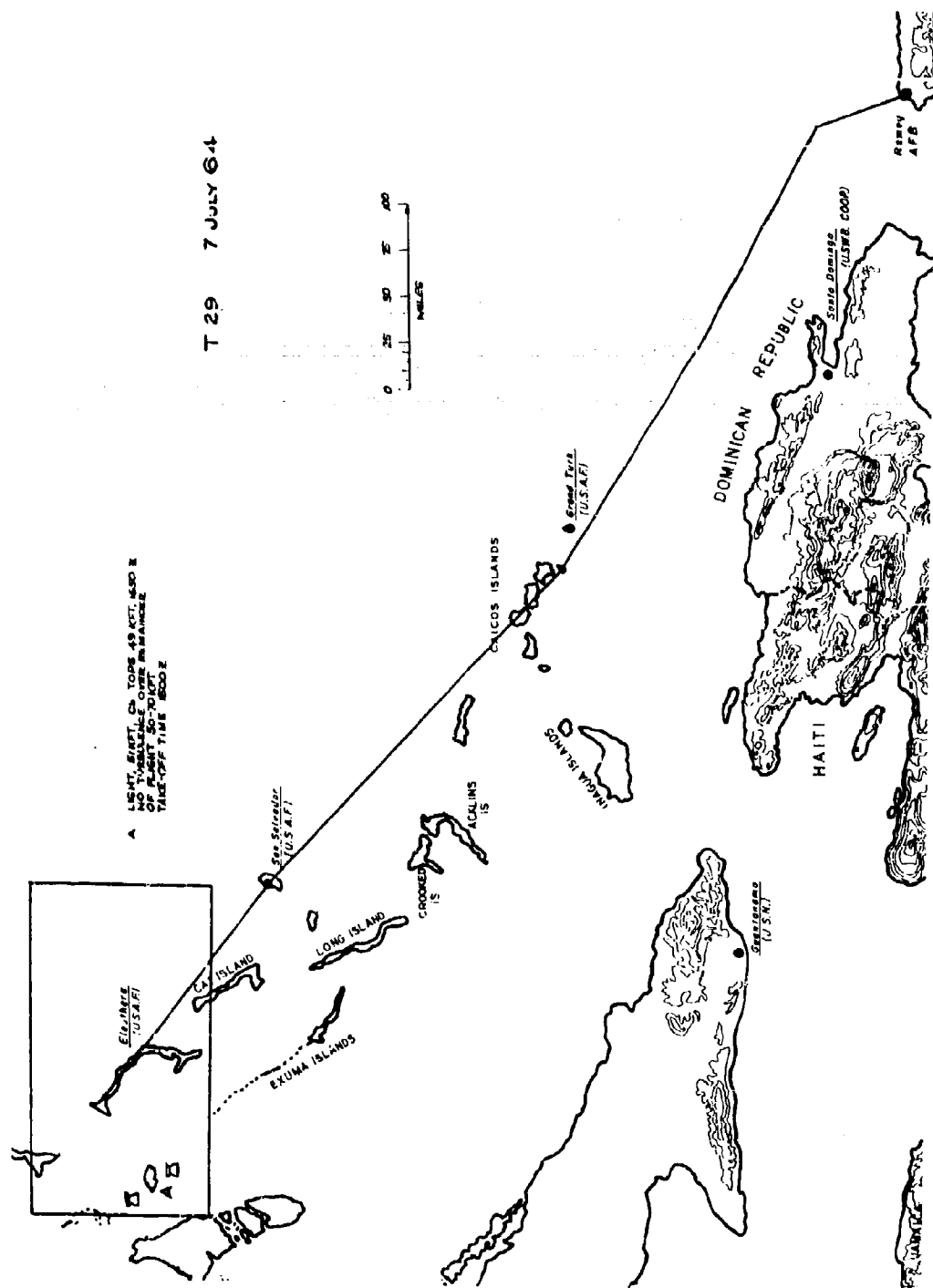
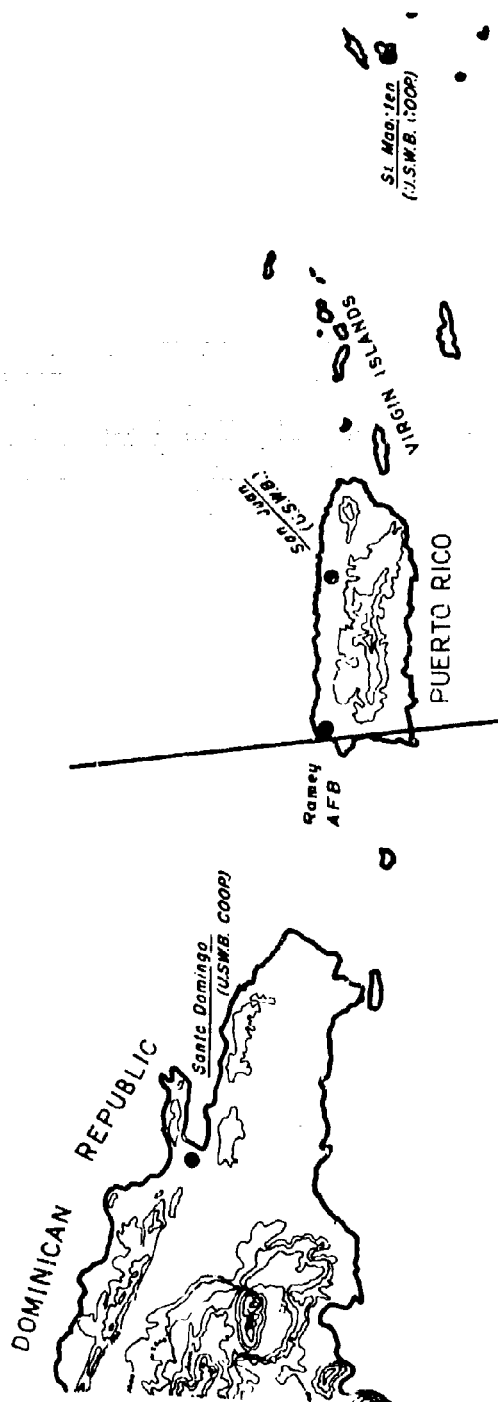


Figure 87. HICAT Track Map, Test 29



T30 15 JULY 64

40.56 OVER CH, TOPS 51KFT
FLIGHT ALTITUDE 52 KFT
FLIGHT TIME 1500-1630Z

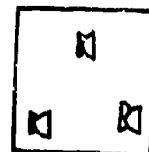


Figure 88. HICAT Track Map, Test 30

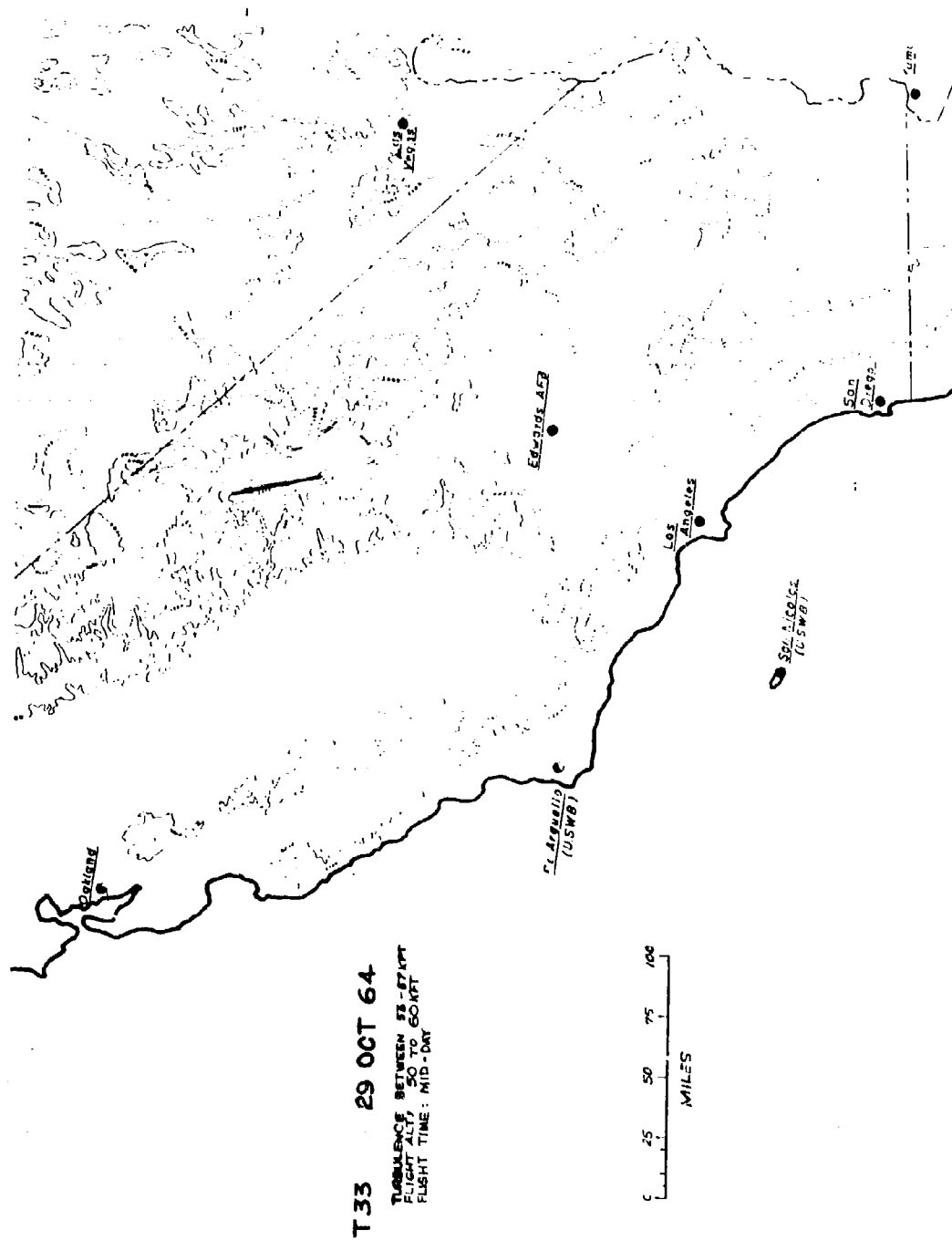


Figure 69. HICAT Track Map, Test 33

APPENDIX III

GUST VELOCITY EQUATIONS

The equations for the determination of the vertical, lateral, and longitudinal gust velocity components are given below:

Vertical Gust Velocity

$$U_V = V_T \Delta \alpha - V_T \Delta \theta + \int_{t_0}^{t_n} \Delta a_N dt$$

where $V_T \Delta \alpha$ = vertical gust velocity relative to the gust probe, i.e., uncorrected for aircraft rotation and translation in the vertical plane

$$= \frac{2 (\Delta P \alpha + m \Delta a_N)}{C_{N\alpha} \rho V_T S_V}$$

Lateral Gust Velocity

$$U_L = V_T \Delta \beta + V_T \Delta \psi - \int_{t_0}^{t_n} (\Delta a_L - g \Delta \phi) dt$$

where $V_T \Delta \beta$ = lateral gust velocity relative to gust probe, i.e., uncorrected for aircraft rotation and translation in the horizontal plane.

$$V_T \Delta \beta = \frac{2 (\Delta P \beta + m \Delta a_L)}{C_{N\beta} \rho V_T S_V}$$

Longitudinal Gust Velocity

$$U_F = \Delta V_T - \int_{t_0}^{t_n} (a_F - g \Delta \theta) dt$$

where ΔV_T = longitudinal gust velocity relative to gust probe uncorrected for aircraft fore-and-aft incremental velocities.

Symbols and sign convention are presented in the preface of this report.

APPENDIX IV

DERIVED EQUIVALENT GUST VELOCITY FORMULA

The derived equivalent gust velocity is a semi-empirical relationship defined as follows:

$$U_{de} = \frac{2 \Delta a_N W}{C_L \alpha \rho_0 K_g V_e S}$$

This formula is popular with aircraft designers because it provides them with a simple approximate relationship for predicting the maximum acceleration a new aircraft design may be expected to experience based upon the gust acceleration experience of an old design or reference airplane. The U_{de} equation is derived from unsteady lift theory and may be applied subject to the following assumptions:

1. The aircraft is a rigid body.
2. The aircraft forward speed is constant.
3. The aircraft is in steady level flight prior to gust entry.
4. The aircraft can rise but cannot pitch.
5. Lift other than from the wings is negligible.
6. The gust velocity is uniform across the wing span and always normal to the longitudinal axis of the aircraft.
7. The gust profile is a 1- cosine shape.
8. The transient lift function is constant with speed.
9. All airplanes are of conventional planform and have the same general characteristics.
10. Relative loads for single isolated gusts are a measure of those from a sequence of gusts.

REFERENCES

1. Hildreth, William W. Jr., et al, High Altitude Clear Air Turbulence, Aeronautical Systems Division Technical Documentary Report No. ASD-TDR-63-440 (LR 16816), June 1963, Unclassified.
2. Coleman, Thomas L.; Steiner, Roy, Atmospheric Turbulence Measurement Obtained From Airplane Operations at Altitudes Between 20,000 and 75,000 Feet for Several Areas in the Northern Hemisphere, NASA TN D-548, October 1960, Unclassified.
3. Hildreth, W. W. Jr., Proposal for a World Wide Clear Air Turbulence Model, Lockheed Report 16574, January 1963, Unclassified.
4. Saunders, K. D., B-66B Low Level Gust Study, Volume XIII. Instrumentation, Wright Air Development Division Technical Report 60-305, March 1961, Unclassified.
5. Fabian, C. B.; Storey, R. E., HICAT Program Preliminary Data Reduction and Analysis Methods, Lockheed Report 17696, March 31, 1964, Unclassified.
6. Hildreth, W. W. Jr.; Court, A.; Abrahms, G., High Altitude Rough Air Model Study, Lockheed Report 18823, May 10, 1965, Unclassified.

UNCLASSIFIED

Security Classification

DOCUMENT CONTROL DATA - R&D		
(Security classification of title, body of abstract and indexing annotation must be entered when the overall report is classified)		
1. ORIGINATING ACTIVITY (Corporate author)		2. REPORT SECURITY CLASSIFICATION
Lockheed-California Co. Burbank, California		Unclassified
		2D GROUP N/A
3. REPORT TITLE		
HIGH ALTITUDE CLEAR AIR TURBULENCE		
4. DESCRIPTIVE NOTES (Type of report and inclusive dates)		
Interim Report (April 1963 - February 1965)		
5. AUTHOR(S) (Last name, first name, initial)		
Crooks, Walter M.		
6. REPORT DATE	7a. TOTAL NO. OF PAGES	7b. NO. OF REFS
September 1965	114	6
8a. CONTRACT OR GRANT NO.	8d. ORIGINATOR'S REPORT NUMBER(S)	
AF 33(657)-11143	AFFDL-TR-65-144	
b. PROJECT NO.	8e. OTHER REPORT NO(S) (Any other numbers that may be assigned this report)	
1469	Lockheed Report No. LR 18794	
c. Task No. - 146902		
d.		
10. AVAILABILITY/LIMITATION NOTICES		
(1) Qualified Requestors May Obtain Copies of this Report From DDC.		
11. SUPPLEMENTARY NOTES		12. SPONSORING MILITARY ACTIVITY
N/A		AFFDL (FDTE) Wright-Patterson AFB, Ohio 45433
13. ABSTRACT		
<p>The purpose of this report is to describe the high altitude clear air turbulence (HICAT) program accomplishments and results as of 15 February 1965, when the program was redirected. The program effort consists of the measurement of HICAT velocity components at altitudes above 50,000 feet in several world areas. The program objective is the statistical definition of the characteristics of HICAT so as to improve structural design criteria.</p> <p>In the work accomplished thus far, an analog FM instrumentation system utilizing a fixed vane gust probe and a 7-hour recording system was installed aboard an Air Force U-2. HICAT searches were conducted at Air Force bases in California, Florida and Puerto Rico. Over seven hours of HICAT associated with jet streams, convective activity due to low level heating, and mountain wave activity were recorded. The latter category provided the most severe turbulence experienced to date, i.e., c.g. normal acceleration incremental peaks up to about $\pm 1g$ and RMS gust velocities in excess of 5 ft/sec.</p> <p>Actual vertical gust velocity time histories containing gust wavelengths from 7' to 2500 feet have been calculated from the measurements and used to obtain gust velocity peak counts and power spectra. Derived equivalent gust velocities, U_{de}, were also calculated and found to be comparable with similar NASA data.</p> <p>The redirected and extended HICAT program will utilize a new digital (PCM) instrumentation system. This system will include a stable platform which will greatly improve the precision of HICAT measurements and permit turbulence wavelengths in excess of 12,000 feet to be measured.</p>		

DD FORM 1 JAN 64 1473

Unclassified

Security Classification

UNCLASSIFIED

Security Classification

14. KEY WORDS	LINK A		LINK B		LINK C	
	ROLE	WT	ROLE	WT	ROLE	WT
High Altitude Clear Air Turbulence Gust Loads						

INSTRUCTIONS

1. **ORIGINATING ACTIVITY:** Enter the name and address of the contractor, subcontractor, grantee, Department of Defense activity or other organization (*corporate author*) issuing the report.

2a. **REPORT SECURITY CLASSIFICATION:** Enter the overall security classification of the report. Indicate whether "Restricted Data" is included. Marking is to be in accordance with appropriate security regulations.

2b. **GROUP:** Automatic downgrading is specified in DoD Directive 5200.10 and Armed Forces Industrial Manual. Enter the group number. Also, when applicable, show that optional markings have been used for Group 3 and Group 4 as authorized.

3. **REPORT TITLE:** Enter the complete report title in all capital letters. Titles in all cases should be unclassified. If a meaningful title cannot be selected without classification, show title classification in all capitals in parentheses immediately following the title.

4. **DESCRIPTIVE NOTES:** If appropriate, enter the type of report, e.g., interim, progress, summary, annual, or final. Give the inclusive dates when a specific reporting period is covered.

5. **AUTHOR(S):** Enter the name(s) of author(s) as shown on or in the report. Enter last name, first name, middle initial. If military, show rank and branch of service. The name of the principal author is an absolute minimum requirement.

6. **REPORT DATE:** Enter the date of the report as day, month, year; or month, year. If more than one date appears on the report, use date of publication.

7a. **TOTAL NUMBER OF PAGES:** The total page count should follow normal pagination procedures, i.e., enter the number of pages containing information.

7b. **NUMBER OF REFERENCES:** Enter the total number of references cited in the report.

8a. **CONTRACT OR GRANT NUMBER:** If appropriate, enter the applicable number of the contract or grant under which the report was written.

8b, 8c, & 8d. **PROJECT NUMBER:** Enter the appropriate military department identification, such as project number, subproject number, system numbers, task number, etc.

9a. **ORIGINATOR'S REPORT NUMBER(S):** Enter the official report number by which the document will be identified and controlled by the originating activity. This number must be unique to this report.

9b. **OTHER REPORT NUMBER(S):** If the report has been assigned any other report numbers (either by the originator or by the sponsor), also enter this number(s).

10. **AVAILABILITY/LIMITATION NOTICES:** Enter any limitations on further dissemination of the report, other than those

imposed by security classification, using standard statements such as:

- (1) "Qualified requesters may obtain copies of this report from DDC."
- (2) "Foreign announcement and dissemination of this report by DDC is not authorized."
- (3) "U. S. Government agencies may obtain copies of this report directly from DDC. Other qualified DDC users shall request through _____."
- (4) "U. S. military agencies may obtain copies of this report directly from DDC. Other qualified users shall request through _____."
- (5) "All distribution of this report is controlled. Qualified DDC users shall request through _____."

If the report has been furnished to the Office of Technical Services, Department of Commerce, for sale to the public, indicate this fact and enter the price, if known.

11. **SUPPLEMENTARY NOTES:** Use for additional explanatory notes.

12. **SPONSORING MILITARY ACTIVITY:** Enter the name of the departmental project office or laboratory sponsoring (paying for) the research and development. Include address.

13. **ABSTRACT:** Enter an abstract giving a brief and factual summary of the document indicative of the report, even though it may also appear elsewhere in the body of the technical report. If additional space is required, a continuation sheet shall be attached.

It is highly desirable that the abstract of classified reports be unclassified. Each paragraph of the abstract shall end with an indication of the military security classification of the information in the paragraph, represented as (TS), (S), (C), or (U).

There is no limitation on the length of the abstract. However, the suggested length is from 150 to 225 words.

14. **KEY WORDS:** Key words are technically meaningful terms or short phrases that characterize a report and may be used as index entries for cataloging the report. Key words must be selected so that no security classification is required. Identifiers, such as equipment model designation, trade name, military project code name, geographic location, may be used as key words but will be followed by an indication of technical context. The assignment of links, rules, and weights is optional.

UNCLASSIFIED

Security Classification